ANTHROPIC SIGNATURES AND PALEOFLOODS IN ALLUVIUM OF THE UPPER LITTLE TENNESSEE RIVER VALLEY, SOUTHERN BLUE RIDGE MOUNTAINS, USA

by

LIXIN WANG

(Under the Direction of David. S. Leigh)

ABSTRACT

This project aimed to compare pre-settlement and post-settlement floodplain sediments and to reconstruct paleoflood history in the upper Little Tennessee River valley, within the Southern Blue Ridge Mountains. The physical and chemical characteristics of overbank sediments at three floodplain sites were studied. Optically stimulated luminescence (OSL), radiocarbon (^{14}C), ^{137}Cs and historic records provided high-resolution chronology. The sedimentation rates and five elements (Ca, P, K, Pb, Hg) clearly differentiate sediments between the two periods. They were designated as anthropic signatures because their significant differences are largely related to increased human activities during post-settlement time. The paleoflood analysis was based on a modern-analog of flood-sedimentology. Two periods with large floods were identified at A.D. 690-875 and A.D. 1100-1350, corresponding to wet climate conditions. The analysis suggested a wetter MWP and a relatively drier LIA.

INDEX WORDS: particle sizes, chemical characteristics, human impact, climate change, paleofloods, hydroclimate, Medieval Warm Period

ANTHROPIC SIGNATURES AND PALEOFLOODS IN ALLUVIUM OF THE UPPER LITTLE TENNESSEE RIVER VALLEY, SOUTHERN BLUE RIDGE MOUNTAINS, USA

by

LIXIN WANG

B.S., Nanjing University, China, 2008

A Thesis Submitted to the Graduate Faculty of The University of Georgia in Partial Fulfillment of

the Requirements for the Degree

MASTER OF SCIENCE

ATHENS, GEORGIA

2010

ANTHROPIC SIGNATURES AND PALEOFLOODS IN ALLUVIUM OF THE UPPER LITTLE TENNESSEE RIVER VALLEY, SOUTHERN BLUE RIDGE MOUNTAINS, USA

by

LIXIN WANG

Major Professor:	David S. Leigh
Committee:	George A. Brook
	Steven M. Holland

Electronic Version Approved:

Maureen Grasso
Dean of the Graduate School
The University of Georgia
August 2010

ACKNOWLEDGEMENTS

This project is supported by the National Science Foundation under grants DEB-9632854 & DEB-0218001 to the Coweeta Long Term Ecological Research program. I thank the P.I., Dr. Ted Gragson from Anthropology department at University of Georgia, for his logistic support of the chemical analysis, radiocarbon and luminescence dates, and the trip to the College of Charleston. I greatly appreciate Dr. Scott Harris in the Department of Geology and Environmental Geosciences at the College of Charleston for letting me to use his CILAS machine to do the particle size analysis. The University of Georgia Luminescence Dating Laboratory processed three OSL ages, for which I am really grateful.

I sincerely thank my advisor David Leigh, who offered excellent guidance and assistance to my master's study and research. This thesis project could not have been completed without his patience, encouragement, and logistic support. I am also very grateful to my committee, George Brook and Steve Holland, for their insightful advice and timely help during the whole process. My appreciation also goes to many other people: to Brad Suther and Jake McDonald, for their great help in my field and lab work; to Jenny Morgan, Amber Ignatius, Genevieve Holdridge, and Fran Rauschenberg, for their kindness in correcting the grammar mistakes in the manuscripts; to Shanqi Zhang, for her help on the graphs; and to all my fellow graduate students, for their friendship during the past two years. Finally, but most importantly, huge thanks go to my family and Taotao Zhu, for their love and consistent support.

TABLE OF CONTENTS

Page

LIST OF TABLES

Page

LIST OF FIGURES

Page

CHAPTER 1

INTRODUCTION AND BACKGROUND

Climate change and human activities are the primary drivers of floodplain sedimentation in the late Holocene (Knighton, 1998; Charlton, 2008). The environmental changes caused by climatic variations and human impacts commonly are recorded in the stratigraphy and sedimentology of floodplain sediments (Gregory et al., 1995; Knighton, 1998; Knox, 1987, 2001, 2006; Macklin, 2003; Lewin, 2005). The dominant driver of environmental change varies depending on the time period. In most parts of the United States, significant human impact on the fluvial system did not begin until after the European settlement, which we refer to as post-settlement time (Trimble, 1974; Jacobson and Coleman, 1986; Knox, 1987; Ambers, 2006). Natural climate change was the dominant driver during pre-settlement time, while human impact was more significant during post-settlement time. Hence, the responses of floodplain sedimentation to environmental changes should reflect the different drivers in the two periods.

In fact, many studies have found significant differences between the two time periods in overbank sediments, in terms of sediment textures, sedimentology and sedimentation rates (Lecce, 1997; Knox, 2001, 2006; Benedetti, 2003). Due to accelerated upland erosion and surface runoff, resulting from intensive human activities such as row-crop agriculture, timber harvest, and land clearing for construction (Glenn, 1911; Happ, 1945; Trimble, 1974, Leigh, 2007), post-settlement sediments generally have been found to be coarser than pre-settlemet sediments, and post-settlement sedimentation rates are much greater than pre-settlement rates (Miller et al., 1993; Knox, 2001, 2006; Benedetti, 2003). Besides the physical characteristics, chemical traits often vary significantly between

the two periods. For example, the lead and zinc content has increased greatly in overbank sediments in the upper Mississippi valley, due to mining activities in the 19th century (Knox, 2006). Mercury (Hg) and gold (Au) were found to have distinctively higher concentrations in post-settlement sediments of the north Georgia gold belt because of gold mining (Leigh, 1994, 1997).

Most studies focused on the impact from human activities during post-settlement time because those impacts were quite significant and easy to track from detailed historical records. On the contrary, information about climate changes during pre-settlement time was scarce. And studies on the paleoclimate reconstruction seldom relied on floodplain overbank sediments because of erosion and disturbance on floodplains (Benito et al., 2003). However, overbank sediments are direct evidence of flood events (Benito et al., 2003).

Floodplain overbank sediments have been used to infer paleofloods (Knox, 2000, 2006; Goman and Leigh, 2004; Werritty et al., 2006). Typically, overbank sediments are composed of silty and fine sandy facies. Silty facies record moderate size overbank floods that are capable of conveying silt and clay in suspension across the floodplain; sandy facies register larger floods that are capable of transporting fine- to medium-sized sand in suspension (Nicholas and Walling, 1997). Paleofloods tend to cluster in certain time periods (Baker, 2008). Although many studies suggest that flood periods coincided with wet climate (Ely, 1997; Goman and Leigh, 2004) or with climate transitional periods (Ely et al., 1993; Knox, 1993), some research reveals that larger floods occur under more arid conditions (Patton and Dibble, 1982). Thus, the relationship between paleofloods and paleoclimate is complicated. However, paleoflood history can still offer insight into paleohydroclimate conditions when studied in conjunction with other climatic indices such as pollen and tree-ring records (Goman and Leigh, 2004).

Few studies regarding the chronology, floodplain sedimentation and sediment chemical characteristics have been conducted in the southern Blue Ridge Mountains. Price and Leigh (2006) studied the stream morphological and sedimentological response to human impact in small highland

streams, but their focus was not on floodplain sedimentation. Leigh and Webb (2006) looked at the long-term average sedimentation rates under different depositional environments at Raven Fork in the Smoky Mountain range. They found higher sedimentation rates during the first half of Holocene than in the last half of Holocene, and attributed it to the frequent heavy rainfall and floods in the early Holocene. They also found that, due to increased human impacts, the post-settlement sedimentation rate was about one order of magnitude greater than pre-settlement rate. In another study, Leigh (2007) calculated the long-term average overbank sedimentation rates at three fluvial stratigraphic sections (State Line, Otto and Riverside) in the upper Little Tennessee River basin. The average of rates was 0.7 mm/yr prior to A.D. 1870, and 12.7 mm/yr from A.D. 1870 to A.D. 2005. However, the scarcity of radiocarbon dates in that study (Leigh, 2007) prevented the investigation from determining a longer, specific relationship between sedimentation rates and time. Few studies is concerned with chemical traits of sediments but one, which use geochemical data as a fingerprint of sediment provenance in Fairfield Lake, an artificial highland lake in the Blue Ridge Mountains of western North Carolina (Miller et al., 2005). Although it mentioned that localized development in the highlands attributed to the much higher sedimentation rates, it did not evaluate the impact of regional development on sediment chemical characteristics.

The long-term (millennial) flood history in the southern Blue Ridge Mountains is unclear due to the short-term record and lack of study. Leigh (2007) related particle size of post-settlement floodplain sediments to gaged flood records in the upper Little Tennessee River basin and found that a relatively high percentage of >0.25 mm particles is a good indicator of the occurrence of large floods; however, he did not examine pre-settlement floods. Although several studies showed a wetter early Holocene in the southeastern United States (Leigh and Feeney, 1995; Goman and Leigh, 2004; Leigh, 2006), the paleoclimate conditions during the last 2000 years are not well known, especially in the southern Blue Ridge Mountains (Leigh, 2008). Therefore, more studies on the stratigraphy, physical and chemical

characteristics of floodplain sediments are needed in order to understand how floodplain sedimentation responded to environmental changes. Also the reconstruction of a long-term flood history is necessary in order to understand the late Holocene hydroclimate conditions in the southern Blue Ridge Mountains.

This project aims to fill these study gaps and thus has two main objectives. The first objective was to identify anthorpic signatures that could differentiate pre-settlement from post-settlement floodplain sediments in the southern Blue Ridge Mountains, which was achieved by studying the physical and chemical characteristics of overbank sediments at three sites in the upper Little Tennessee River valley. The second objective was to reconstruct flood history and hydroclimatic conditions for the past 2000 years in the southern Blue Ridge Mountains, which was accomplished by building a modern flood-sedimentology analog and comparing it to other climate indices. Established techniques were adopted, but several features in this study are worth mentioning. First, compared with the traditional particle size analysis methods such as sieve, hydrometer or pipette, the automatic laser analyzer in this study produced high-resolution particle size results, facilitating the discrimination of different allostratigraphic units and the identification of paleofloods. Second, the increased number of dates from optically stimulated luminescence (OSL), radiocarbon dating, ^{137}Cs and historic records allowed the construction of non-linear depth-age models, which helped to determine the relationship between sedimentation rates and time and to establish a paleoflood chronology. Third, statistical analyses on chemical elements objectively identified signature elements that distinguished post-settlement from pre-settlement sediments, which was the first investigation of its kind in the southern Blue Ridge Mountains.

Chapter 2 focuses on the first objective concerning the anthropic signatures of floodplain overbank sediments. Chapter 3 focuses on the second objective, which involves the paleofloods and

paleohydroclimate during the past 2000 years. These two chapters will be submitted to the journal "The Holocene". And finally, major findings of this project are highlighted in Chapter 4.

CHAPTER 2

PRE-SETTLEMENT VESUS POST-SETTLEMENT FLOODPLAIN SEDIMENTS IN THE UPPER LITTLE TENNESSEE RIVER VALLEY, USA[1]

[1] Wang, L., Leigh, D.S., Brook, G.A. To be submitted to *The Holocene*.

Abstract: Physical and chemical characteristics of floodplain overbank sediments were studied at three sites in the upper Little Tennessee River valley of the southern Blue Ridge Mountains. High-resolution particle size analysis (2-2000 μm) from an automatic laser analyzer facilitated the determination of the allostratigraphic unit boundaries. The buried A horizons, Hurst color index, and weight loss on ignition (LOI) values identified the pre-settlement/post-settlement boundary, and the percentage of >0.25 mm fraction, mean, D90, and skewness of particle size distributions best defined the pre-settlement lateral accretion/vertical accretion boundary. The pre-settlement chronology came from radiocarbon and optically stimulated luminescence (OSL) dating, and post-settlement chronology came from ^{137}Cs and historical gaged flood records. The high-resolution dates helped to build a non-linear power relationship between depth and age of vertical accretion sediments, which suggested decreasing sedimentation rates with time before A.D. 1870, and increasing rates with time after A.D. 1870. Though the sedimentation rates, sediment texture and chemical elements varied at the three study sites, they all showed great differences between post-settlement and pre-settlement periods. Long-term average sedimentation rates after A.D. 1870 were 3-12 mm/yr, up to one order of magnitude greater than before A.D. 1870, when rates were less than 1.2 mm/yr. The pre-settlement vertical accretion showed a fining-upward trend, but the post-settlement sediments showed a coarsening-upward trend. Chemical analysis identified five signature elements (Ca, Hg, K, P, Pb) that are significantly different between post-settlement and pre-settlement sediments. The significant differences and substantial changes between the two periods were related to the environmental changes caused by intensified human activities, such as timber harvest, agriculture, and mining activities during the early post-settlement time, as well as population growth and urbanization after A.D. 1970. Even though autogenic processes of floodplain development and natural climate change in the past decades may have contributed to these changes, direct human impact dominates. Therefore, we viewed the sedimentation rates, sediment texture, and

the five signature elements as anthropic signatures, which discriminate human impact from other influences on floodplain sedimentation in the southern Blue Ridge Mountains.

Keywords: stratigraphy, sedimentology, soil chemistry

Introduction

Climate change and human activities are two important factors that affect the fluvial system (Knox, 1977, 1987; Knighton, 1998; Charlton, 2008). Understanding how floodplains respond to these two factors is a long standing issue in fluvial geomorphology. Various studies have shown that floodplain sedimentation is responsive to environmental changes caused by climate change and human activities (Miller et al., 1993; Knox, 1977, 1987, 2001, 2006; Macklin, 2003; Lewin, 2005). Stratigraphic records of floodplain sedimentation provide important information about variations in climate, human impact on the landscape, and geomorphic processes (Gregory et al., 1995; Knighton, 1998; Wohl, 2000).

In most parts of the United States, significant human impact on fluvial systems did not occur until after the non-indigenous immigration and settlement, which primarily was characterized by people of European and African heritage in the southeastern United States. This period is often referred to as post-settlement time (e.g. Trimble, 1974; Jacobson and Coleman, 1986; Knox, 1987, 2001; Ambers, 2006). Thus, during pre-settlement time, natural changes with little human disturbance controlled floodplain sedimentation, while human influence became more significant during post-settlement time. Following the settlement of Euro-Americans, intensive agricultural practices greatly accelerated soil erosion. For example, Happ (1945) estimated that about 15 cm of surface soils were eroded within 150 years, due to agricultural land use in the Carolina Piedmont; and Trimble (1974) estimated that an average of 19 cm surface soils were eroded from the upper Piedmont of Georgia between A.D. 1800 and A.D. 1970. These eroded sediments were transported and deposited in valleys, leading to increased

floodplain sedimentation. The change from forest and prairie land to cropland and pastureland that was associated with European settlement in the upper Mississippi River valley increased the rates and magnitudes of floodplain sedimentation by at least one order of magnitude (Lecce, 1997; Knox, 1987, 2006). Besides the sedimentation rates, chemical characteristics of overbank sediments also proved to be different between pre-settlement and post-settlement periods, in relation to the regional mining activities. For instance, lead and zinc content greatly increased in post-settlement overbank sediments in the upper Mississippi valley due to intensive mining activities in the Zinc-Lead District (Lecce and Pavlowsky, 2001; Knox, 2006). Mercury (Hg) and gold (Au) were found in distinctively higher concentrations in post-settlement sediments of the north Georgia gold belt because of gold mining (Leigh, 1994, 1997).

Many studies of agricultural and mining districts have found differences between the two periods in overbank sediments, in terms of sedimentology, sedimentation rates, and chemical characteristics (Miller et al., 1993; Knox, 2001, 2006; Benedetti, 2003; Leigh, 1994, 1997). However, little is known of the more remote highlands of the southern Blue Ridge Mountains where this study is focused. Subsistence agriculture was discontinuous and mining activities were scattered in this region, but intensive timber harvest was significant (Harden, 2004). Leigh and Webb (2006) found that, due to timber harvest and land clearing at Raven Fork in the Smoky Mountain range, the post-settlement floodplain sedimentation rates were 5.8-6.5 mm/yr, about one order of magnitude greater than pre-settlement rates. Leigh (2007) investigated the long-term average floodplain sedimentation rates in the upper Little Tennessee River valley and found the rate was 12.7 mm/yr after A.D. 1870, much higher than the 0.7 mm/yr before A.D. 1870. In general, however, studies relating sedimentation rates to human impact in this region are few, and even fewer studies are concerned with the chemical trait of sediments, except for Miller et al. (2005). They did chemical analysis on the sediments in Fairfield Lake, an artificial highland lake in the Blue Ridge Mountains of western North Carolina, and used the

geochemical data as a fingerprint of sediment provenance. Although they mentioned that the localized development in the highlands contributed to high sedimentation rates, they did not talk about human impact on sediment chemical characters. Generally, the chemical distinctions between post-settlement and pre-settlement floodplain sediments in the Blue Ridge province have not been thoroughly studied, which provided an impetus for this research.

Thus, one of the main objectives of this study is to elucidate physical and chemical differences between pre-settlement and post-settlement sediments in a mountainous region that has not been heavily influenced by agricultural and mining activities. It is assumed that the physical and chemical distinctions, in terms of sediment texture, sedimentation rates and chemical element contents, are significant between the two periods, and that certain anthropic signatures could be identified as they relate to post-settlement human impacts in the region.

Study Area

The upper Little Tennessee River drains a 363 km^2 catchment above the United States Geological Survey (USGS) gaging station near Prentiss (USGS 03500000), with elevation of 510-1600 m in northeast Georgia and western North Carolina (Figure 2.1). The characteristic bedrock of the region is quartz dioritic gneiss and biotite gneiss, containing certain amount of precious metal such as gold and copper (Hatcher, 1988; Daniel and Payne, 1990; Robinson et al., 1992). Bedrock has been weathered to form a 1-30 m thick mantle of saprolite. The texture of saprolite ranges from sand to clay loam, providing abundant fine sediments to the drainage network (Price and Leigh, 2006; Leigh, in press (b)). The upper Little Tennessee River flows north and is fed predominantly by east- and west-flowing tributaries (Figure 2.1). The morphology of the channel is characterized by meandering riffles and pools with coarse bed sediments such as cobble, gravel and sand, and with finer overbank sediments such as fine sand, silt and clay (Price and Leigh, 2006; Leigh, in press (a)). Entisols and inceptisols are common on floodplains and the first terraces, which are developed from retransported saprolite, alluvium or

colluvial deposits (Leigh, in press (b)). The region lies in the humid subtropical climate zone, with a 30-year (1971-2000) average annual precipitation of 183 cm and an average annual temperature of 12.7 °C, as recorded at the low elevation station of the Coweeta hydrologic laboratory (NCDC, 2003).

The area lies in the gold-bearing belt in the southeast U.S. and scatted mining activities were active during the late 19th and early 20th century (Robinson et al., 1992). However, most of these activities were prospecting and only one mine location was recorded within the study area, the Otto Zn-Cu mine (Location is shown in Figure 2.1). Three specific sites in the bottomland of the upper Little Tennessee River valley were selected between the headwater and the lower main stem (Figure 2.1). Currently, all three sites are pastureland, and the catchment contains a variety of land cover type (pasture, forest, cropland, suburban, and roads). The Keener site is located in the valley of a small tributary with a drainage area of 7.2 km^2 (Price and Leigh, 2006), and the cores were taken about 25 meters away from the channel next to Price and Leigh's (2006) core site KE1. The State Line and Riverside sites (Leigh, 2007) are located downstream along the main stem of the upper Little Tennessee River, and samples were taken on the bank directly next to the channel. Previous studies (Price and Leigh, 2006; Leigh, 2007) identified the ages of overbank sediments at these three sites to be within the last 2500 years, bracketing the Medieval Warm Period (MWP, A.D. 800-1300) and the Little Ice Age (LIA, A.D. 1400-1800), the two climate anomalies that are of great interest in late pre-settlement time. Although sedimentation rates at two of the three sites have been studied by Leigh (2007), this study extends that work. New radiocarbon and optical stimulated luminescence (OSL) dates increased the age resolution and allowed a better chronology. Higher-resolution particle size results facilitated the discrimination between different stratigraphic units. In addition to the physical properties such as particle sizes, sedimentation rates, and organic matter content, we also looked at the chemical elements that were absorbed on particle surfaces, in an effort to identify diagnostic anthropic signatures.

Methods

Field Methods

Field work was conducted in March 2009. Solid cores (7.5 cm diameter) were taken with a trailer-mounted Giddings hydraulic coring rig. Each core was wrapped with plastic and aluminum foil in the field and returned to the laboratory. Two adjacent cores were taken at the Keener site for comparison. In addition to cores, at the State Line and Riverside sites, monolith samples were obtained by pounding metal or PVC trough into the vertical cutbank profile and then meticulously excavating the soils out. The advantage of monoliths is that they are not compressed and preserve undisturbed layers in the best possible condition. Later in the laboratory, based on the stratigraphic correlation and particle size analysis results, data from cores and monoliths were combined into a single profile to take advantage of the intact monolith samples.

OSL samples were taken from the State Line and Riverside sites' cutbank profile by pounding gray plastic tubes (5 cm diameter by 15 cm long) into sand strata and then wrapping both ends with black duct tape. OSL samples for the Keener site came directly from the core sample. Additionally, flecks of charcoal were collected from the outcrops at the State Line and Riverside sites for radiocarbon dating.

Laboratory Methods

All cores and monoliths were cleaned, photographed and described according to the U.S. Department of Agriculture Soil Survey Manual (Soil Survey Division Staff, 1993), and the descriptions are available in the appendices (Appendix A). Samples were taken from each core and monolith in 2-14 cm increments to approximate 50-yr time intervals for pre-settlement sediments and 10-yr time intervals for post-settlement sediments, based on the previous chronology (Price and Leigh, 2006; Leigh, 2007). Abrupt and clear boundaries were captured by smaller sampling intervals in order to be reflected in the laboratory data. Samples were oven dried at 55 °C for at least 48 hours and then sieved through 2 mm

mesh. Particles larger than 2 mm were weighed and discarded, while particles smaller than 2 mm were retained for further analysis.

Particle size: About 0.5 g samples were taken for particle size analysis on an automatic laser particle size analyzer (CILAS 1180) in the Department of Geology and Environmental Geosciences at the College of Charleston. Samples were pretreated with 30% hydrogen peroxide (H_2O_2) to remove humus and then with a sodium metaphosphate solution (50 g/L) to disperse clay aggregates before being introduced into the machine. The machine measures particles from 0.04 µm to 2500 µm and produces a continuous distribution of particle sizes. Traditional wet sieve and pipette methods were also run on certain samples to be compared with the CILAS results (Figure 2.2); and the sieve and pipette results were transformed to CILAS-based results according to the relations shown in Figure 2.2. Descriptive statistics of the particle size range 2-2000 µm were performed on the program *GRADISTAT 4.0* (Blott, 2000).

Organic matter content: Loss on ignition (LOI) was used to estimate the content of organic matter in the sediment according to procedures of Dean (1974) and Cuniff (1998). Approximately 5 g samples were measured and dried at 110°C for 12 hours and then burned in a muffle furnace at 550°C for 4 hours. Weight loss from this process primarily occurs from the combustion of organic matter, but also includes some dewatering of clay minerals and oxides (Beaudoin, 2003; Smith, 2003; Santisteban et al., 2004). However, the percentage of weight loss is generally accepted to primarily represent the proportion of organic matter (Dean, 1974; Heiri et al., 2001).

Geochemical analysis: The chemical analyses were completed by a private commercial laboratory (ALS Chemex) using an aqua regia (hot 1:3 nitric-hydrochloric acids) digestion on the <0.25 mm fraction to remove extractable elements. Concentrations of 34 extractable elements were determined by inductively coupled plasma-atomic emission spectroscopy and mercury was analyzed by

cold vapor atomic absorption spectrometry. The precision of the analytical methods are certified by Chemex to be within 10% at 200 times the detection limits.

Chronology: In addition to the previous radiocarbon ages at three sites (Price and Leigh, 2006; Leigh, 2007), new OSL and radiocarbon ages were obtained for pre-settlement age control. The light-sealed central part of an intact sandy section in one of the Keener cores, along with the OSL samples taken from the State Line and Riverside sites, were dated in the University of Georgia Luminescence Dating Laboratory. Sediments were washed with water, and then treated with 10% HCl and 30% H_2O_2 to remove carbonates and organic material. Sieving isolated the 120-150-mm-size fraction and then density separation using Na-polytungstate (2.58 g/cm^3) was used to separate quartz from feldspar minerals. The quartz fraction was etched with 48% HF for 80 min followed by 36% HCl for 40 min to remove the alpha skin. Quartz grains were mounted on stainless steel discs with the help of Silkospray^{TM}. Light stimulation of quartz mineral extracts was undertaken with a RISØ array of combined blue LEDs centered at 470 nm. Detection optics consisted of two Hoya 2.5-mm-thick U340 filters and a 3-mm-thick Schott GG420 filter coupled to an EMI 9635 QA photomultiplier tube. Measurements were taken with an RISØ TL-DA-15 reader. A 25-mCi $^{90}Sr/^{90}Y$ built-in source was used for sample irradiation. A thick source Daybreak alpha counting system was used to estimate U and Th for dose rate calculation. Potassium was measured by ICP90, with a detection limit of 0.01%, using the sodium peroxide fusion technique at the SGS Laboratory in Toronto, Canada. Water content was assumed to be 10±5% for all samples. The single-aliquot regenerative-dose protocol (Murray and Wintle, 2000) was used to determine paleodose. A five-point measurement strategy was adopted with three dose points to bracket the paleodose, a fourth zero dose and a fifth repeat-paleodose point. The repeat paleodose was measured to correct for sensitivity changes and ensure that the protocol was working correctly. All measurements were made at 125 °C for 100 s after a pre-heat to 220 °C for 60 s. Ten to fourteen

aliquots were used for each sample. For all aliquots, the recycling ratio between the first and the fifth point ranged from 0.95 to 1.05. Data were analyzed using the *ANALYST* program of Duller (1999).

Charcoal samples were radiocarbon dated at the University of Georgia Center for Applied Isotope Studies using a National Electrostatics Corporation Model 1.5SDH-1500 kV Accelerator Mass Spectrometer, following pretreatment with an acid-alkali-acid wash and combustion to create graphite targets from CO_2 gas. Radiocarbon dates were calibrated to calendar year age using *CALIB 5.0.2* (Stuiver and Reimer, 1993); and the mid-point of the age range was converted to ages before 2009 to maintain consistency with OSL ages.

The radioactive isotope ^{137}Cs and historical records were used as age controls for post-settlement sediments. The maximum content of ^{137}Cs in the sediments represents the year A.D. 1963 (Walling and He, 1997). The ^{137}Cs content of sediments was measured by gamma spectrometry with a high purity germanium crystal system coupled with an Ortec digital spectrometer in the University of Georgia Geomorphology Laboratory, with count times of 5000 to 10000 seconds to achieve analytical errors <10%. Ages of certain sand layers were estimated by correlating the sedimentological evidence of large floods (such as 1902 and 1964 floods) with USGS gaged flood records and served as time markers for post-settlement sediments (Knox, 2006).

Statistical Analysis

The physical and chemical characteristics of sediments were compared between pre-settlement and post-settlement vertical accretion using statistical analysis. Particle sizes strongly influence the concentration of absorbed elements because finer particles have a relatively larger surface area so they can absorb more elements (Horowitz, 1991). Given the variations of sediment particle sizes, we tried different techniques to standardize the concentration of chemical elements, such as using the residual value of regression analysis on sand (63-250 μm) percentage or LOI value, or using the ratio to concentration of Ti or Al (Horowitz, 1991). Standardized data was checked for normality using the

Shapiro-Wilk method in *Stata 10*. Non-normally distributed data were transformed using log10, inverse, and square root et al. Statistical t-tests and Mann-Whitney U-tests were run to assess the differences of means of physical and chemical characteristics between pre-settlement and post-settlement sediments, for normally and non-normally distributed data separately. Discriminant function analysis (DFA) is an effective method to determine which variables differ among groups (Owens et al., 1999), so we also ran DFA to objectively screen out signature elements, whose concentrations (relative to Al) are significantly different between the two periods.

Results

Allostratigraphy

A buried A horizon (Ab), which contains more organic matter and has a darker color than the overlying most recent sediments, is prevalent in the stratigraphy of older floodplains or terraces and represents the land surface that existed prior to the time of initial European settlement (Happ, 1945; Trimble, 1964; Costa, 1975; Jacobson and Coleman, 1986; Knox, 2001; Leigh, in press (a)). Sediments above the Ab horizon were deposited from the erosive land use during the post-settlement time, and Leigh (in press (a)) established that the top of the Ab horizon represents a temporal boundary of approximately A.D. 1870 in the upper Little Tennessee valley. At all three sections, the distinct boundary between an obvious dark-colored Ab horizon and overlying sediments divided the deposits into two major allostratigraphic units. The lower unit (unit 1) represents the pre-settlement sediments while the upper unit (unit 2) represents the post-settlement sediments (Figure 2.3).

Generally the three sites have similar stratigraphic characteristics. Three facies were observed in the pre-settlement sediments of unit 1. The bottom facies (facies 1) consists of gravels and coarse sand; the gravels are mostly sub-rounded to well-rounded with diameters smaller than 1 cm, although several gravels have a diameter as large as 1.5-2 cm. The middle facies (facies 2), which has a clear boundary with the underlying facies 1, is composed primarily of medium and coarse sand, with massive

to weak blocky structure and redox features. The lower part of facies 2 at the Keener and State Line sites contains interbedded peat and sand layers. Sediments in facies 2 show a fining upward trend and gradual transitions to the upper facies (facies 3), which is primary silt clay loam and exhibits pedogenic features such as moderate fine to medium blocky structures. The top of facies 3 is the dark-colored Ab horizon. Although generally fine textured, several stratified sand layers are clear in facies 3, especially at the State Line and Riverside sites. Referring to the sediment texture and stratigraphic characters of typical floodplain deposits of meandering streams (Nichols, 1999; Bogg, 2006), the bottom facies represents the bedload deposits that are transported and deposited in the previous channel. Sediments of the middle facies are point bar deposits from lateral migration of the meander river, called lateral accretion. The upper facies represents the vertical accretion of the floodplain, which is composed of fine particles that settled out of suspension during overbank flooding, and sand layers from large overbank flood events. Therefore, we designated the three facies as 1B, 1LA, and 1VA, to represent the pre-settlement bedload, lateral accretion, and vertical accretion deposits, respectively.

Post-settlement sediments of unit 2 are composed of fine sand and silt loam, including several distinct light-colored medium and coarse sand layers. Sediments present massive, laminated and thinly bedded structure at the State Line and Riverside sites, while pedogenic features (granular and blocky structure) predominate at the Keener site. Cumulic soils have developed as evidenced by the dark-colored fine sediment layers. Roots and evidence of bioturbation are common in this unit. The upper part of the unit exhibits a coarsening-upward trend at all of the three sites. Sediments in this unit were deposited by overbank flooding after the European settlement and thus were designated as post-settlement vertical accretion (unit 2VA).

The exact depth of stratigraphic boundaries was defined based on the visual observation and quantitative results of sediment analysis (Figure 2.3). The pre-settlement/post-settlement boundary was delineated on the top of the most pronounced Ab horizon. Hurst color index and LOI values also

distinguished the boundaries (Figure 2.3). The exact depth of the boundary between pre-settlement lateral and vertical accretion was defined primarily on the results of particle size analysis. Statistics of particle size distributions, such as mean, sorting (standard deviation), skewness, kurtosis, D90, and percentage of sand fractions were plotted against depth, as shown in Figure 2.3. The lateral accretion is dominated by medium and coarse sand (>0.25 mm), while no medium or coarse sand appears in the vertical accretion deposits, except in large flood deposits or late post-settlement sediments. The distribution of particle sizes is symmetrical in the lateral accretion deposits but left-skewed in the vertical accretion deposits. Mean and D90 of lateral accretion and vertical accretion deposits are different across the three sites, but they all clearly show larger values in lateral accretion sediments than in vertical accretion sediments. Although kurtosis of particle size distribution clearly differentiates the vertical and lateral accretion at the Keener site, with lateral accretion leptokurtic and vertical accretion mesokurtic, such distinctions at the State Line and Riverside sites are not significant. At all three sites, the lateral and vertical accretion sediments are poorly sorted, so sorting (standard deviation) does not differentiate the two units. Therefore, we used the percentage of >0.25 mm particles, mean, D90 and skewness of particle size distribution to delineate the lateral and vertical accretion boundary. Based on these criteria, the pre-settlement lateral/vertical boundaries at the Keener, State Line and Riverside sites are at depths of 95 cm, 290 cm and 200 cm, respectively (Figure 2.3).

The thickness, sediment color, and texture of each stratigraphic unit varied across the three sites. The post-settlement deposit at the Keener site is much thinner than at the State Line and Riverside sites; visually, the sediments at the Keener site are darker and finer than at the State Line and Riverside sites. The t-test of mean, D90, and percentage of sand between the two allounits did not show much difference at two of the three sites. As shown in Table 2.1, the sediments of unit 2VA are significantly coarser than sediments of unit 1VA at the Riverside site, but no significant difference exists between the two periods at the Keener and State Line sites. Particularly, at the Keener site, mean of

these particle size parameters of pre-settlement sediments has higher values than post-settlement sediments (Table 2.1). Generally, however, at all three sites, the deposits of pre-settlement vertical accretion exhibit a fining-upward trend while post-settlement vertical accretion deposits show a coarsening-upward trend (Figure 2.3).

Chronology and Depth-age Model

Radiocarbon and OSL age results are shown in Table 2.2 and 2.3. Compared with the OSL ages and previous non-charcoal radiocarbon ages, the two new radiocarbon ages from charcoal (SL Mono 206 cm and RS Mono 200 cm) are obviously too old. This charcoal may have been derived from reworked sediments so their ages are considered unreliable. Previous radiocarbon ages (from Price and Leigh, 2006 and Leigh, 2007) and new OSL ages were used, and the depths of previous radiocarbon ages were adjusted to the new sections based on stratigraphic correlations (Table 2.2 and Figure 2.3). Based on these dates, the long-term average lateral accretion rates were 3.75 mm/yr at the Keener site and 3.67 mm/yr at the Riverside site. Since the two rates were very close, it is reasonable to assume that the State Line site, which is spatially between the Keener and the Riverside sites, had a similar lateral accretion rate (using 3.71 mm/yr, the average of the two). Thus, the age of pre-settlement lateral/vertical accretion boundary of each site was calculated based on the assumption of constant and relatively fast lateral accretion rates.

The population, agriculture, logging and mining activities in this region significantly increased circa A.D. 1870, which is a reasonable date for the pre-settlement/post-settlement boundary atop the Ab horizon, as indicated by Leigh (2007, in press (a)), and thus is used here to separate allostratigraphic units 1 and 2.

A post-settlement age of A.D. 1963 was expected from the ^{137}Cs peak content, but given the leaching of ^{137}Cs peak concentration in the profile (Walling and He, 1997) and the evidence of bioturbation in the upper part of post-settlement sediments, we decided to use the sedimentological

record of the 1964 flood as an age marker for post-settlement vertical accretion. The 1964 (October 4, 1964) flood is the largest flood recorded at the Prentiss gaging station and left an obvious sedimentary bed, evidenced by the pronounced increase of sand fraction in the profile (see Chapter 3). Additionally, the depth of this sedimentological record is very close to the depth of peak concentration of ^{137}Cs, giving us confidence in assigning the basal depth of this sand layer an age of 1964. The depth of A.D. 1964 of each site is shown in Figure 2.3.

At the State Line site, another post-settlement age control came from the historical record. Railroad grade materials were found in a nearby core at 23.5 cm above the Ab horizon and were believed to have an age a few years earlier than 1905, the year the railway reached the state line (D.S. Leigh, personal communication). In addition, there was a large flood in 1902, which was the largest recorded at the Judson gaging station (location shown on Figure 2.1). Based on the stratigraphic correlation of the two cores and sedimentological record of the 1902 flood, the sandy layer at 16 cm above the buried soil horizon (at the depth of 144 cm) was assigned an age of A.D. 1902 (Figure 2.3).

We expressed the depth-age relations of vertical accretion by power functions. Given that under natural conditions with little human disturbance, overbank sedimentation rates decrease with time as the floodplain surface builds up (Wolman and Leopold, 1957), we found the power relationship between average floodplain overbank sedimentation rate (R, in cm/yr) and the deposition time (t, in year) proposed by Bridge (2003) to be the best way to model this concept. Therefore, we adopted Bridge's (2003) quantitative expression ($R=10t^{-0.33}$) and adjusted the constant and exponents to fit our depth and age data for pre-settlement vertical accretion. The power function curves with exponents smaller than 1 turned out to fit the data quite well ($r^2=0.99$) (Figure 2.4). Because human impact during post-settlement time became important, Wolman and Leopold (1957)'s concept is not as valid. Linear, power, and exponential functions were tried on the depths and ages of post-settlement vertical accretion, and the power functions with exponents greater than 1 were the best fit to the data ($r^2=0.99$)

(Figure 2.4). As a result, based on the chronology and concept of floodplain sedimentation, we used non-linear power functions to model the depth-age relationship of vertical accretion, separately for pre-settlement and post-settlement periods.

Sedimentation Rates

The sedimentation rates R (cm/yr) were derived from the depth-age model in the form of power functions with deposit time t (years) (Table 2.4). The exponents of the functions are negative for pre-settlement vertical accretion and positive for post-settlement vertical accretion. The long-term average overbank sedimentation rates (thickness/time) at different time intervals were also calculated (Table 2.5), and found to vary across the three sites. The State Line site had the highest rates for both post-settlement and pre-settlement time; the lowest post-settlement rate was at the Keener site; and the lowest pre-settlement rate was at the Riverside site. However, broadly similar trends exist at all three sites. Post-settlement (A.D. 1870-2009) long-term average sedimentation rates were 3-12 mm/yr, and about one order of magnitude greater than pre-settlement (Before A.D. 1870) rates, which were less than 1.2 mm/yr. For the two periods within post-settlement time, long-term average sedimentation rates after A.D. 1964 were nearly twice as large as those before A.D. 1964 (Table 2.5).

Special attention was paid to the sedimentation rates during the MWP and the LIA. Although the onsets and terminations of these periods varied from region to region (Hughes and Diaz, 1994; Bradley and Jones, 1995; Bradley et al., 2003), it is generally accepted that the maximal range for the periods are from A.D. 800 to A.D. 1300 for the MWP, and from A.D. 1400 to A.D. 1800 for the LIA (Grove, 1988; Grove and Switsur, 1994). The depth and thickness of deposits during the two periods were determined using the pre-settlement depth-age model and then sedimentation rates were calculated. The MWP appears to have slightly higher sedimentation rates than the LIA (Table 2.5).

Chemical Characteristics and Signature Elements

Besides the physical characteristics of sediments such as sediment texture and sedimentation rates, we also looked for the chemical distinctions between the vertical accretion facies of the pre-settlement versus post-settlement allounits with statistical analysis. Both the residual value of regression on sand (63-250 μm) percentage and the ratio to Al well represented the difference between the two periods. However, considering the small r^2 (could be as low as 0.01) of the regression analysis of some elements, and the fact that Al is a good proxy for the aluminum-silicate clays that constitute most of the adsorption surface (%Al and %clay correlation coefficients are 0.87, 0.87, and 0.81 for the Keener, State Line and Riverside sites, respectively), we used the ratio to Al in the statistical analysis to eliminate particle size influences.

DFA was run on log10 transformed data at each site, and expected to pick up signature elements, elements that differ significantly between post-settlement and pre-settlement sediments, but the results were not satisfactory. As shown in Table 2.6, no single element contributed the same to the differences between post-settlement and pre-settlement sediments at all three sites. For example, log P has a negative contribution at the Keener site but positive contributions at both the State Line and Riverside sites; contribution from log Ti is most negative at the Keener site but most positive at the State Line site (Table 2.6). The unsatisfactory result of DFA probably resulted from the non-normal distribution of the majority of the data and the high correlation between these variables.

Mann-Whitney U-test on the chemical data (ratio to Al) identified four elements (Ca, Hg, P, Pb) that are significantly different (99% confidence level) between the two units at two of three sites, and all the four elements have higher concentrations (relative to Al) in unit 2VA than in unit 1VA at all three sites (Table 2.7). We also plotted the chemical data (ratio to Al) against depth to examine the down-core trends of each element visually (Figure 2.5). Ca/Al and P/Al have similar trends that they have consistently low values throughout the vertical accretion, but increase significantly at the surface of unit

2VA (Figure 2.5). Hg/Al of sediments in unit 2VA presents different trends at the three sites. It increases steadily from the bottom of the unit up to the surface at the Keener site, but keeps a high value at the State Line site. At the Riverside site, the value is low at the bottom of unit 2VA, increases to a peak in the middle, and then decreases at the surface (Figure 2.5). Pb/Al shows a similar trend to Hg/Al at all three sites. In addition to the four elements identified by the U-test, we found the trend of K/Al with depth to also showes significant changes between the two units. Generally, the K/Al decreases upward in unit 1VA but increases upward in unit 2VA, with the lowest value at or near the pre-settlement/post-settlement boundary at all three sites (Figure 2.5). Therefore, five elements, Ca, Hg, K, P, and Pb, were identified as signature elements that differentiate the two units.

Discussion

Allostratigraphy

Accurate identification of allostratigraphic unit boundaries is crucial because it affects the determination of boundary ages and the calculation of sedimentation rates. We defined the pre-/post-settlement boundary mainly by referring to the Ab horizon, but this boundary is also reflected by the Hurst color index and LOI values. The Hurst color index is a good indicator of iron content in the sediments (Hurst, 1977), but here we used it to represent the soil color quantitatively, with darker colors having larger values. The Hurst color index value appears as an obvious change in the boundary with higher values below the boundary and lower values above the boundary (Figure 2.3). Generally, the LOI values represent organic matter content, in that the values are relatively higher in Ab horizons. However, clay and oxide content seems to have affected the LOI value as well. The relatively high LOI values of the lower part of unit 2VA at the State Line site and the middle part of unit 2VA at the Riverside site probably are the result of finer particles and higher content of clay mineral and oxides in these sediments.

For the pre-settlement lateral accretion/vertical accretion (unit 1LA/1VA) boundary, observations of sediment color and texture alone were insufficient. Fortunately, the high-resolution particle size information helped to determine the exact depth of the boundary. Overbank sediment texture is directly controlled by the suspended materials in the floods, which are influenced by the flood magnitude and vegetation cover (Lecce et al., 2004). The maximum particles in suspension typically is 0.5 mm and overbank sediments are predominantly clayey silt and fine sand with small amounts of medium sand from high-magnitude flood events (Alexander and Fielding, 2006; Heitmuller and Hudson, 2009). The suspended sediment particle size data from Little Tennessee River at Riverside also support shows that suspended sediments are smaller than 0.5 mm (Oblinger, 2003). Therefore, we had intended to use the appearance of particles larger than 0.5 mm as the criterion to define lateral/vertical accretion boundary. However, our particle size results showed similar trends for the percentage of >0.25 mm and >0.5 mm, and because the percentage >0.5 mm particles are generally very low, the distinction between lateral and vertical accretion was much clearer in terms of >0.25 mm fractions (Figure 2.3). Thus, we used the percentage of > 0.25 mm as the criterion. Compared with vertical accretion, lateral accretion has a clear increase of percentage of >0.25 mm with depth. The vertical accretion layers that contain particles larger than 0.25 mm appear to be deposits from high-magnitude overbank flooding.

The coarsening-upward trend of the late post-settlement vertical accretion possibly results from three factors. First is lateral migration of the channel and levee progradation. As the channel shifts laterally, sediments on the cutbank side are eroded. The newer sediments on top of the cutbank are generally coarser than the underlying sediments because the deposition is closer to the channel (Lecce, 1997; He and Walling, 1998). Second, the source sediments may be getting coarser. Sediments in the drainage basin may have come primarily from slope erosion in the upland soil (Glenn, 1911). Early post-settlement erosion removed much of the fine surface soils, causing later erosion to erode relatively

coarser underlying saprolite from gullies (Leigh and Webb, 2006). The third factor relates to land use changes during post-settlement time. The change from forest to pasture and urbanized land may have increased surface runoff and produced larger flood discharges that were able to transport and deposit coarser sediments during overbank floods (Knox, 2001; Sutherland et al., 2002; Chin, 2006). It is not clear which one of the three factors contributed most, and all of them may have played a role in the coarsening-upward trend.

Depth-Age Model

A proper depth-age relationship is important in determining sedimentation rates over time. Although we used a linear thickness-time relation for lateral accretion, the non-linear power relationship worked much better for vertical accretion. The power curves best fit the data, and in addition, the power functions clearly separate the pre-settlement and post-settlement vertical accretion units. The pre-settlement sedimentation rates derived from the pre-settlement depth-age model have negative exponents, indicating a decreasing sedimentation rate over time. This agrees with Wolman and Leopold's (1957) concept that under natural conditions with little human disturbance, overbank sedimentation rates decrease with time as floodplain surface builds up. As a result, although the two pre-settlement ages at the Keener and Riverside sites can fit any kind of function curve, we believe the power functions work best here, given the theoretical basis and great fit at the State Line site.

On the contrary, the post-settlement rates derived from the post-settlement depth-age model have positive exponents, indicating an increasing vertical accretion rate with time. This makes sense given the natural levee progradation during late post-settlement time, and the recently intensified human impacts related to second-home reconstruction and population growth in the region, especially after the 1970s (Leigh, 2007).

The depth-age model assumed that vertical accretion was continuous and gradual. However, flood deposits have spatial and temporal variations depending on the floodplain geomorphology, flood

magnitude, suspended materials concentration, and vegetation (Walling, 1995; Lecce, 1997; Walling and Fang, 2003). The actual depth-age relationship is more complicated than the model suggests. More age controls may help us better understand the depth-age relationship, but given the available dates, and the high r^2 value (r^2=0.99), we think the model works well, and are confident with the depth range of the MWP and the LIA derived from the model.

Sedimentation Rates

As mentioned above, the sedimentation rates derived from the depth-age model demonstrated the differences between floodplain sedimentation in pre-settlement and post-settlement time, but the specific values of long-term-average rates made it even easier to see the differences. Spatial variations of sedimentation rates across the three sites reflected the differences of geomorphic conditions, although the low pre-settlement sedimentation rate at the Riverside site might be largely due to the long deposition time. The higher sedimentation rates during the MWP than during the LIA may have resulted from a wetter MWP (Stahle et al., 2003; Liang, 2008) with more overbank flooding and sedimentation (Chapter 3). However, as pre-settlement sedimentation rates decreased with time as a power function, and since the MWP was before the LIA, the higher MWP rate might just be the result of inherent processes of overbank accretion. Thus, the effects of climate change on sedimentation rates are unclear, due to the complicated relationship between climate, floods, sediment yield and overbank deposits (Gomez et al., 1995; Lecce et al., 2004; Leigh and Webb, 2006). However, the order of magnitude greater post-settlement overbank sedimentation rates is consistent with studies in other regions (Lecce, 1997; Benedetti, 2003; Lichtenstein, 2003; Knox, 2001, 2006; Leigh and Webb, 2006), and it is most likely related to human impacts during post-settlement time that accelerated erosion and sedimentation rates.

Human impact in the upper Little Tennessee River basin could date back to the Late Archaic Period (ca. 3000 years ago). Although Native Americans were present in the area, they had

comparatively little influence on the environment with practices such as limited forest clearance and subsistence crop cultivation (Hudson, 1976; Delcourt et al., 1986; Delcourt and Delcourt, 2004). After the Euro-American settlement, human impact intensified. Although agricultural practices were not as significant as in other areas, clearing-cutting for timber harvest was intensive and row-crop agriculture also occurred during the late 19th and early 20th century (Harden, 2004). These practices accelerated soil erosion on slopes and sedimentation in valleys, as noted by Glenn (1911), leading to downstream floodplain aggradation. The federal acquisition of Appalachian land in 1911 established national forests and regulated development on federal land (Yarnell, 1998; Harden, 2004), but human disturbance on private land persisted in the form of forest clearing, agriculture, urbanization, and road construction (Price and Leigh, 2006). Especially beginning in the 1970s, as more people migrated to this area (Figure 2.6), the exurban development of second-homes and road building occurred on high relief areas of the basin (Leigh, 2007; in press (b)). These disturbances from human activities led to accelerated soil erosion and hillslope failures, which provided substantial amounts of sediments to floodplains (Leigh and Webb, 2006; Knox, 2006), resulting in the significant increases of post-settlement vertical accretion rates.

Signature Elements and Human Activities

Since there is no single element that is significantly (99% confidence level) different between pre-settlement and post-settlement periods at all three sites, we set the criterion to be significantly different at two of three sites. The five signature elements demonstrate differences of vertical accretion sediments between the two periods, either by statistical analysis or by observations of the down-core trend. All other analyzed elements that were not picked up also logically had no relation to human activities.

Although the mean values of K/Al are not significantly different between the two periods, the down-core trend clearly shows the distinction. Because the Al concentration does not change much in

pre-settlement sediments (Figure 2.5), the decreasing-upward of K/Al probably reflects the pedogenesis and weathering of potassium-bearing minerals occurring before Euro-American settlement. The degree of weathering strengthens within the epipedons of pre-settlement floodplain surface so that the concentration of K and thus the K/Al value decrease. In contrast, the post-settlement sediments have not been heavily weathered due to the short time. The increasing value of K/Al in post-settlement sediments, to a certain extent, probably is related to the decreasing concentration of Al in relation to the coarsening-upward trend of sediments with fewer aluminum-silicate clays, but other factors also contributed to the increase. The sediments eroded from the weathered (potassium-depleted) epipedons on uplands and hillslopes provided the main supply to floodplains during early post-settlement time (Glenn, 1911). In contrast, the upper post-settlement sediments may have resulted from the later erosion of gullies cutting down into potassium-enriched saprolite. Therefore, a change of sediment source may have contributed to the increase in K/Al values in recent time. In addition, since K is an important element for plant growth, the use of potash as fertilizer on farmland, pastures and household lawns and gardens (Messick et al., 2001) provides additional K into soils, possibly contributing to the increase of K/Al as well.

Although the decreases of Al concentration may partly explain the increase of Ca/Al and P/Al in the upper post-settlement sediments, the increase of the ratio values is substantial, especially considering the coarse particle sizes. This probably indicates an extra input of Ca and P into the late post-settlement sediments. Soils in the southern Blue Ridge Mountains are generally acidic, so farmers and homeowners apply lime in order to reduce soil acidity (Messick et al., 2001). In addition, phosphate is widely applied to farmland, pastures, and hay fields as fertilizer to increase agricultural production (Messick et al., 2001). Therefore, the addition of Ca and P in late post-settlement sediments probably is related to the fertilizer use and lime input from agricultural activities.

Mercury was used extensively in gold mining in the Blue Ridge Piedmont to amalgamate and recover gold from sluices and stamp mills (Pardee and Park, 1948). Much of the mercury was transported and reworked by fluvial process, and is currently stored in overbank sediments (Leigh, 1994, 1997). Some mercury has been added to the atmosphere (Nriagu, 1994), making atmospheric fallout another important source of mecury to soils. Although there were no major gold mining operations near the study sites and only one mine location was recorded within the study area (Otto Zn-Cu mine), because the area lies in the region of gold-bearing rock in the southeast United States (Pardee and Park, 1948), scattered gold mining (mostly prospecting) was active during the early post-settlement time in the late 1800s and early 1900s (Robinson et al., 1992). Located in the upper headwaters, the Keener site probably was least affected by the gold prospecting, but the State Line and Riverside sites might have been more affected given the contributions from several different tributaries. The increase of Hg/Al in post-settlement sediments at the Keener site may be explained by the decreasing of Al concentrations and the addition of mercury into the sediments from atmospheric fallout (Nriagu, 1994). In the lower part of post-settlement sediments at the State Line site and in the middle part of post-settlement sediments at the Riverside site, the Hg/Al values are comparatively high even though the concentrations of Al are relatively high. This indicates additions of Hg to these sediments, which probably is related to the gold mining activities. Although extensive mining ended in the 1940s (Robinson et al., 1992), the channel migration and cutbank erosion could have reworked the sediments and redistributed the mercury in the watershed (Leigh, 1997), so the Hg/Al values remains relatively high.

Lead was a minor associate of the gold ore in the gold-belt, so the lead mining was also active in the region during the early post-settlement time (Eller, 1982; Robinson et al., 1992). Similarly to Hg, the increase of Pb content in post-settlement sediments may be related to mining activities and atmospheric fallout. Moreover, with the regional development, more and more automobiles came into

use, consuming gasoline. Both the North Carolina and Georgia highway use of gasoline rose steadily since the 1950s, and especially after the 1980s (Figure 2.7). Lead has been blended with gasoline since the early 1920s and automobile exhaust emission was an important source of lead pollution to the air and water. Even though the United States Environmental Protection Agency (U.S. EPA) began regulating lead content in gasoline in 1973, leaded fuel was still available until the Clean Air Act became effective in 1996 (U.S. EPA, 1996). The use of leaded gasoline by automobile probably introduced more Pb into the soils during post-settlement time. Even if the lead pollution from gasoline use decreased after the 1970s, the reworking of sediments and the redistribution of Pb in the watershed may have maintained Pb at higher levels in the overbank sediments.

Justification of Anthropic Signatures

In spite of the geomorphic and sedimentologic variability of the three sites, the physical and chemical characteristics of floodplain overbank sediments showed significant differences between post-settlement and pre-settlement periods. Therefore, post-settlement vertical accretion is differentiated from pre-settlement vertical accretion based on the clear buried A horizon, sedimentation rates, sediment textures, and the signature elements. Post-settlement overbank sedimentation rates increased with time while pre-settlement rates decreased with time, and the long-term average sedimentation rates during post-settlement time were one order of magnitude greater than that during pre-settlement time. The pre-settlement vertical accretion has a fining-upward trend, but the post-settlement vertical accretion shows a coarsening-upward trend. Concentrations (relative to Al) of signature elements in post-settlement sediments were significantly higher than in pre-settlement sediments. As a result, when identifying the Ab horizon is difficult due to coring disturbance or flood scouring (Happ, 1945), these physical and chemical characters provide other indicators for dividing the two periods.

We designated sedimentation rates and the five signature elements as anthropic signatures to indicate human influences. However, changes in sedimentation rates and sediment textures were not caused solely by human activities. The autogenic process of floodplain development, such as natural levee progradation following channel lateral migration, was at least partly responsible for the increased sedimentation rates and the coarsening-upward trend in the upper post-settlement sediments at the State Line and Riverside stream bank sites. The annual precipitation at the Little Tennessee River during the past 100 years did not show a clear trend of increase or decrease (Leigh, 2007), but the frequency of high-magnitude floods did increase in the past several decades according to gaging records from the Prentiss and Judson gages on the Little Tennessee River (Chapter 3). More large floods contribute to the increased sedimentation rates as well (Knox, 2006; Leigh and Webb, 2006). However, the change of flood regime possibly is related to changes in land use, which yield more surface runoff with the same amount of precipitation. Multiple factors are acting on the fluvial system and it is difficult to separate human impacts from natural influences. However, given the substantial changes and their relationship with human activities, and referring to the descriptions in Glenn (1911), we believe that direct human impacts played a very important role and overshadowed all other factors during post-settlement time. Therefore, these anthropic signatures appear to be good indicators of human influence.

Conclusion

The physical and chemical characteristics of floodplain vertical accretion sediments at three sites in the upper Little Tennessee River valley showed great differences between post-settlement and pre-settlement sediments in terms of sedimentation rates, sediment texture and the chemical element concentrations. Post-settlement sedimentation rates decreased with time while post-settlement sedimentation rates increased with time, and the long-term average sedimentation rates during post-settlement time were about one order of magnitude greater than those in pre-settlement time. Generally, the pre-settlement vertical accretion showed a fining-upward trend but post-settlement

sediments showed a coarsening-upward trend. The chemical analysis identified five signature elements with significantly higher contents (relative to Al) in post-settlement sediments (Ca, Hg, P, Pb) or with different downcore trend between the two periods (K). The significant differences and substantial changes between the two periods likely were related to intensified human impacts, such as timber harvest and gold mining during early post-settlement time, agricultural and home fertilizer use, and land clearing for urbanization after the 1970s. Even though the autogenic process of floodplain development and climate changes in the recent decades also accounted partly for these changes, direct human impacts overshadowed these factors. Therefore, we designated sedimentation rates, sediment texture and five elements (Ca, Hg, K, P, Pb) as anthropic signatures, the manifestations of human impacts on the floodplain sediments during post-settlement time.

Table 2.1. Results of t-test on particle size parameters between pre-settlement and post-settlement vertical accretion sediments

	Keener			State Line			Riverside		
	mean	**D90**	**%sand**	**mean**	**D90**	**%sand**	**mean**	**D90**	**%sand**
post-settlement	21.12	62.98	10.37	54.71	172.02	43.96	59.79	193.81	46.94
pre-settlement	23.40	65.96	12.46	52.22	140.27	44.63	37.15	101.28	31.62
P	0.3	0.62	0.49	0.55	0.14	0.78	0.0003	0.0009	<0.0001

Note: t-test was run on *Stata 10*. Null hypothesis is no difference exists between pre-settlement and post-settlement vertical accretion sediments. Reject null hypothesis when $p<0.05$.

Table 2.2. Results of radiocarbon ages.

sample	sample ID	material	$\delta^{13}C$ (‰)	$\delta^{13}C$ corrected Radiocarbon Age	CALIB (2 sigma) AD/BC [1]	Midpoint age AD/BC	cal yr before 2009
SL Mono 206cm	UGAMS#05231	charcoal	-22.2	1380±30	AD 607-680	AD 644	1366±37
RS Mono 200cm	UGAMS#05230	charcoal	-25.9	2700±30	BC 904-806	BC 855	2863±49
[2]State Line 312 cm	UGA #14480	leaf stem	-26.18	1380±40	AD 619-663	AD 641	1368±22
[2]Riverside 304 cm	UGA# 9054	leaf stem	-26.43	2530±40	BC 767-581	BC 674	2683±93
[3]Keener 200 cm	UGA# 14485	acorn	-25.79	1610±40	AD 408-514	AD 461	1548±53

Note: [1] Radiocarbon ages were calibrated using CALIB 5.0.3.

[2] ages from Leigh, 2007. Depths were adjusted to the new sections

[3] age from Price and Leigh, 2006. Depth was adjusted to the new section

Table 2.3. OSL dating results

Sample	Lab No.	U (ppm)	Th (ppm)	K (%)	Water Content (%)	Dose Rate (Gy/Ka)	Mean(Gy) Paleodose	Mean Age (Ka) (±2 sigma)	AD/BC
Riverside 200 cm	UGA09OSL-669	3.93±0.74	7.54±2.52	1.83	10±5	3.1±0.3	7.31±0.79	2.4±0.3	BC 391
State Line 225 cm	UGA09OSL-670	4.04±0.45	10.21±1.59	1.98	10±5	3.4±0.3	3.69±0.28	1.1±0.1	AD 909
Keener1c 107 cm	UGA09OSL-672	3.89±0.22	5.0±1.28	1.71	10±5	2.8±0.2	3.65±0.22	1.3±0.1	AD 709

Table 2.4. Vertical accretion sedimentation rates derived from "depth-age" model

Site	post-settlement	pre-settlement
Keener	$R=0.026t^{0.6}$	$R=0.28t^{-0.31}$
State Line	$R=0.082t^{0.64}$	$R=2.96t^{-0.59}$
Riverside	$R=0.384t^{0.2}$	$R=0.19t^{-0.26}$

Note: R=sedimentation rate (cm/yr); t=deposition time (year).

Table 2.5. Long-term average vertical accretion sedimentation rates

Age Interval	Average Overbank Sedimentation Rate (mm/yr)		
	Keener	State Line	Riverside
MWP (AD 800-1300)	0.52	1.00	0.28
LIA (AD 1400-1800)	0.35	0.50	0.25
Before AD 1870	0.46	1.11	0.34
After AD 1870	3.09	11.51	8.63
AD 1870-1964	2.45	8.83	7.96
AD 1964-2009	4.44	17.11	10.00

Table 2.6. Results of DFA on log-transformed chemical data (ratio to Al)

Keener		State Line		Riverside	
variable	**Coefficient**[1]	**variable**	**coefficient**	**variable**	**coefficient**
Mg	4.25	**Ti**	3.32	Mg	6.79
[2]**Co**	3.90	**Zn**	3.02	**V**	2.26
Cr	3.78	Cr	2.55	**P**	2.17
Zn	3.14	Mg	2.10	LOI	1.87
Sr	2.24	**P**	1.25	**Pb**	0.96
Hg	0.86	**Mn**	1.25	Mn	0.53
Sc	0.56	Ba	0.86	**Ni**	0.53
Pb	0.41	**Hg**	0.54	Cu	0.13
Ca	0.00	Sc	0.10	**La**	0.06
La	-0.13	**La**	-0.04	Cr	0.03
Cu	-0.22	Cu	-0.27	Sc	0.03
Fe	-0.22	Sr	-0.36	**Co**	-0.24
LOI	-0.99	Ni	-0.38	**Ca**	-0.70
Ni	-1.01	Pb	-0.39	Hg	-0.84
V	-1.58	Co	-0.42	**Ba**	-1.03
K	-1.69	LOI	-0.49	Sr	-1.09
Mn	-2.01	**Fe**	-0.98	**Ti**	-2.08
Ba	-2.75	Ca	-2.19	**Zn**	-2.18
P	-4.61	V	-2.69	**Fe**	-2.24
Ti	-5.31	K	-6.07	**K**	-2.47

Note: [1] coefficient is the standardized discriminant function analysis (DFA) coefficient, the larger the absolute value of coefficient, the greater contribution to the differences. The sign represents the contribution direction; positive coefficient represents positive contribution, while negative coefficient represents negative contribution.

[2] bolded letters indicate the log-transformed data were non-normally distributed.

Table 2.7. Mann-Whitney U-test of five signature elements

		Ca/Al	Hg/Al	P/Al	Pb/Al	K/Al
Keener	[1]P	0.0013	0.0027	0.0001	<0.0001	0.9424
	[2]prob	0.830	0.807	0.904	0.930	0.493
State Line	P	0.3004	<0.0001	0.0005	<0.0001	0.8466
	Prob	0.592	0.943	0.809	0.939	0.517
Riverside	P	<0.001	0.022	0.6929	0.3333	0.0003
	Prob	0.999	0.704	0.535	0.586	0.821

Note: [1] When P <0.01, reject H0 (H0 = no difference between the two periods).

[2] prob is the probability of post-settlement value is larger than pre-settlement value.

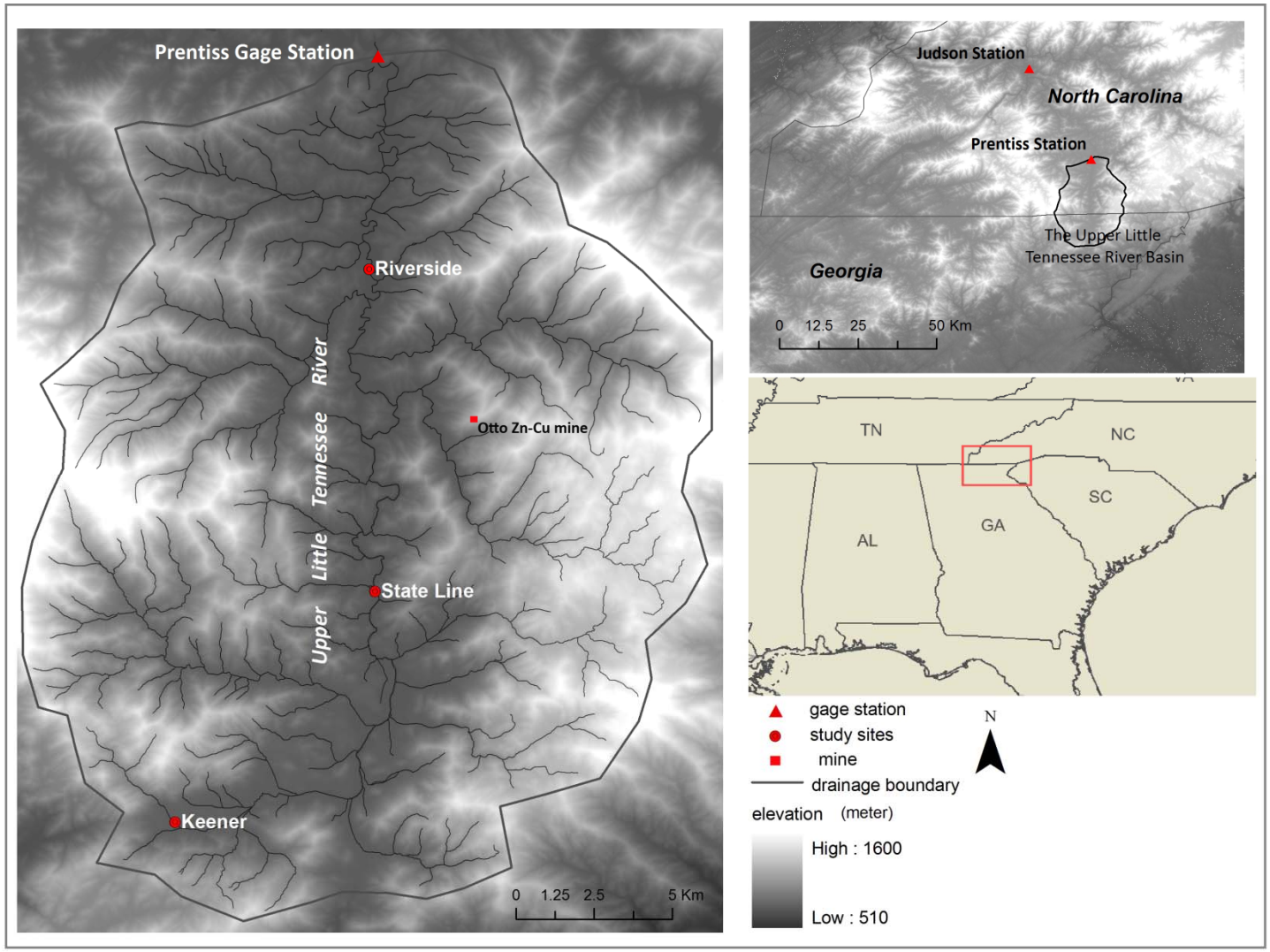

Figure 2.1. Location of the upper Little Tennessee River Valley and the three study sites.

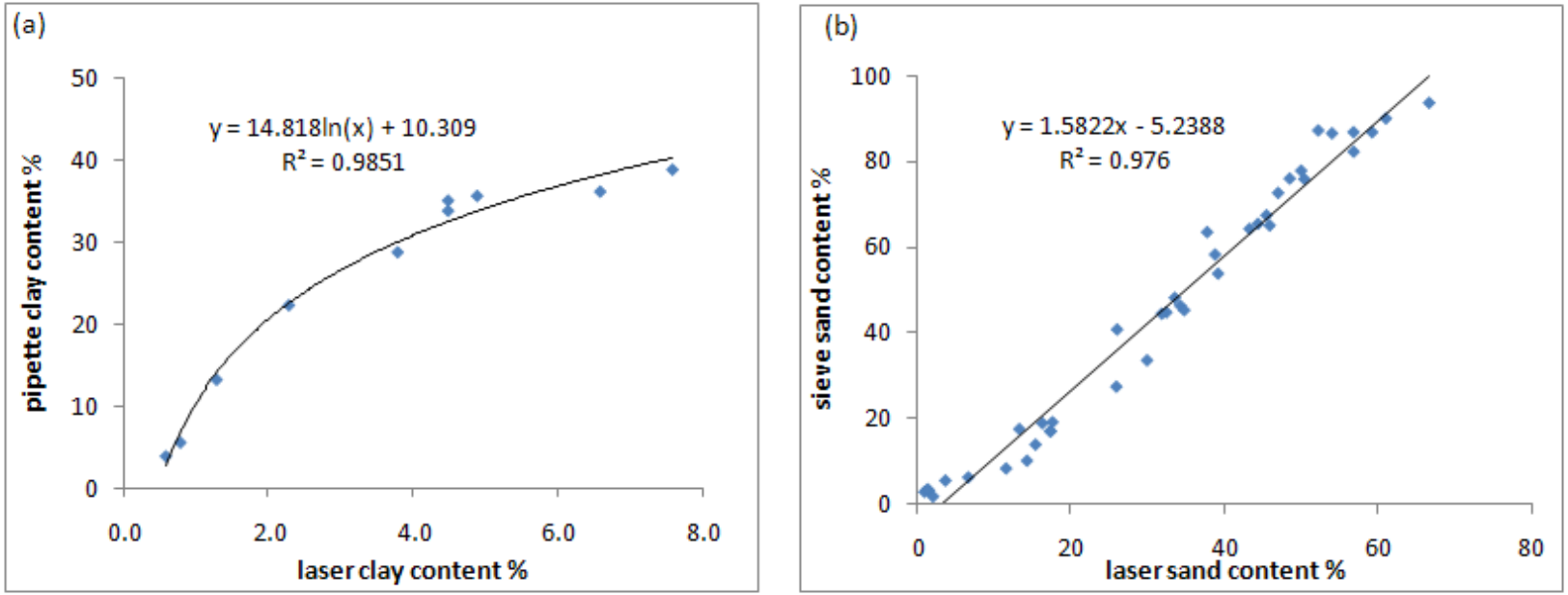

Figure 2.2. Comparison of clay and sand measurement between the CILAS laser method and traditional methods.

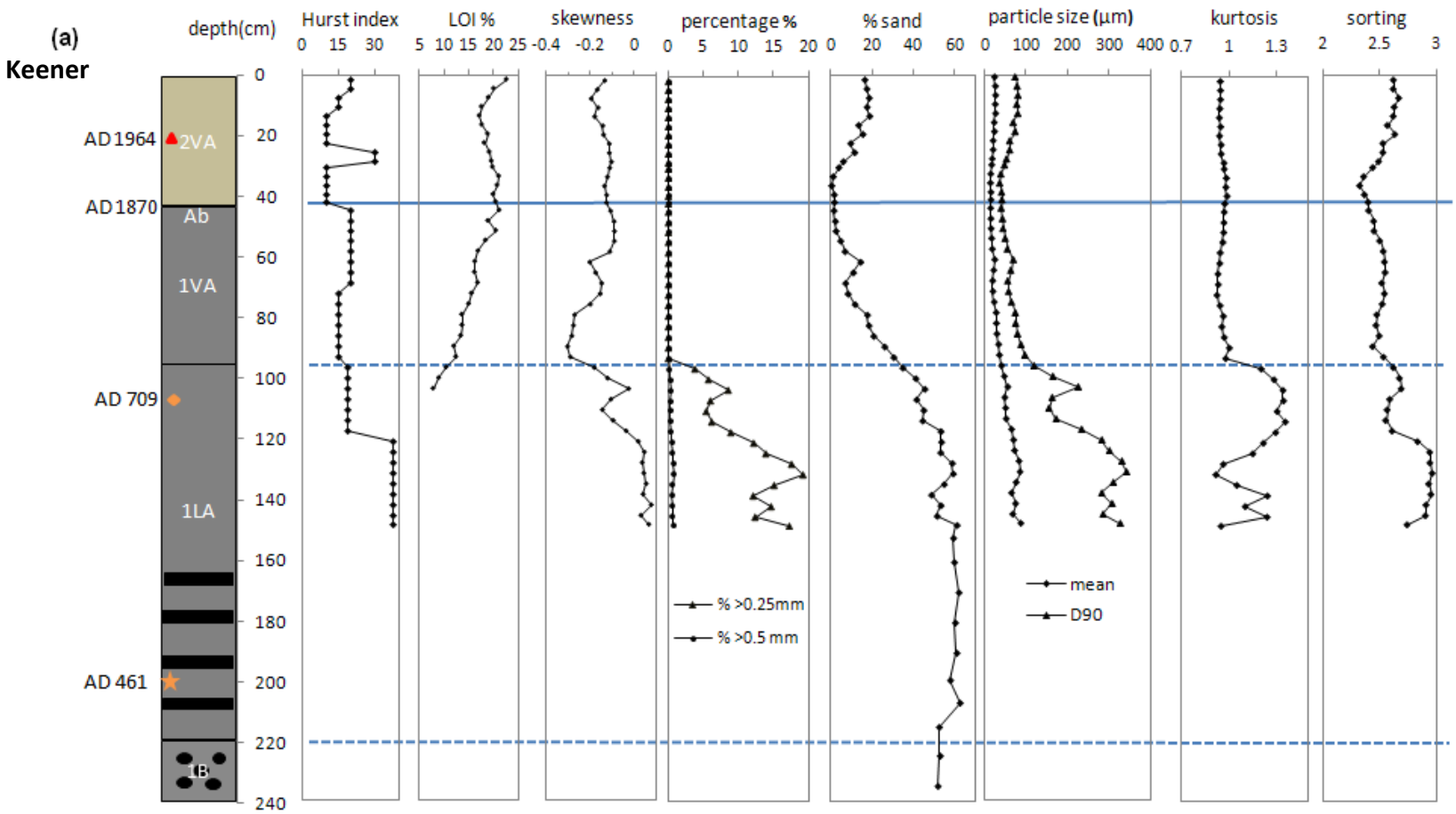

note 1: 1B: bedload
1LA: pre-settlement lateral accretion
1VA: pre-settlement vertical accretion
2VA: post-settlement vertical accretion

historic gage record
OSL date
Radiocarbon date

bedload
peat layer

Hurst index = hue*value/chroma

note 2: statistic parameters calculated based on the Folk & Ward Method (Geometric) using GRADISTAT 4.0 (Blott, 2000).
skewness: <-0.1, left skewed; -0.1-0.1, symmetrical; >0.1, right skewed
kurtosis: <0.9, platykurtic; 0.9-1.11, mesokurtic; >1.11, leptokurtic
sorting:<0.7, well sorted; 0.7-1, moderately sorted; >1, poorly sorted

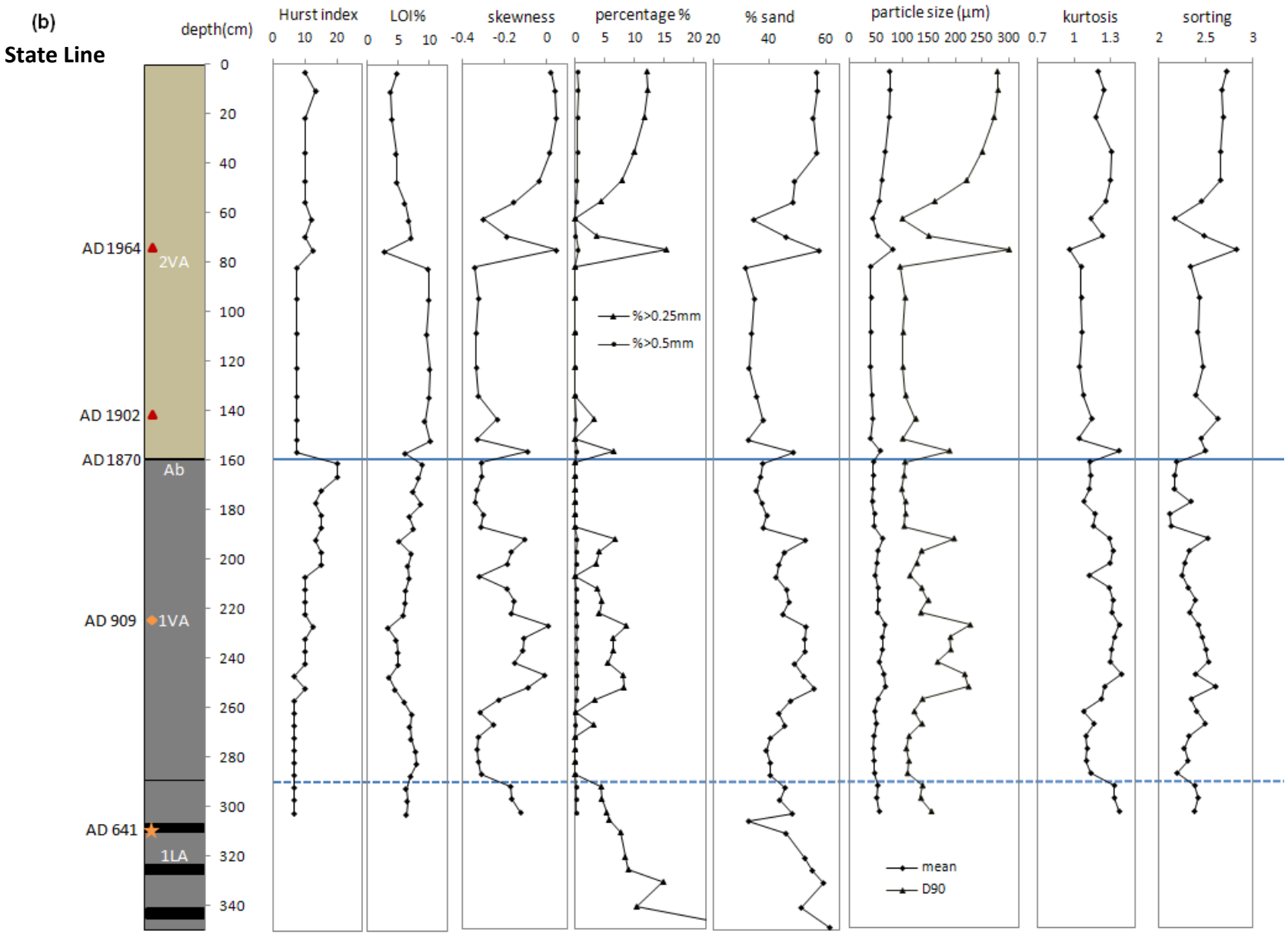
(b)
State Line
depth(cm)
Hurst index
LOI%
skewness
percentage %
% sand
particle size (µm)
kurtosis
sorting
AD 1964
2VA
AD 1902
AD 1870
Ab
AD 909
1VA
AD 641
1LA
%>0.25mm
%>0.5mm
mean
D90

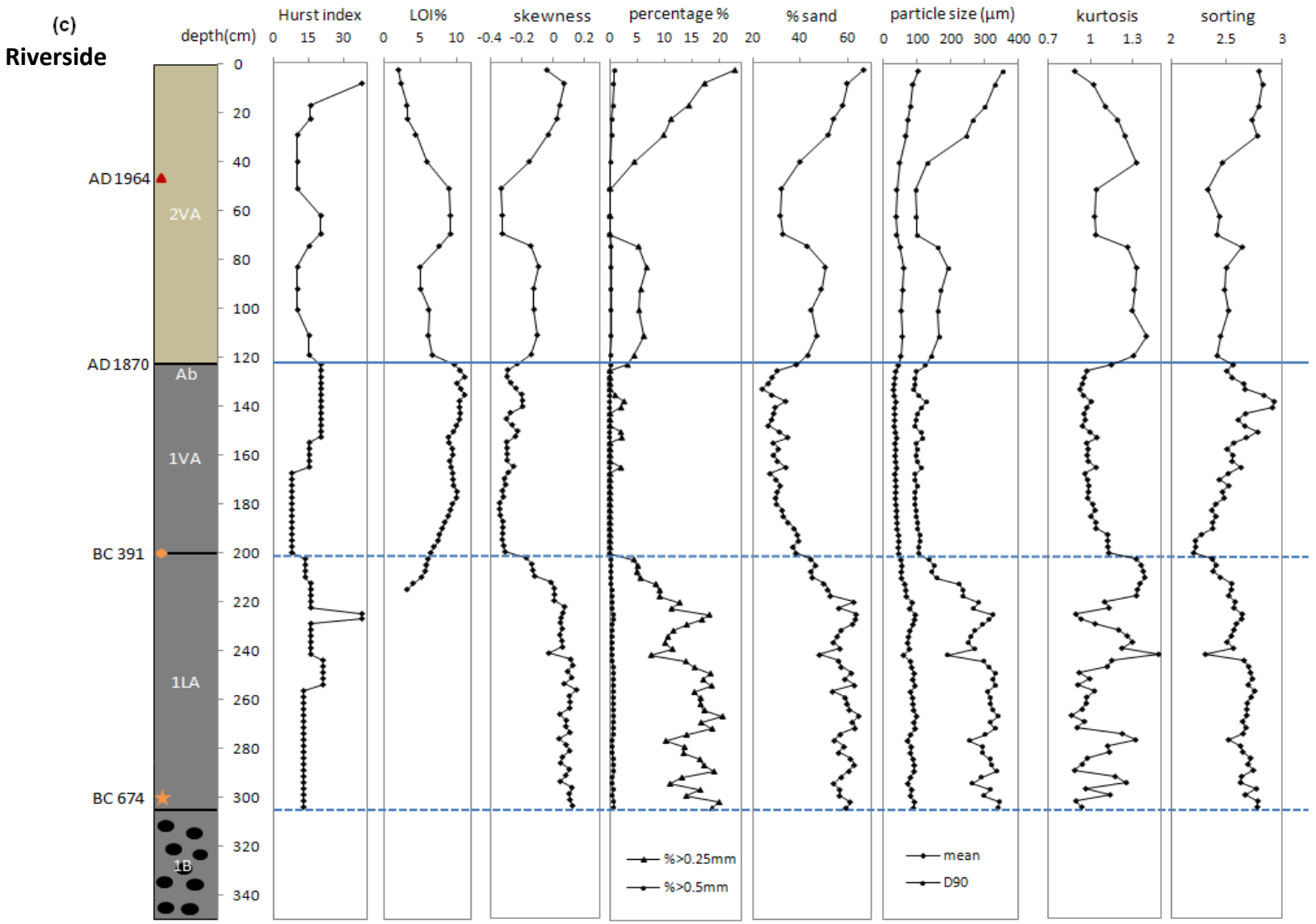

Figure 2.3. Allostratigraphic units, chronology, and physical character of sediments. (a) the Keener site; (b) the State Line site; (c) the Riverside site. Notes are shown in (a).

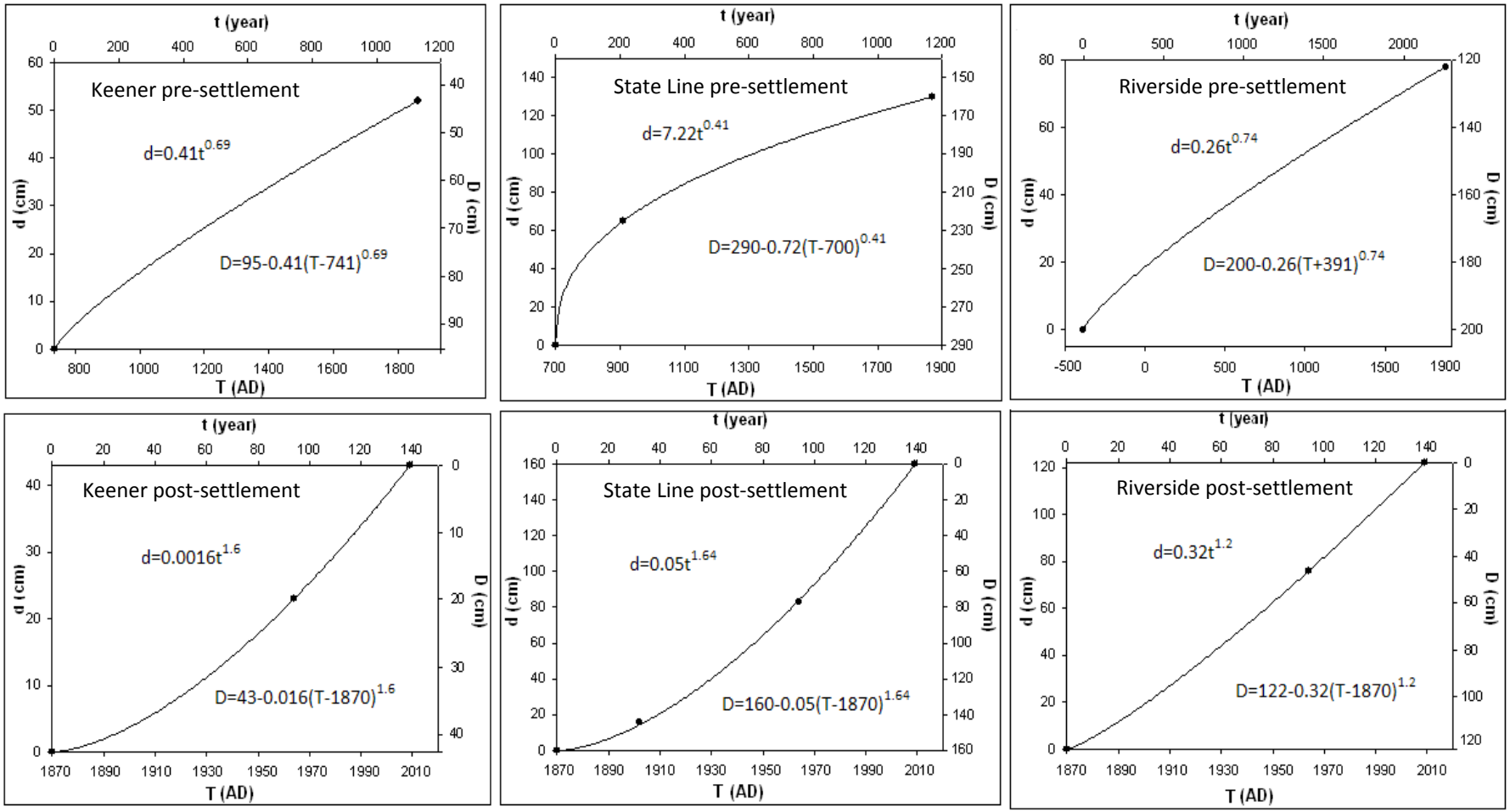

Note: d, deposition thickness; t, deposition time; D, depth below the surface; T, calendar year (AD, negative number means BC).

Figure 2.4. Depth-age curves of vertical accretion.

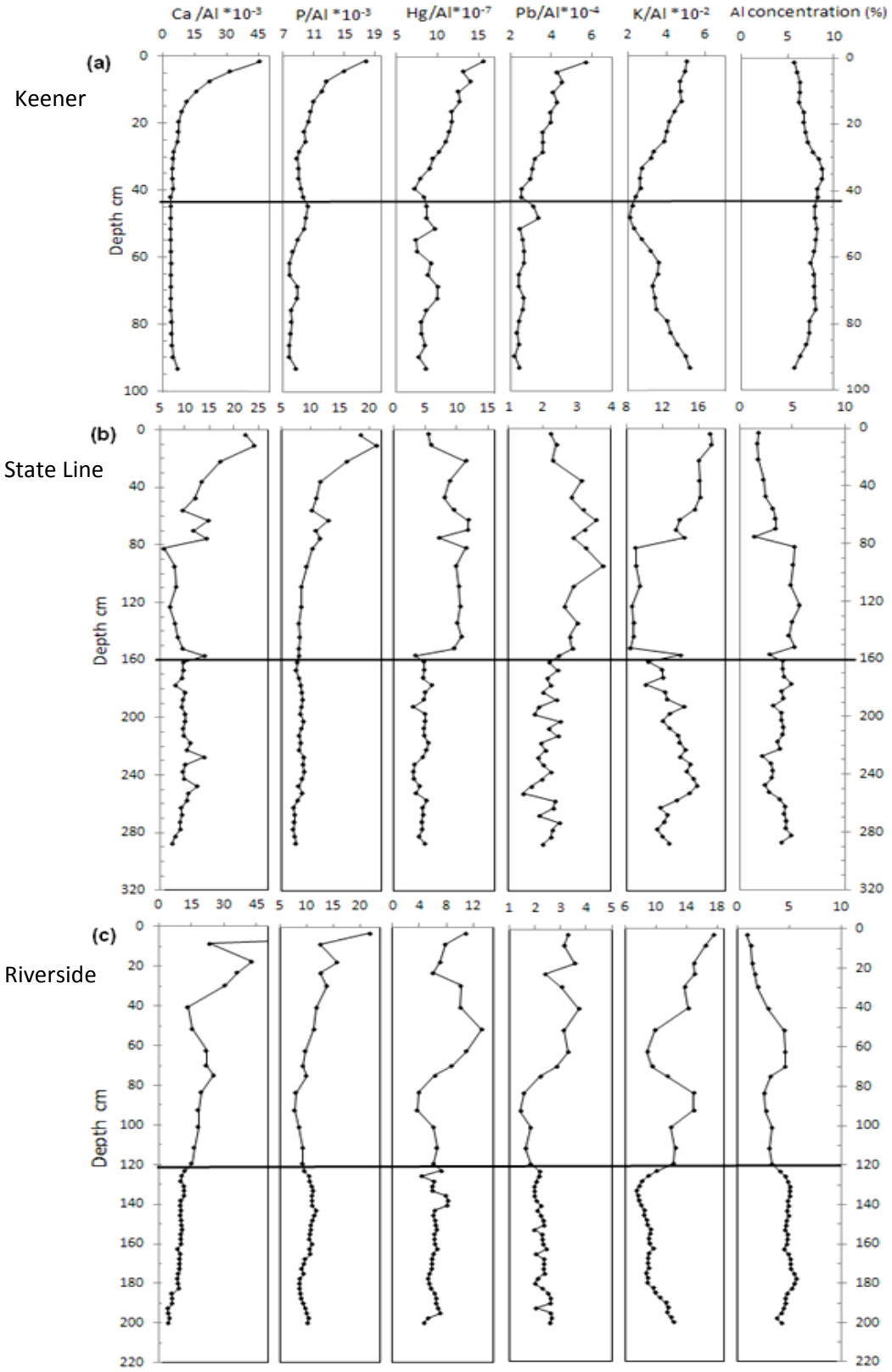

Figure 2.5. Down-core trend of five signature elements (ratio to Al) and concentration of Al. (a) the keener site; (b) the State Line site; (c) the Riverside site. The solid black line in each profile represents the boundary of pre-/post-settlement sediments, above the line are post-settlement sediment, below the line are pre-settlement sediments.

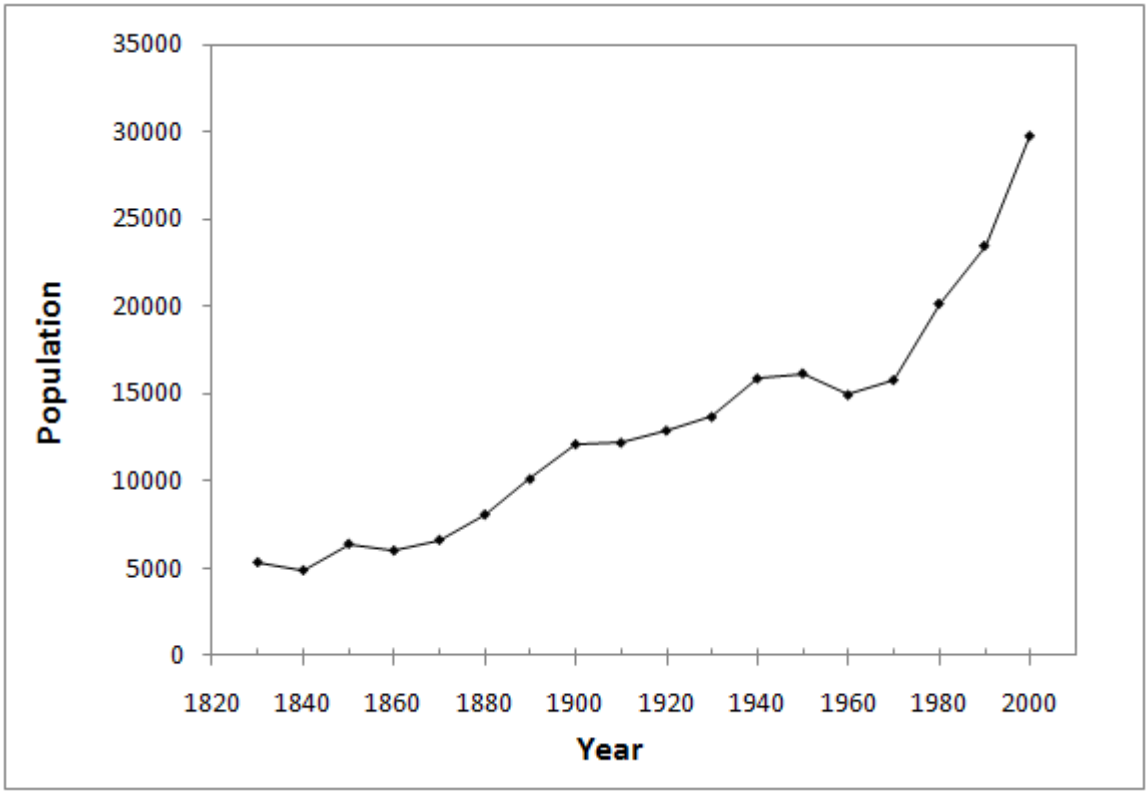

Figure 2.6. Historic population in the Macon County, North Carolina.

Data source: 1830-1960 (http://mapserver.lib.virginia.edu/php/newlong3.php); 1960-2000 (http://www.census.gov/population/www/censusdata/cencounts).

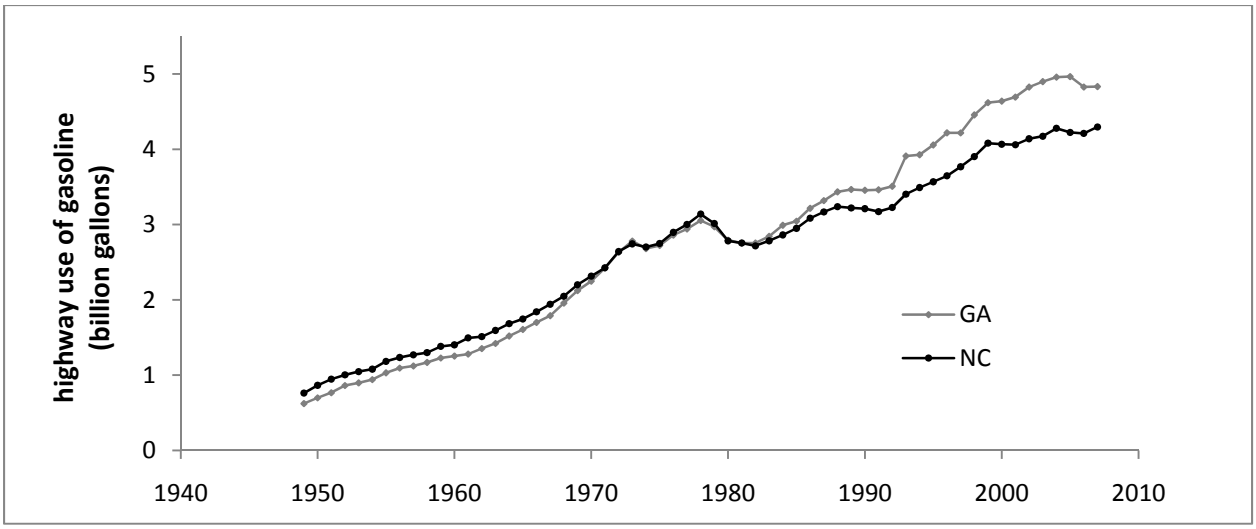

Figure 2.7. Highway use of gasoline in Georgia and North Carolina.

Data are from U.S. Department of Transportation Federal Highway Administration Highway Statistics (http://www.fhwa.dot.gov/policy/ohpi/qffuel.cfm)

CHAPTER 3

LATE HOLOCENE PALEOFLOODS IN THE UPPER LITTLE TENNESSEE RIVER VALLEY, SOUTHERN BLUE RIDGE MOUNTAINS, USA[1]

[1] Wang, L., Leigh, D.S. To be submitted to *The Holocene*.

Abstract: A paleoflood history during the past 2000 years was reconstructed by analyzing floodplain overbank sediments in the upper Little Tennessee River valley, within the southern Blue Ridge Mountains. Distinct buried A horizons and organic matter contents defined the boundary of pre-settlement and post-settlement vertical accretion. Radiocarbon and luminescence dates were used for pre-settlement age control, while ^{137}Cs and historical records provided age control for post-settlement time. Particle sizes were measured in 3-14 cm intervals using an automatic laser analyzer. The sedimentological characteristics of post-settlement sediments were compared with gaged flood records. The comparison demonstrated that sorting, the normalized percentage of 0.125-0.25 mm particles, and the shape of the particle size distribution curves can be used to discern floods larger than a 15-year event. The modern analog was applied to pre-settlement sediments and two periods were identified with high-magnitude floods, although the magnitude of these floods was uncertain. The non-linear power relation between depth and age defined the ages of the two periods at A.D. 690-875 and A.D. 1100-1350. These periods corresponded to extremely wet years and time intervals that lacked severe and extreme droughts as indicated by tree-ring records. It suggests that high-magnitude paleofloods probably occurred under wetter climate conditions. The hydroclimate conditions of the MWP and the LIA were also examined, and the sedimentology of overbank sediments indicates a wetter MWP and possibly a relatively drier LIA.

Keywords: particle size, sediments, hydroclimate

Introduction

A long-term flood history is essential for flood risk analysis (Benito, 2004; Werritty et al., 2006) and for understanding the relationship between floods and climate (Ely et al., 1993; Knox, 2000; Baker, 2008). Modern instrumental records of floods only go back to a little over 100 years ago at best, which

is too short a time frame for a long-term flood history. Historic documents that archived large flood events provide great amounts of information in certain parts of the world like China and Europe (Benito, 2004). However, such detailed historic information is not always available. Even historic documents typically go back only several hundred years at most, which is still not enough for a millennial-scale analysis. As a result, information on paleofloods, which are past or ancient floods that occurred without being recorded by instruments or historic documents (Baker, 2008), is necessary to reconstruct a long-term flood history.

Where river channels are confined by stable bedrock, evidence of paleofloods is usually found in slackwater deposits and bedrock scour features (Baker et al., 1983; Benito, 2003). Such studies have been conducted in many regions of the world such as Australia, South Africa, Europe, East Asia, and North America, particularly the southwest United States (Baker, 2008). In humid temperate environments where slackwater deposits are less well expressed, paleoflood records can be reconstructed using dendrogeomorphic evidence (Sigafoos, 1964), but more commonly by analyzing floodplain overbank sediments (Knox, 2000; Goman and Leigh, 2004; Werritty et al., 2006). Typically, overbank sediments are composed of silty and fine sandy facies. Silty facies record moderate-sized overbank floods that are capable of conveying silt and clay in suspension across the floodplain; while sandy facies register larger floods that are capable of transporting fine- to medium-sized sand in suspension (Nicholas and Walling, 1997; Knox, 2006; Werritty et al., 2006). If ages of sandy facies are known, then a paleoflood history can be reconstructed back to the earliest of vertical accretion facies (Werritty et al., 2006).

Climate is an important driver in hydrologic systems, and floods are quite sensitive to even modest changes in climate (Knox, 1993, 2000). Long-term variations in the magnitude and frequency of floods commonly are related to changes in the climate and prevailing large-scale atmospheric circulation patterns (Ely, 1997). Paleofloods tend to cluster in certain time periods (Knox, 1993; Baker, 2008).

Although many studies suggest that flood periods coincide with wet climate (Ely, 1997; Goman and Leigh, 2004) or with climate transitional periods (Ely et al., 1993; Knox, 1993), some research also reveals that large floods occur under more arid conditions (Patton and Dibble, 1982). Even though the relationship between paleofloods and climate is uncertain, paleofloods present direct evidence of the occurrence of an individual hydrological event (Benito et al., 2003).

Native Americans have lived in the southern Blue Ridge Mountains since the Paleoindian Period (ca. 12,000 years ago) but they did not have written language until the early 19th century; thus, historic documents of large floods prior to European settlement are not available and a long-term flood history is not well known. Slackwater deposits in this area are not well-developed, so reconstructing the paleoflood history relies on floodplain overbank sediments or vertical accretion facies. Leigh (2007) related particle sizes of post-settlement vertical accretion sediments with gaged flood records in the upper Little Tennessee River basin and found that a relatively high percentage of >0.25 mm particles is a good indicator of the occurrence of large floods; however, he did not investigate the floods during pre-settlement time. In this study, we further explored the relationship between overbank sediments and large flood events, and built a pre-settlement flood history.

Several studies showed a wetter early Holocene in the southeast United States (Leigh and Feeney, 1995; Goman and Leigh, 2004; Leigh, 2006). However, the paleoclimatic conditions during the last 2000 years are not well known, especially in the southern Blue Ridge Mountains (Leigh, 2008). Paleoflood history may help resolve the hydroclimate conditions in this area. Therefore, the objectives of this research are: (1) to reconstruct late pre-settlement paleofloods in the upper Little Tennessee River valley by using a modern flood-sedimentology analog; and (2) to infer hydroclimate conditions in the southern Blue Ridge Mountains during the past 2000 years.

Study Area

The upper Little Tennessee River, which flows north and is fed predominantly by east- and west-flowing tributaries, drains a 363 km^2 catchment above the United States Geological Survey (USGS) gaging station near Prentiss (USGS 03500000) within the southern Blue Ridge Mountains in northeast Georgia and western North Carolina (Figure 3.1). The characteristic bedrock of the region is quartz dioritic gneiss and biotite gneiss (Hatcher, 1988; Daniel and Payne, 1990; Robinson et al., 1992), which has been weathered to form a 1-30 m thick mantle of saprolite. The texture of saprolite ranges from sand to clay loam, providing abundant fine sediments to the drainage network (Price and Leigh, 2006; Leigh, in press (b)). The morphology of the river channel is characterized by meandering riffles and pools with coarse bed sediments, such as cobble, gravel and sand, and finer overbank sediments such as fine sand, silt and clay (Price and Leigh, 2006; Leigh, in press (a)).

The region lies in the humid subtropical climate zone. The climate record at the low elevation station of the Coweeta hydrological laboratory during 1971-2000 shows a 30-year average annual temperature was 12.7 °C, with July being the hottest month and January the coldest month; the 30-year average annual precipitation was 183 cm. Rainfall is most abundant in winter and minimal in late summer and early fall (Figure 3.2). Precipitation is affected by tropical storms as well as frontal storms. The inland tracks of tropical storms from the Atlantic Ocean and the Gulf of Mexico occasionally provide exceptional amounts of intense precipitation to the region during the late summer and fall, tending to trigger landslides, debris flows, and floods (Leigh, in press (b)).

Three sites were selected in the bottomland of the upper Little Tennessee River valley at locations from headwaters to the lower main stem (Figure 3.1). Previous studies (Price and Leigh, 2006; Leigh, 2007) have identified the ages of overbank sediments, and Leigh (2007) found a relationship between sediment particle sizes and flood events, which provide a basis for looking into paleofloods in this study. The Keener site is located on the first terrace of a small tributary in the headwaters with a

drainage area of 7.2 km^2 (Price and Leigh, 2006). The Keener cores were taken about 25 meters away from the channel on the valley flat. The State Line and Riverside sites are located further downstream on active floodplains of the mainstem of the upper Little Tennessee River. Samples at these two sites were taken on the natural levee immediately adjacent to the cutbank of the channel.

Methods

Field work was conducted in March 2009. Solid cores (7.5 cm diameter) were taken using a trailer-mounted Giddings hydraulic coring rig. Generally, coring continued until hitting gravels at the bottom. Each core was wrapped with plastic wrap and aluminum foil in the field and returned to the laboratory. In addition to cores, at the State Line and Riverside sites, monolith samples were obtained by pounding metal or PVC trough into the vertical cutbank profile and then meticulously excavating the soils out. The advantage of monoliths is that they are not compressed and preserve undisturbed layers in the best possible condition. Later in the laboratory, based on the stratigraphic correlation and particle size analysis results, data from cores and monoliths were combined into a complete profile to take advantage of the intact monolith samples. Optically stimulated luminescence (OSL) and charcoal samples also were collected for dating analysis.

All cores and monoliths were cleaned, photographed and described according to the U.S. Department of Agriculture Soil Survey Manual (U.S. Division of Soil Survey, 1993), and the descriptions are available in the appendices (Appendix A). Buried A horizons (Ab) were used to define the boundary between pre-settlement and post-settlement time periods (Knox, 1987; Leigh, in press (a)). Samples were taken from each core and monolith in 2-14 cm increments to approximate 50-yr time intervals for pre-settlement sediments and 10-yr time intervals for post-settlement sediments based on the previous chronology (Price and Leigh, 2006; Leigh, 2007). Abrupt and clear boundaries were captured by smaller sampling intervals in order to be reflected in the laboratory data. Samples were oven dried at 55°C for

at least 48 hours and then sieved through 2 mm mesh. Particles larger than 2 mm were weighed and discarded while particles smaller than 2 mm were retained for further analysis.

Approximately 0.5 g samples were taken for particle size analysis on an automatic laser particle size analyzer (CILAS 1180) in the Department of Geology and Environmental Geosciences at the College of Charleston. Samples were pretreated with 30% hydrogen peroxide (H_2O_2) to remove humus and then with a sodium metaphosphate solution (50 g/L) to deflocculate clay aggregates before being introduced into the machine. The CILAS machine measures particles from 0.04 μm to 2500 μm and produces a continuous distribution of particle sizes. Traditional wet sieve and pipette methods were also run on certain samples to be compared with the CILAS results (Figure 3.3). The comparison showed a substantial underestimation of clay content using CILAS, possibly because the pretreatment did not deflocculate clay well before putting into CILAS, or the high content of mica in the sample, whose flat sheet shape might result in different sizes by CILAS measurement (Hayton et al., 2001). Anyway, given the fact that sand content is more important to our study, we only adopted 2-2000 μm particles in our analysis. Descriptive statistics of the particle size (2-2000 μm) were performed on the GRADISTAT 4.0 (Blott, 2000). The percentage of particle size fractions were normalized by dividing the largest amount in the sample set (separately for pre-settlement and post-settlement periods).

Discharge records (annual duration series) of the Little Tennessee River were obtained from the Prentiss gaging station (USGS 03500000, from 1945 to 2008) and the Judson gaging station (USGS 03507000, from 1897 to 1944) (locations are shown in Figure 3.1). Because the Judson station has a larger drainage area (1600 km^2) than the Prentiss station (363 km^2), the absolute peak discharges from the two gauges are different and cannot be compared directly. We normalized the gage data by dividing the peak discharge by the drainage area ($m^3/sec/km^2$) so that they are similarly scaled. To verify this adjustment, we normalized the peak discharge from the Bryson gaging station (USGS 03513000, from 1898 to 2009), whose drainage area (1720 km^2) is close to the Judson Station but with a much more

continuous record. Comparison of the normalized data showed that some frequent floods (2-yr, 5-yr and 10-yr time interval), and very large floods (100-yr time interval) registered similar values at three sites (Figure 3.4 and Table 3.1), giving us confidence in connecting the data from the Prentiss and Judson stations.

According to Leigh (in press (a)), the boundary of pre-settlement and post-settlement occurred at about A.D. 1870. A complete chronology of each sample in vertical accretion facies was obtained by fitting power function curves to the absolute ages, which were derived from radiocarbon, OSL, ^{137}Cs, and correlation of prominent flood layers to historical gaging records (See Chapter 2).

Results

Modern Flood-sedimentology Model

Particle size characteristics of post-settlement sediments, including the percentage of particle size fractions and statistics of the particle size distribution, were compared to the normalized gage records by plotting these data against time (Figure 3.5). The comparison showed that sorting and the normalized percentage of 0.125-0.25 mm particles broadly correspond to floods that are larger than a 15-year event, which was calculated using the Weibull equation (Charlton, 2008, p31). A pronounced increase of fine sand (0.125-0.25 mm) content in the sediments corresponds to extremely large floods like the 1964 flood and the 1902 flood (Figure 3.5). Even though all samples are poorly sorted, the extremely large floods are more poorly sorted than the smaller floods with larger sorting values (Figure 3.5). These correspondences are best expressed at the State Line site, but not as well at the Keener and Riverside sites. We also did correlation analysis to see how well particle size data correlate to the gage records. The normalized annual peak discharges were averaged within each time interval of the sediment samples, and then used for correlation analysis with particle size characteristics. As shown in Table 3.2, the correlation coefficient r-values at the State Line and Riverside sites are very low (<0.3) and virtually uncorrelated with high p-value, while the r-values at the Keener site are relatively higher.

In addition, we found the shape of the particle size distribution curve also helped differentiate high-magnitude floods from smaller floods (Figure 3.6). At the State Line and the Riverside sites, the high-magnitude floods have "shoulders" on the coarse end of the curve (ϕ= 1-2) while the small floods present a sharp decrease to zero at the coarse end (ϕ=2). At the Keener site, the particle size distribution curves do not have "shoulders" at the coarse end, but curves drop to zero at ϕ=2 for high-magnitude floods and at ϕ=3 for smaller floods; and the two peaks of bimodal curves differ significantly for high-magnitude floods but are rather even for smaller floods (Figure 3.6).

In summary, three particle size characteristics, sorting, normalized percentages of 0.125-0.25 mm particles, and the shape of particle size distribution curve, visually demonstrate a relationship with flood records. Thus, these measures of particle sizes are adopted from the modern flood-sedimentology model, for use in identifying time periods with large floods in the pre-settlement strata as described below.

Paleofloods

We derived the age of each sample from the depth-age model (Chapter 2) and then plotted the sorting and normalized percentage of 0.125-0.25 mm particles on the time scale for each site (Figure 3.7). At the State Line and Riverside sites, sorting and the normalized percentage of fine sand generally correspond, when the percentage of fine sand increases, the sorting value increases as well. According to the modern analog, we identified the samples with significantly higher content of fine sand and larger sorting value as deposits from large floods. This approach identified three large flood periods at the State Line and Riverside sites (Figure 3.7). At the Keener site, however, sorting and the normalized fine sand percentage do not quite correspond. Sorting does not have much variation though time but the percentage of fine sand shows a minor increase around A.D. 1350 and a sharp increase around A.D. 800 at the bottom of vertical accretion sediments (Figure 3.7). We also examined the particle size

distribution curve of each sample, and the shape difference of the curves generally supported the identification of paleofloods by the other two particle size characteristics (Figure 3.6).

Age errors of each inferred paleoflood were calculated by combining the dating error and predicted error from the "depth-age"model (Chapter 2), as shown on Figure 3.7. Comparing the derived large flood events at the three sites, we conclude that large flood events were temporally clustered within two periods: from A.D. 690 to A.D. 875 and from A.D. 1100 to A.D. 1350 (Figure 3.7).

Discussion

Flood-sedimentology Model

In the flood-sedimentology model, even though the 1902 and 1964 floods were the largest on record, without the dating information, we could not have been confident in relating the highest peaks of particle size characteristics to them. As shown in the gage record, the frequency of high-magnitude floods increased substantially after 1964, but the annual precipitation record from a long-term gage in the region (Coweeta Hydrologic Laboratory at Otto, NC, from 1935-2009) did not show clear trend of changes during the past decades (Figure 3.8). We also looked at the rainfall amount in the months with floods, and found that the flood discharge does not correlate well to the rainfall amount of that month ($r=0.54$). Therefore, the increased frequency of large floods probably is more related to the intensified human activities (Knox, 2006). After the 1970s, the road building and second-home construction in the mountainous areas reduced forest cover, thereby increasing surface runoff and leading to a larger discharge given the same amount of precipitation (Leigh, 2007; Chapter 2). Human impact was so significant that it overshadowed other factors during post-settlement time (Chapter 2). Because the drivers of large flood events are different between the two periods, with human impact being dominant in post-settlement time and natural climate changes more important in pre-settlement time, the absolute percentage of fine sand is meaningless in the flood-sedimentology model. We used the normalized percentage of 0.125-0.25 mm particles, which is the percentage of fine sand in each sample

relative to the largest amount in the sample set (separately for pre-settlement and post-settlement periods). This not only eliminated the spatial difference of fine sand content among the three sites, but it also separated human factors from natural climate factors.

The coarse sampling intervals of post-settlement sediments, which resulted in 6- to 15-year time intervals based on the power-function chronology, only allowed the model to discern floods larger than a 15-year flood. Finer sampling intervals probably would have provided a better correlation to large floods and would help to identify floods with smaller magnitudes, as was found by Leigh (2007). However, considering bioturbation and pedogenesis, and the coarse resolution of pre-settlement sediments, the current sampling strategy was sufficient to allow the identification of high-magnitude floods and was most appropriate for comparison with the even longer time intervals represented by the pre-settlement samples. The 1964 and 1902 floods were not well-represented at the Riverside and Keener sites. The coarse sampling interval at Riverside may have averaged the sediments from several floods, thus preventing the identification of an individual flood. Because the Keener site is in the headwaters, it may not pick up the same floods as the mainstem sites. This may also be true for pre-settlement time since there are few large paleofloods indicated at the Keener site. The significant increase of fine sand percentage in the first period (A.D. 690-875) at the Keener site actually might be deposits from large floods, but it is also related to the initial rapid overbank sedimentation under higher energy on a new surface, which may compromise its integrity as a true paleoflood.

Suitability of Floodplain Overbank Sediments for Paleoflood Reconstruction

Although it is agreed that moderate flood events have stronger impact on channel and floodplain geomorphology because of their frequent occurrence (Wolman and Miller, 1960), it has been difficult to achieve consensus on the role large floods played in landscape modification. One large flood may deposit a large amount of sediments on a floodplain; it may also produce minor geomorphic changes with little or no deposition (Gomez et al., 1995; Lecce et al., 2004). Overbank deposition relies

not only on the magnitude of floods, but also on other factors such as the suspended material concentration, previous flood events, and the duration of the flood (Nicholas and Walling, 1997; Lecce et al., 2004). Therefore, not every flood would leave evidence in overbank sediments, and the thickness and particle size of an overbank deposit would not necessarily reflect the magnitude of the flood that deposited it. Using overbank sediments as evidence of floods runs the risk of portraying incomplete flood records and makes it difficult to determine flood magnitude. This is also the reason that we can identify the age of paleoflood periods but not the magnitude of these paleofloods. But without other proxies to reconstruct paleofloods, it is the best available technique. Although the correlation analysis showed no strong correlation between the particle size data and gaged record, particular at the State Line and Riverside sites, the broad visual trends provide valuable information for understanding the flood-sedimentology relationship. The good correspondence of the trends gave us confidence in the modern analog and the paleofloods derived from it.

Hydroclimate Conditions During the Past 2000 Years

Large floods frequently occur under wet climate conditions and deposit coarse overbank sediments (Knox, 1993; Ely, 1997; Goman and Leigh, 2004). Under arid climate conditions, however, one large flood can also produce substantial sandy deposits (Patton and Dibble, 1982). It is difficult to determine whether the sandy sediments were deposited by one large flood or by a sequence of large floods based solely on the stratigraphic and sedimentological information provided by the cores; and the low temporal resolution further increased such difficulty. As a result, although two periods of high-magnitude floods have been identified from the pre-settlement overbank sediments, the hydroclimate conditions (wet or dry) of the two periods are not certain, and other paleoclimate proxies should be considered.

Good pollen records in the study area are scarce. Most pollen records in the southeast United States usually extend back to the late Pleistocene and early Holocene (Watts, 1970; Delcourt et al.,

1986) and have rather coarse resolution during the last 3000 years. The pollen record from Black Pond dates back to 3000 yr B.P. but its vegetation record mainly reflects disturbance by Native Americans (Delcourt et al., 1986). Viau (2006) reconstructed mean July temperature during the past 14,000 years using pollen records but did not derive the hydroclimate conditions. Thus, efforts to relate pollen records with our study failed.

Fortunately, high-resolution tree-ring records near the study area provided insight into the hydroclimate conditions. We related the paleofloods to the reconstructed Palmer Drought Severity Index (PDSI) data from Cook et al. (2004), which are available at the NOAA website: http://www.ncdc.noaa.gov/paleo/newpdsi.html (Grid cell 238). We found that the two periods with high-magnitude paleofloods corresponded well to time intervals that contain extremely wet years and without severe or extreme drought (Figure 3.7). This comparison indicates that these high-magnitude floods occurred under relatively wetter climate conditions.

During the last 1500 years, the most significant climate anomalies are the Medieval Warm Period (MWP) and the Little Ice Age (LIA). The two periods are named based on the temperature variations that MWP was warmer than present and LIA was cooler than present. However, the hydroclimate conditions are not clear, and are supposed to vary from region to region relating to large-scale circulation patterns (Bradley et al., 2003). Although the onsets and terminations of these periods varied from region to region (Hughes and Diaz, 1994; Bradley and Jones, 1995), it is generally accepted that a maximal time range for the two periods are from A.D. 800 to A.D. 1300 for the MWP, and from A.D. 1400 to A.D. 1800 for the LIA (Grove, 1988; Grove and Switsur, 1994). Under this time frame, the first reconstructed high-magnitude flood period (A.D 690-875) in this study happen to occur during the transition into MWP and the early MWP, and the second reconstructed high-magnitude flood period (A.D. 1100-1350) right falls at the end of MWP and the transition period from MWP to LIA. Thus, it appears to indicate a generally wetter MWP (A.D. 800-1300) in the Southern Blue Ridge Mountains. This

is compatible with another tree-ring chronology of eastern red cedar from Cedar Knob, West Virginia, which has wider ring widths indicating a wetter period during the MWP (A.D. 950- 1100) (Stahle et al., 2003). The inference is also consistent with the isotopic records of a stalagmite in the Desoto Cavern in northeastern Alabama, which suggested a wetter MWP (A.D. 850-1200) in the southeast United States (Liang, 2008). On the other hand, if we use a narrower time range for the MWP as used in Stahle et al. (2003), the two flood periods would fall into the transitional periods into and out of the MWP, indicating a wetter climate during the transitional periods.

No paleofloods that are as large as those during the MWP were identified from the sedimentological record of floodplain sediments during the LIA, indicating less frequent large floods and possibly drier climate conditions during the LIA. However, the PDSI data shows that there were very wet years as well as severe drought years during AD 1400 – 1800, indicating fluctuated hydroclimate conditions. The coarse sampling intervals and low temporal resolution limited our understanding of hydroclimate conditions during the LIA, but compared with the MWP or transitional periods, it should be relatively drier during the LIA.

Conclusion

By correlating the particle size characteristics of post-settlement floodplain overbank sediments with the USGS gaged flood record, we found that sorting, normalized percentages of 0.125-0.25 mm particles, and shape of particle size distribution curves readily discern floods that are larger than a 15-year event (annual duration series). Applying this modern analog to the pre-settlement sediments, we identified two periods (A.D. 690-875 and A.D. 1100-1350) that have high-magnitude floods, though the magnitude was difficult to determine. These periods correspond to time intervals that contained extremely wet years and lacked severe and extreme droughts as indicated by tree-ring records and the paleo-PDSI. Thus, the derived paleofloods probably occurred under wetter climate conditions. The sedimentology of floodplain overbank sediments suggested a wetter MWP or transitional periods. The

coarse sampling intervals and low temporal resolution limited our understanding of hydroclimate conditions during the LIA but it appears relatively drier than the MWP.

Table 3.1. Comparison of normalized peak discharge of different recurrence interval (RI) between three gaging stations

	A.D. 1898-2008		A.D. 1898-1944		A.D. 1945-2008	
RI	Bryson	Judson & Prentiss[1]	Bryson	Judson	Bryson	Prentiss
2yr	0.29	0.23	0.29	0.23	0.27	0.25
5yr	0.42	0.36	0.42	0.34	0.42	0.41
10yr	0.51	0.51	0.65	0.48	0.50	0.52
15yr	0.54	0.66	0.68	0.59	0.51	0.71
25yr	0.65	0.73	0.81	0.74	0.52	0.77
50yr	0.80	0.87			0.55	0.92
100yr	0.99	0.94				

Note: [1] data of 1898-1944 are from Judson gaging station, data of 1944-2008 are from Prentiss gaging station.

Data are calculated using the Weibull equation.

Table 3.2. Correlation coefficient (r) of averaged normalized discharge and particle size characteristics

site	N[1]		sorting	%0.125-0.25mm	%0.25-0.5mm	%0.5-1mm	%>0.25 mm	%sand	D50	D90	skewness	kurtosis
Keener	14	r	0.59	0.61	-[3]	-	-	0.60	0.59	0.59	-0.53	-0.58
		[2]P	0.03	0.02	-	-	-	0.02	0.03	0.03	0.05	0.03
State Line	16	r	0.28	0.28	0.17	0.13	0.17	0.17	0.16	0.13	0.15	-0.08
		p	0.29	0.29	0.52	0.63	0.52	0.53	0.56	0.63	0.59	0.76
Riverside	13	r	0.13	0.13	0.21	0.21	0.21	0.14	0.18	0.16	0.17	-0.03
		p	0.68	0.67	0.48	0.49	0.48	0.65	0.56	0.59	0.59	0.92

Note: [1] N is the number of observation

[2] p-value is the probability of null hypothesis (H0: no correlation, r=0)

[3] r is not available because these particle size data are zero

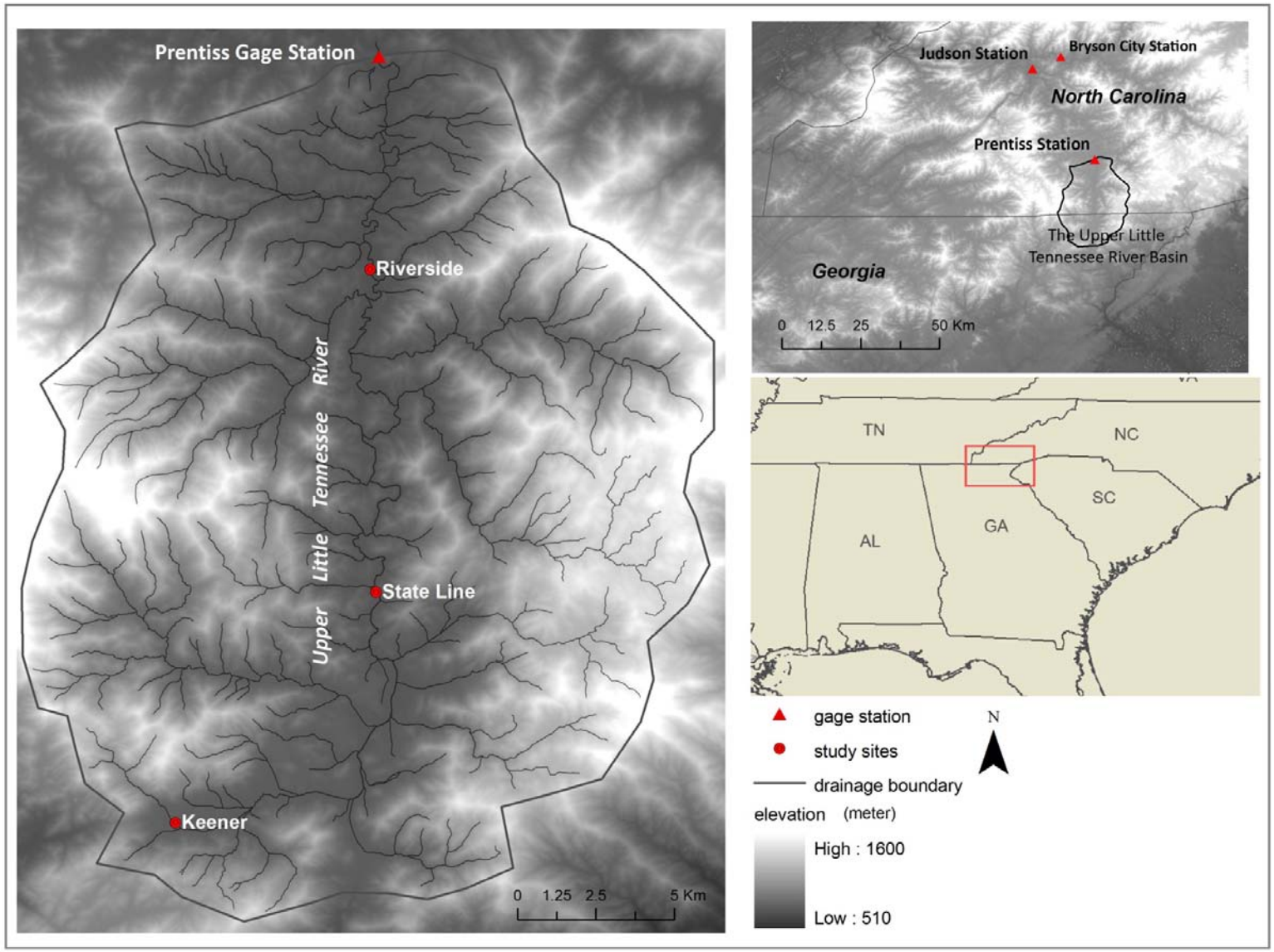

Figure 3.1. Location of the upper Little Tennessee River Valley and the three study sites.

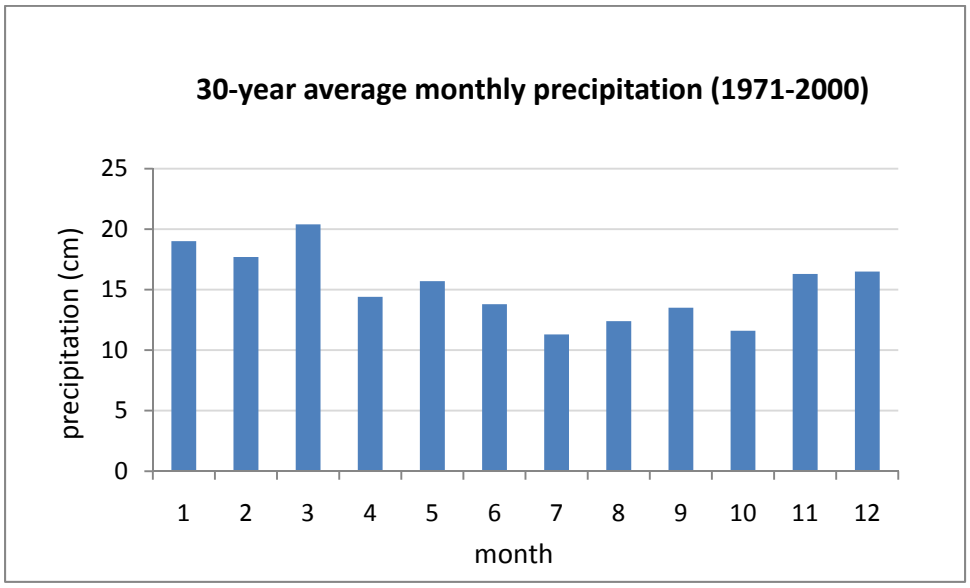

Figure 3.2. 30-year average monthly precipitation (1971-2000) at Coweeta Experiment Station. Data are from website of State Climate Office of North Carolina (http://www.nc-climate.ncsu.edu/cronos/normals.php?station=312102)

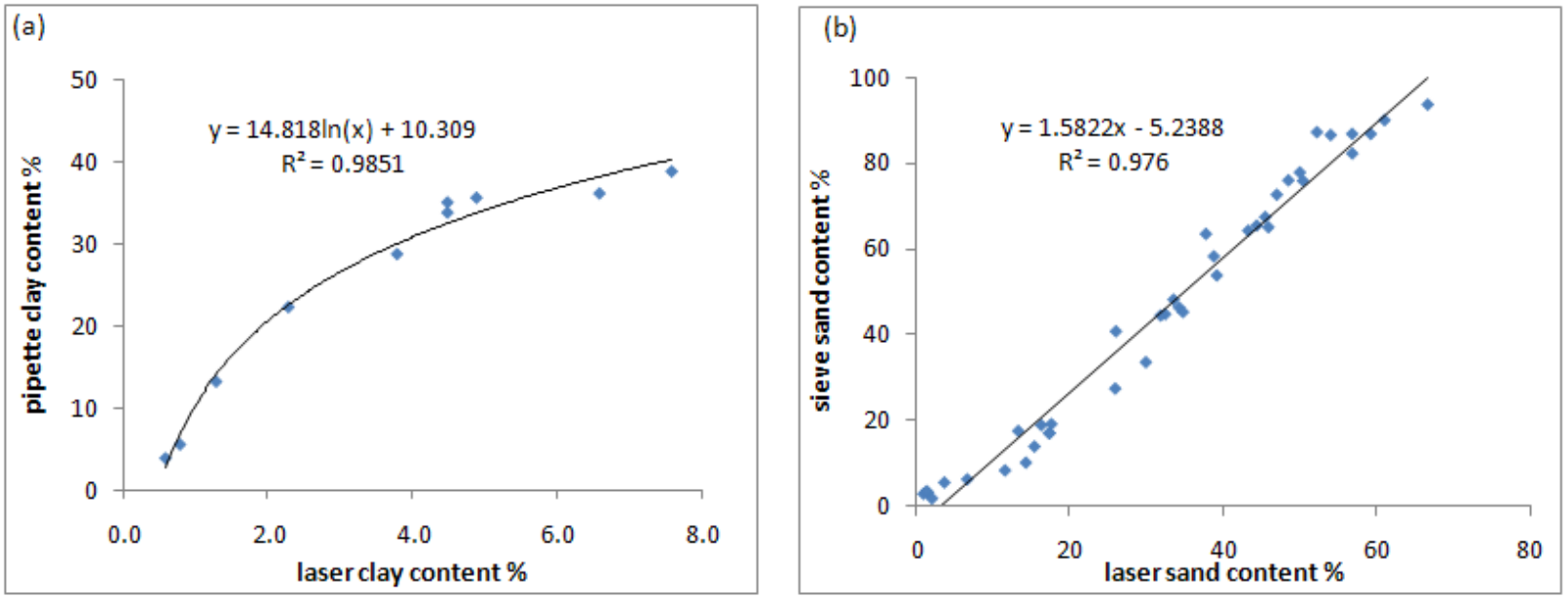

Figure 3.3. Comparison of clay and sand measurement between the CILAS laser method and traditional methods.

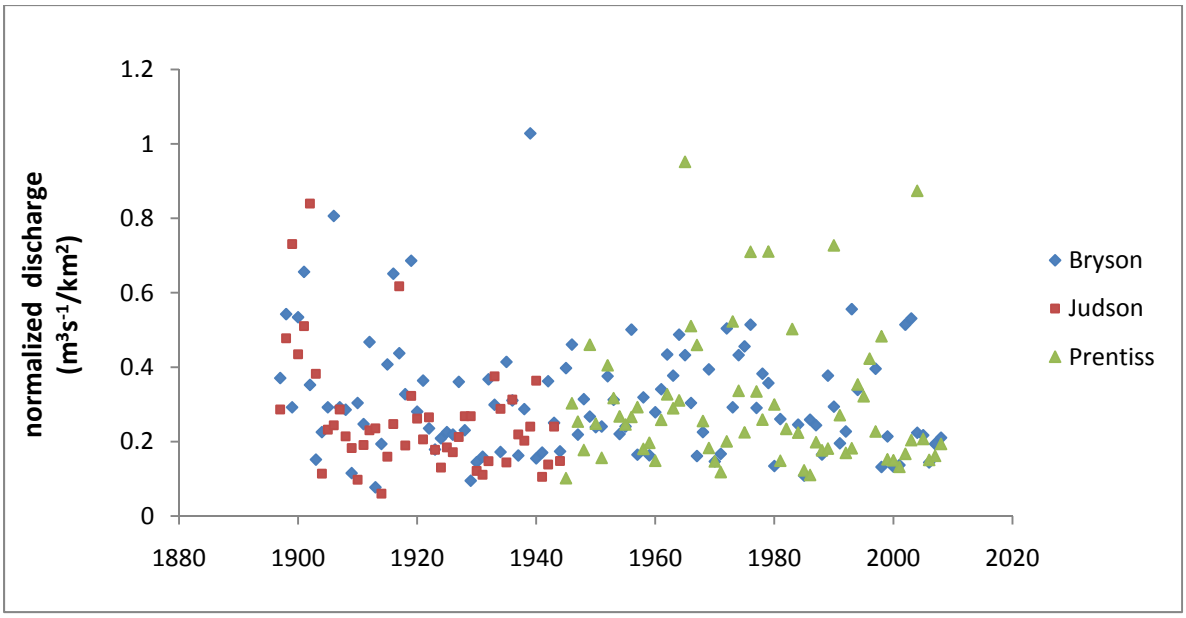

Figure 3.4. Comparison of normalized annual peak discharge at three gaging stations. normalized discharge = annual peak discharge / drainage area.

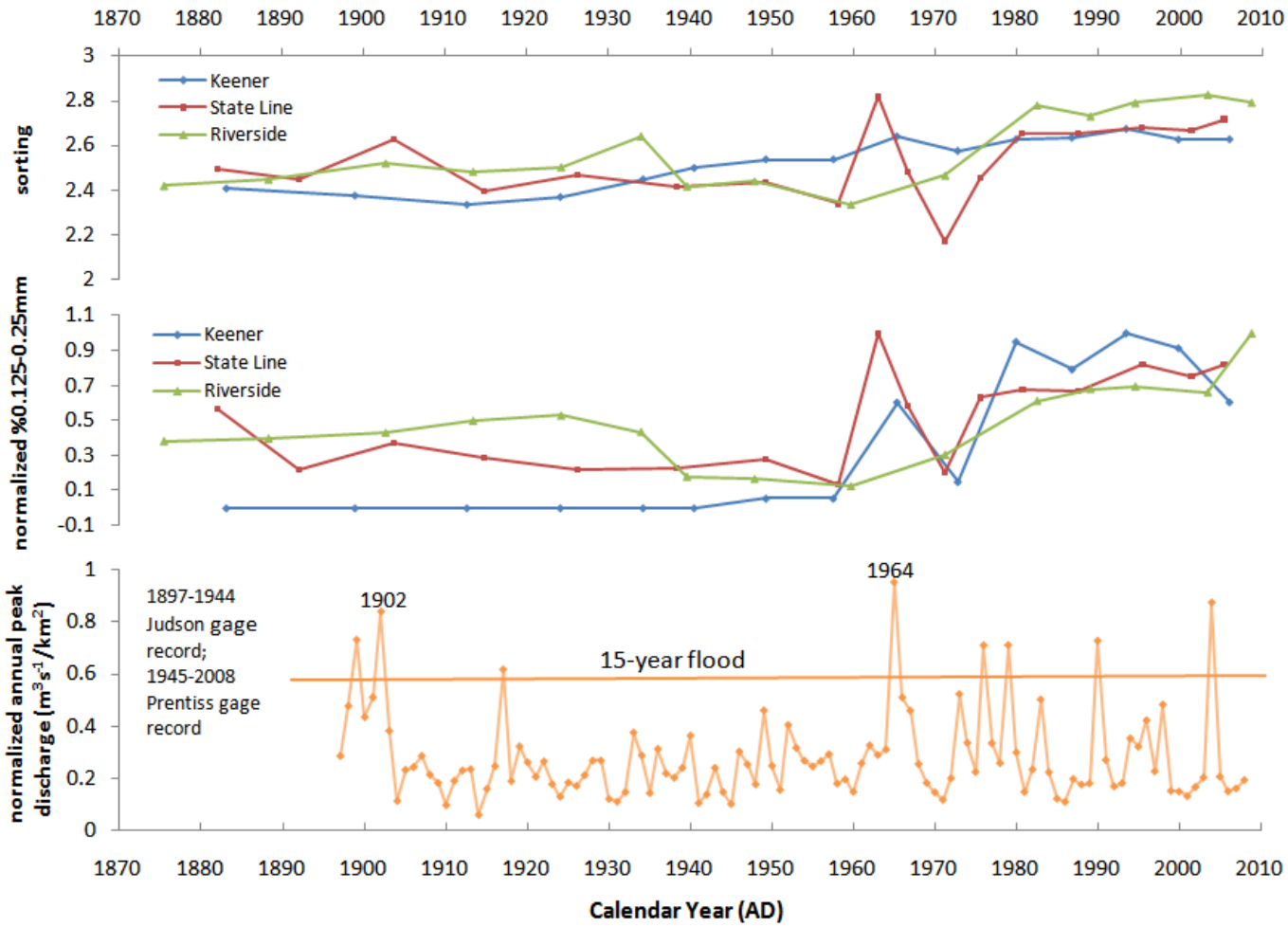

Figure 3.5. Comparison between particle size characteristics of post-settlement sediments and gaged flood records. Sorting is based on the Folk & Ward Geometric method. Normalized % of 0.125-0.25 mm particles refers to the percentage of 0.125-0.25 mm particles in each sample relative to the maximum content of 0.125-0.25 mm particles in the post-settlement sediments. Normalized annual peak discharge is the annual peak discharge divided by the drainage area, record of 1897-1944 is from the Judson gaging station and 1945-2008 is from the Prentiss gaging station.

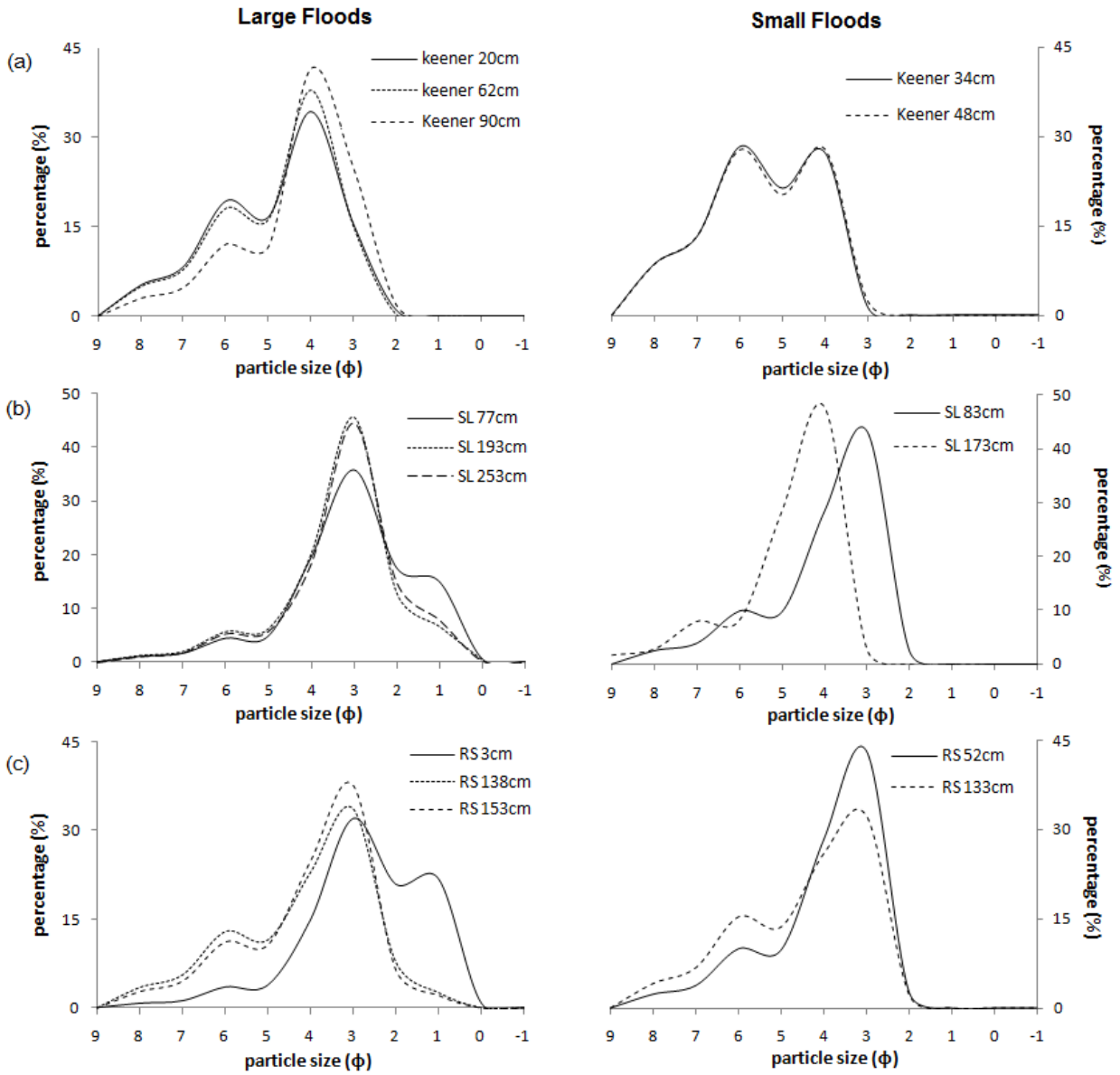

Figure 3.6. Particle size distribution curves of large floods and small floods. (a) the Keener site; (b) the State Line site; (c) the Riverside site. The solid curves represent post-settlement floods (Keener 22cm and SL 77cm represent 1964 flood, RS 3cm probably represent 2004 flood), the dotted curves represent pre-settlement floods.

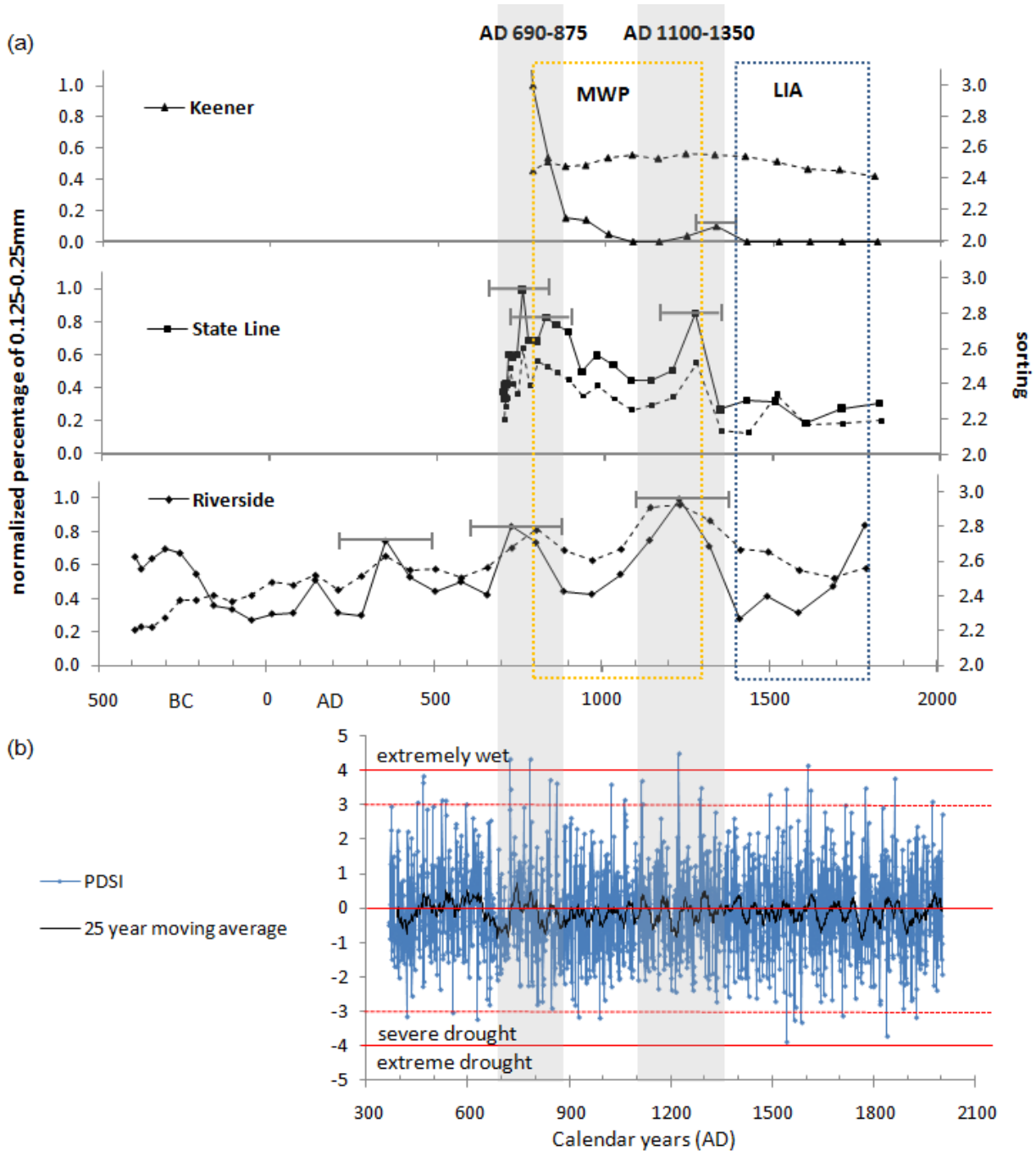

Figure 3.7. Reconstructed paleofloods (a) and its comparison with the tree-ring record (b). In (a), solid lines refer to normalized percentage of 0.125-0.25 mm particles, dotted lines represent sorting. The bars on the figure indicate age error (50 yr for Keener, 75 yr for State Line, and 170 yr for Riverside).

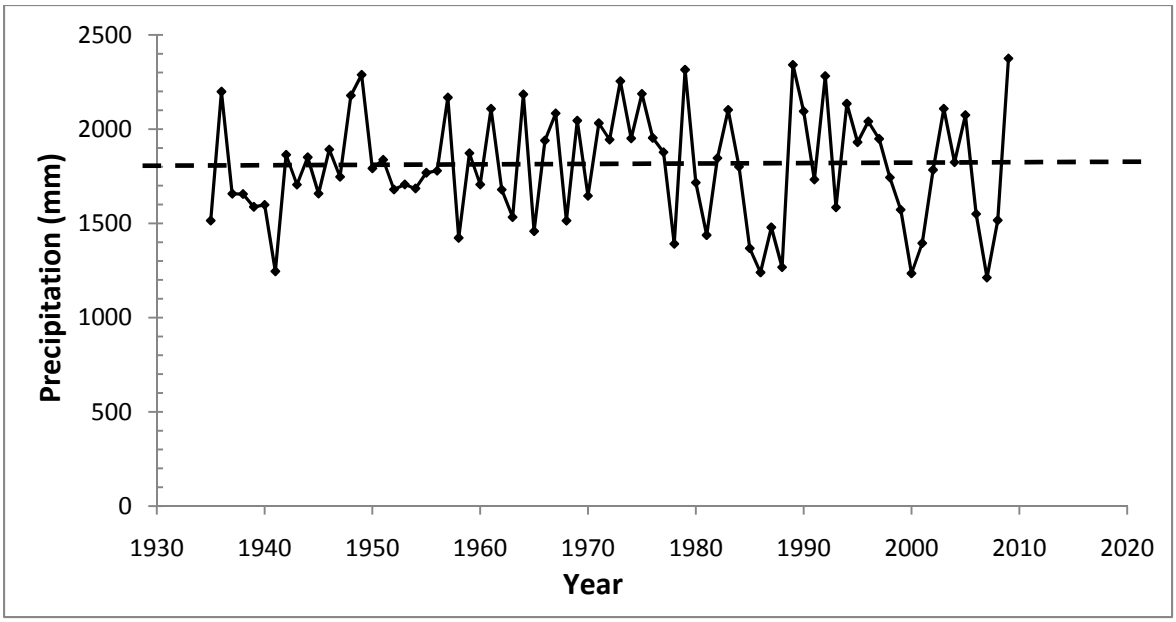

Figure 3.8. Annual precipitation at the Coweeta Hydrologic Laboratory, Otto, NC. Data from 1935-2009, downloaded at http://www.srs.fs.usda.gov/coweeta/data/. The dashed line represents the 74-yr mean precipitation.

CHAPTER 4

CONCLUSIONS

This study of the physical and chemical characteristics of floodplain sediments at three sites in the upper Little Tennessee River valley identified anthropic signatures in overbank sediments and reconstructed the paleoflood history during the last 2000 years. The results aid in understanding how floodplain sedimentation responded to late Holocene climatic changes and human impacts in the Southern Blue Ridge Mountains. Moreover, the reconstructed flood history provides insight into the hydroclimate conditions during the past 2000 years.

The overbank sedimentation rates, sediment texture and five chemical elements showed significant differences between pre-settlement and post-settlement sediments. Sedimentation rates decreased with time during pre-settlement time but increased with time during post-settlement time in the form of power functions. The long-term average sedimentation rates during post-settlement time were 3-12 mm/yr, up to one order of magnitude greater than rates in pre-settlement time, which were less than 1.2 mm/yr. Pre-settlement overbank sediments showed a fining-upward textural trend while the pre-settlement overbank sediments showed a coarsening-upward trend. Signature elements Ca, P, Pb, and Hg had greater concentrations (relative to Al) in post-settlement sediments. The value of K/Al had different trends in the two periods; it decreased upward in pre-settlement sediments but increased upward in post-settlement sediments, and exhibited a minimum value near the boundary of pre-settlement and post-settlement sediments. All these significant differences and substantial changes were related to post-settlement human impacts such as timber harvest, mining, intensive agricultural activities, and urbanization. Although autogenic processes of floodplain development also contributed to these changes, direct human impacts overshadowed all other factors. These anthropic signatures not

only differentiate sediments between the two periods, they also serve as good indicators of human impacts on floodplain sedimentation.

Comparing high-resolution particle size results and the post-settlement gaged flood records suggested that sorting, normalized percentages of 0.125-0.25 mm particles, and the shape of particle size distribution curves readily discern floods that are larger than a 15-year event. The modern flood-sedimentology analog identified two periods with high-magnitude floods at A.D. 690-875 and A.D. 1100-1350, but the magnitude of floods was difficult to determine. Although flood-climate relationship is complicated, we found that the two identified periods corresponded to extremely wet years and time intervals without severe and extreme droughts, as indicated by tree-ring records. The derived paleofloods probably occurred under wetter climate conditions. The sedimentological characteristics of floodplain overbank sediments suggested a wetter MWP and possibly relatively drier LIA.

REFERENCES

Alexander J, Fielding C.R., 2006. Coarse-grained floodplain deposits in the seasonal tropics: Towards a better Facies model. Journal of sedimentary research 76, 539-556.

Ambers, R.K.R., Druckenbrod, D.L., Ambers, C.P.; 2006. Geomorphic response to historical agriculture at Monument Hill in the Blue Ridge Foothills of Central Virginia. Catena 65, 49-60.

Baker, V.R., Pickup, G., Polach, H.A., 1983. Desert paleofloods in central Australia. Nature 301, 502–504.

Baker, V.R, 2008. Paleoflood hydrology: Origin, progress, prospects. Geomorphology 101, 1-13.

Beaudoin, A. 2003. A comparison of two methods for estimating the organic matter content of sediments. Journal of Paleolimnology 29, 387-390.

Benedetti, M.M., 2003. Controls on overbank deposition in the Upper Mississippi River. Geomorphology 56, 271-290.

Benito, G., Sopena, A. et al., 2003. Palaeoflood record of the Tagus River (Central Spain) during the Late Pleistocene and Holocene. Quaternary Science Reviews 22, 1737-1756.

Benito, G., Lang, M., Barriendos, M., et al., 2004. Use of Systematic, Palaeoflood and Historical Data for the Improvement of Flood Risk Estimation. Review of Scientific Methods. Natural Hazards 31, 623-643.

Blott, S., 2000. GRADISTAT Version 4.0, A Grain Size Distribution and Statistics Package for the Analysis of Unconsolidated Sediments by Sieving or Laser Granulometer.

Boggs, S., 2006. Principles of sedimentology and stratigraphy, 4th ed. Pearson Prentice Hall, Upper Saddle River, N.J. P662.

Bradley, R. S and Jones, P. D, 1995: Recent developments in studies of climate since A.D.1500. In Bradley, R. S. and Jones, P. D., editors, Climate Since AD 1500 [Revised Edition],London: Routledge, 666-679.

Bradley, R. S., Hughes, M. K. and Diaz, H. F., 2003. Climate change: Climate in Medieval Time. Science 302, 404-405.

Bridge, J.S., 2003. Rivers and Floodplains: Forms, Processes, and Sedimentary Record. Blackwell Science Ltd, Xoford, UK. P504, 268-269.

Brown, A.G., 1998. Fluvial evidence of the Medieval Warm Period and the late Medieval climatic deterioration in Europe. In: Benito G., Baker V.R., Gregory K.J. (Eds.), Paleohydrology and Environmental Change. Wiley, Chichester, pp. 43-52.

Charlton, R., 2008. Fundamentals of Fluvial Geomorphology. Routledge, London and New York, 234 pp.
Chin,A., 2006. Urban transformation of river landscapes in a global context. Geomorphology 79, 460-487.

Cook et al., 2004. North American Drought Atlas PDSI Reconstructions, Time Series Plots. NOAA Paleoclimatology Program.

Costa, J.E., 1975. Effects of agriculture on erosion and sedimentation in Piedmont province, Maryland. Bulletin of Geological Society of America 86, 1281-1286.

Cuniff, P. A. (ed), 1998. Official Methods of Analysis of AOAC International, 16th edition. AOAC International, Gaithersburg, Maryland. Method 2.7.08. Chapter 2. p 37.

Daniel III, C.C., Payne, R.A., 1990. Hydrogeologic unit map of the Piedmont and Blue Ridge provinces of North Carolina. Water Resources Investigations Report, Vol 90-4035. U.S. Geological Survey, Raleigh, NC.

Dean, W. E., Jr. 1974. Determination of carbonate and organic matter in calcareous sediments and sedimentary rocks by loss on ignition: Comparison with other methods. Journal of Sedimentary Petrology 44, 242-248.

Delcourt, P.A, Delcourt, H.R, Cridlebaugh, P.A, and Chapman, J., 1986. Holocene ethnobotanical and paleoecologicalrecord of human impact on vegetation in the Little Tennessee River Valley, Tennessee. Quaternary Research 25, 330-349.

Duller, G.A.T., 1999. Luminescence Analyst computer programme v2.18. Department of Geography and Environmental Science.University of Wales, Aberystwyth.

Eller, R. D., 1982. Miners, Millhands, and Mountaineers: Industrialization of the Appalachian South 1880–1930. Knoxville, TN: University of Tennessee Press.

Ely, L.L, Enzel, Y, Baker, V.R, Cayan, D.R, 1993. A 5000-Year Record of Extreme Floods and Climate Change in the Southwestern United States. Science 262, 410-412.

Ely, L.L, 1997. Response of extreme floods in the southwestern United States to climatic variations in the late Holocene. Geomorphology 19, 175-201.

Fitzpatrick, F. A., Knox, J.C., 2000. Spatial and temporal sensitivity of hydrogeomorphic response and recovery to deforestation, agriculture, and floods. Physical geography 21, 89-108.

Folk, R.L. and Ward, W.C.,1957. Brazos River bar: a study in the significance of grain size parameters. Journal of Sedimentary Petrology 27, 3-26.

Glenn, 1911. Denudation and erosion in the southern Appalachian region and the Monongahela Basin. USGS Professional Paper 72, 137

Goman, M., Leigh, D.S., 2004. Wet early to middle Holocene conditions on the upper coastal plain of North Carolina, USA. Quaternary Research 61, 256–264

Gomez, B., Mertes, L. A. K., Phillips, J. D., Magilligan, F. J., and James, L. A., 1995. Sediment characteristics of an extreme flood: 1993 upper Mississippi River valley. Geology 23, 963–966.

Gregory, K.J., Starkel, L., Baker, V.R., 1995. Global Continental Palaeohydrology. Wiley, Chichester.

Grove, J. M., 1988. The Little Ice Age. Methuen, London. 498pp.

Grove, J.M., Switsur, R., 1994. Glacial Geological Evidence for the Medieval Warm Period. Climate change 26, 143-169.

Happ, S.C., 1945. Sedimentation in South Carolina Piedmont Valleys. American Journal of Science 243(3), 113-126.

Harden, C.P., 2004. Fluvial response to land-use change in the southern Appalachian region: a century of investigation. Physical Geography 25, 398-417.

Hatcher, R.D., 1988. Bedrock geology and regional geologic setting of Coweeta Hydrologic Laboratory in the eastern Blue Ridge. In: W.T. Swank and D.A. Crossley, Jr. (Editors), Forest Hydrology and Ecology at Coweeta. Springer-Verlag, New York, pp. 81-92.

Hayton,S., Nelson,C.S., Ricketts, B.D., Cooke, S., Wedd, M.W., 2001. Effect of Mica on Particle-Size Analyses Using the Laser Diffraction Technique. Journal of Sedimentary Research 71, 507 - 509.

He, Q., Walling, D.E., 1998. An investigation of the spatial variability of the grain size composition of floodplain sediments. Hydrological Processes 12, 1079– 1094.

Heiri, O., A. F. Lotter, and G. Lemcke. 2001. Loss on ignition as a method for estimating organic and carbonate content in sediments: Reproducibility and comparability of results. Journal of Paleolimnology 25, 101-110.

Heitmuller F.T., Hudson P.F., 2009. Downstream trends in sediment size and composition of channel-bed, bar and bank deposits related to hydrologic and lithologic controls in the LIano River watershed, central Texas, USA. Geomorphology 112, 246-260.

Horowitz, A.J., 1991. A Primer on Sediment-trace Element Chemistry. Lewis, MI, USA, pp. 134.

Hughes, M.K., Diaz, H.F., 1994. Was there a “Medieval Warm Period”, and if so, where and when? Climate change 26: 109-142.

Hurst, V.J. , 1977. Visual estimation of iron in saprolite. Geological Society of America Bulletin 88, 174-176.

Jacobson, R.B., Coleman, D.J., 1986. Stratigraphy and recent evolution of Maryland Piedmont floodplains. American Journal of Science 286, 617-637.

Knighton, A.D., 1998. Fluvial Forms and Processes: A New Perspective, and edition. Arnold, London.

Knox, J.C., 1977. Human impacts on Wisconsin stream channels. Annals of the Association of American Geographers 67, 323–342.

Knox, J.C., 1985. Responses of floods to Holocene climatic change in the Upper Mississippi Valley. Quaternary Research 23 (3), 287–300.

Knox, J.C., 1987. Historical valley floor sedimentation in the upper Mississippi Valley. Annals of the Association of American Geographers 77, 224–244.

Knox, J.C., 1993. Large increases in food magnitude in response to modest changes in climate. Nature 361, 430-432.

Knox, J.C., 2000. Sensitivity of modern and Holocene floods to climate change. Quaternary Science Reviews 19, 439-457.

Knox, J.C., 2001. Agricultural influence on landscape sensitivity in the Upper Mississippi River Valley. Catena 42, 193-224.

Knox, J.C., 2006. Floodplain sedimentation in the Upper Mississippi Valley: Natural versus human accelerated. Geomorphology 79, 286-310.

Kochel, R.C., 1988. Geomorphic impact of large floods: Review and new perspectives on magnitude and frequency. In V. R. Baker, R. C. Kochel, and P. C. Patton, eds., Flood Geomorphology. New York, NY: John Wiley and Sons, 279-300.

Lecce, S.A., 1997. Spatial patterns of historical overbank sedimentation and floodplain evolution, Blue River, Wisconsin. Geomorphology 18, 265-277.

Lecce, S.A., Pavlowsky, R.T., 2001. Use of mining-contaminated sediment tracers to investigate the timing and rates of historical flood plain sedimentation. Geomorphology 38 (1–2), 85–108.

Lecce, S.A., Pease,P.P, Gares, P.A., Rigsby, C.A., 2004. Floodplain sedimentation during an extreme flood: The 1999 flood on the tar river, eastern North Carolina. Physical Geography 25, 334-346.

Leigh, D.S., 1994. Mercury contamination and floodplain sedimentation from former gold-mines in north Georgia. Water resources bulletin 30, 739-748.

Leigh, D.S., 1997. Mercury-tainted overbank sediment from past gold mining in north Georgia, USA. Environmental Geology 30, 244-251.

Leigh, D. S., 2006. Terminal Pleistocene braided to meandering transition in rivers of the southeastern USA. Catena 66, 155-160.

Leigh, D.S., 2007. Human influence on Floodplain Sedimentation in the Upper Little Tennessee River Valley, Southern Blue Ridge Mountains, USA. Paper presented at the Annual Meeting of the Association of American Geographers, April 2007, San Francisco, CA.

Leigh, D.S., 2008. Late Quaternary climates and river channels of the Atlantic Coastal Plain, Southeastern USA. Geomorphology 101, 90-108.

Leigh, D.S., in press (a). Morphology and channel evolution of small streams in the southern Blue Ridge Mountains of western North Caronlina. Southeastern Geographer.

Leigh, D.S., in press (b). The Southern Blue Ridge Mountains. Book chapter, Gragson, T editor.
Leigh, D. S. and Feeney, T. P., 1995. Paleochannels indicating wet climate and lack of response to lower sea level, Southeast Georgia. Geology 23, 687-690.

Leigh, D.S., Webb, P.A., 2006. Holocene erosion, sedimentation, and stratigraphy at Raven Fork, Southern Blue Ridge Mountains, USA. Geomorphology 78, 161-177.

Lewin, J., Macklin, M.G., 2005. Interpreting alluvial archives: sedimentological factors in the British Holocene fluvial record. Quaternary Science Review 24, 1873-1889.

Lichtenstein, K.P., 2003. Historic alluvial sedimentation and allostratigraphy of the South Fork of the Broad River, Northeast Georgia. Unpublished MS Thesis, University of Georgia, Athens, Georgia, USA.

Macklin, M.G., Lewin, J., 2003. River sediments, great floods and centennial-scale Holocene climate change. Journal of Quaternary Science 18, 101-105.

Magilligan, F. J., Phillips, J. D., James, L. A., and Gomez, B., 1998. Geomorphic and sedimentological controls on the effectiveness of an extreme flood. Journal of Geology 106, 87–95.

Messick, D.P., Joseph, J.W., Adams, N.P., 2001. Tilling the Earth, Georgia's Historic Agricutural Heritage-A context. Online resources. <http://gashpo.org/assets/documents/tilling_the_earth.pdf>

Miller, S.O., Ritter, D.F., Kochel, R.C., Miller, J.R., 1993. Fluvial responses to land-use changes and climatic variations within the Drury Creek watershed, southern Illinois. Geomorphology 6, 309–329.

Miller, J.R., Lord, M., Yurkovich, S., Mackin, G., Kolenbrander, L., 2005. Historical Trends in Sedimentation Rates and Sediment Provenance, Fairfield Lake, Western North Carolina. Journal of the American Water Resources Association 41, 1053-1075.

Moss, J. H. and Kochel, R. C., 1978. Unexpected geomorphic effects of the Hurricane Agnes storm and flood, Conestoga drainage basin, southeastern Pennsylvania. Journal of Geology 86, 1–11.

Murray, A.S., Wintle, A.G., 2000. Luminescence dating of quartz using an improved single-aliquot regenerative-dose protocol. Radiation Measurements, 27, 171 – 184.

National Climate Data Center (NCDC), 2003. Climatography of the United States no. 84, 1971-2000.

Nichols, G., 1999. Sedimentology and stratigraphy. Blackwell Science Ltd, Oxford, UK. P355.

Nicholas, A.P., Walling, D.E., 1997. Modeling flood hydraulics and overbank deposition on floodplains. Earth Surface Processes and Landforms 17, 687-697.

Nriagu, J.O., 1994. Mercury pollution from the past mining of gold and silver in the Americas. Science of the Total Environment 149, 167–181.

Oblinger, C.J., 2003. Suspended Sediment and Bed Load in Three Tributaries to Lake Emory in the Upper Little Tennessee River Basin, North Carolina, 2000-02. U.S. Geological Survey Water-Resources Investigations Report 03-4194.

Owens, P.N., Walling, D.E., Leeks, G.J.L., 1999. Use of floodplain sediment cores to investigate recent historical changes in overbank sedimentation rates and sediment sources in the catchment of the River Ouse, Yorkshire, UK Source. Catena 36, 21-47.

Patton, P.C., Dibble, D., 1982. Archeologic and geomorphic evidence for the paleohydrologic record of the Pecos river in west Texas. American Journal of Science 282, 97-121.

Pardee, J.T., Park, C.F., 1948. Gold Deposits of the Southern Piedmont. US Geological Survey Professional Paper 213, 156.

Price, K., Leigh, D.S., 2006. Morphological and sedimentological responses of streams to human impact in the southern Blue Ridge Mountains, USA. Geomorphology 78, 142-160.

Robinson, G.R., Lesure, F.G., Marlowe II, J.I., Foley, N.K., Clark, S.H., 1992. Bedrock geology and mineral resources of the Knoxville 1 degrees by 2 degrees quadrangle, Tennessee, North Carolina, and South Carolina. Bulletin, vol. 1979. U.S. Geological Survey, Reston, VA.

Santisteban, J.I., Mediavilla, R., Lopez-Pamo, E., Dabrio, C.J., Zapata, M.B.R., Garcia, M.J.G., et al. (2004). Loss on ignition: A qualitative or quantitative method for organic matter and carbonate mineral content in sediments. Journal of Paleolimnology 32, 287–299.

Sigafoos, R.S., 1964. Botanical Evidence of Floods and Flood-Plain Deposition.Professional Paper, vol. 485A. United States Geological Survey. 35 pp.

Smith, J.G. (2003). Aspects of the loss-on-ignition (LOI) technique in the context of clay-rich glaciolacustrine sediments. Geografiska Annaler 85, 91–97.

Soil Survey Division Staff, 1993. Soil survey manual. Soil Conservation Service. U.S. Department of Agriculture Handbook 18.

Stahle, D. W. and Cleaveland, M. K., 1994. Tree-ring reconstructed rainfall over the Southeastern U.S.A. during the Medieval Warm Period and Little Ice Age. Climatic Change 26, 199-212.

Stahle, D. W., Cleaveland, M. K. and Hehr, J. G., 1988. North Carolina climate changes reconstructed from tree rings: A.D. 372 to 1985. Science 240, 1517-1519.

Stuiver, M., Reimer, P.J., 1993. Extended C-14 data-base and revised Calib 3.0 C-14 age calibration program. Radiocarbon 35 (1), 215-230.

Sutherland, A.S., Meyer, J.L., and Gardiner, E.P., 2002. Effects of land cover on sediment regime and fish assemblage structure in four southern Appalachian streams. Freshwater Biology 47, 1791-1805.

Trimble, S. W., 1974. Man-induced soil erosion on the Southern Piedmont, 1700-1970. Soil Conservations Society of America, pp 180.

U.S. Environmental Protection Agency, 1996. EPA Takes Final Step in Phaseout of Leaded Gasoline. Press release. http://www.epa.gov/history/topics/lead/02.htm.

Viau, A.E., K. Gajewski, M.C. Sawada, and P. Fines. 2006. Millennial-scale temperature variations in North America during the Holocene. Journal of Geophysical Research, Vol. 111, D09102, doi:10.1029/2005JD006031.

Walling, D.E. 1995. Suspended sediment yields in a changing environment. In Gurnell, A. and Petts, G. Changing River Channels. Wiley, Chichester.

Walling, D.E., He, Q., 1997. Use of fallout 137Cs in investigations of overbank sediment deposition on river floodplains. Catena 29, 263-282.

Walling, D.E. and Fang, D. 2003. Recent trends in the suspended sediment loads of the world's rivers. Global and Planetary Change 39(1-2), 111-126.

Watts, W.A. 1970. The full-glacial vegetation of northwestern Georgia. Ecology 51, 17-33.

Werritty, A., Paine, J.L., Macdonald, N., Rowan, J.S., McEwen, L.J., 2006. Use of multi-proxy flood records to improve estimates of flood risk: Lower River Tay, Scotland. Catena 66, 107-119.

Wohl, E., 2000. Mountain rivers. Water Resources Monograph 14. American Geophysical Union, Washington, D.C.

Wolman, M.G., and Leopold, Luna B., 1957, River Flood Plains: Some Observations on their Formation, U.S. Geological Survey Professional Paper 282-C, 30p.

Wolman, M.G., Miller, J.P., 1960. Magnitude and Frequency of Forces in Geomorphic Processes. The journal of Geology, 54-74.

Yarnell, S.L., 1998. The Southern Appalachians: A History of the Landscape. General Technical Report SRS-18, U.S. Department of Agriculture Forest Service Southern Research Station, Asheville, N.C.

APPENDIX A

CORE AND MONOLITH DESCRIPTIONS

Keener 1b Core Description

Ap – 0-6 cm, 10YR2/1, silt loam, moderate fine granular structure, common roots, abrupt boundary

A – 6-12 cm, 10YR3/2, fine loam, weak blocky parting to very fine granular structure, common roots, gradual boundary, feel a little bit of compacted

AB – 12-24 cm, 10YR3/3, silt loam, moderate medium granular structure, common roots, clear boundary, less compacted than above

Ab – 24-29 cm, 10YR3/1, silt loam, moderate medium granular structure, clear boundary

Bb – 29-43 cm, 10YR3/3, silt clay loam, moderate medium subangular blocky structure, clear boundary, redox features (Fe concentration, 5YR4/6)

Ab' – 43-53 cm, 10YR2/1, silt clay loam, weak fine granular structure, clear boundary

Bgb – 53-92 cm, 10YR3/2, silt clay loam, moderate fine/medium blocky structure, gradual boundary

BCg – 92-100 cm, 2.5Y3/2, silt loam, weak blocky structure, gradual boundary, redox feature (root channel, Fe concentration, 10YR5/8, relatively yellower than above Fe concentration)

CBg – 100-120 cm, 2.5Y3/2, fine sandy loam to sandy loam, weak blocky structure, gradual boundary, one plant root form redox features, 5YR4/6

Cg – 120-145 cm, 2.5Y3/1, coarse sandy loam to loamy sand, massive, clear boundary

Cg & Oi – 145-220 cm, sand layers and peat beds interbedded.

145-156 cm, 162-168 cm, 170-174 cm, 190-195 cm, 204-211 cm, sand, 2.5Y6/3

211-220 cm, sandy loam to loamy sand, 2.5Y6/3

156-162 cm, 168-170 cm, 174-190 cm, 195-204 cm are peats, gley 2.5/N, leaves, roots, twigs, producing unpleasant odor

Cg2 – 220-240 cm, 2.5Y3/1, sandy loam to loamy sand, bottom is coarse sand and gravel (bedload)

State Line Core Description

A – 0-7 cm, 10YR3/3, loamy sand, massive, clear boundary, common roots

AC – 7-15 cm, 10YR4/3, loamy sand, massive, clear boundary

C – 15-60 cm, 10YR4/4, loamy sand, massive, contain a light sand layer in 15-19 cm, and sand pockets in 40 cm, 45 cm

Ab – 60-66 cm, 10YR3/2.5, loam, weak subangular blocky structure, clear boundary

AC – 66-74 cm, 10YR4/4, loamy sand, massive, abrupt boundary

C – 74-77 cm, 10YR5/4, sand, massive, abrupt boundary

Ab' – 77-88 cm, 7.5YR3/3 (from 77 cm to 155 cm, soil is redder relative to above or below, maybe still in 10YR page), loam, weak fine subangular blocky structure, clear boundary

Bwb – 88-155 cm, 7.5YR4/4, sandy loam to sandy clay loam, weak fine subangular blocky structure, clear boundary, in 130-139 cm, weak redox feature developed (5YR5/6)

C – 155-159 cm, 10YR5/6, thin stratified loamy sand to fine sand, massive, abrupt boundary

Ab'' – 159-230cm, 10YR3/2, thick Ab horizon with sand layers (possible sand lenses) in 170-176 cm, 200-201 cm (10YR4/6). The top part at 159-170 cm are best expressed

AC – 230-245 cm, 10YR4/6, sandy loam, massive, gradual boundary

C1 – 245-312 cm, 10YR4/6, loamy sand, massive, 298-300 cm develop redox features (7.5YR5/8), 300-312 cm are darker (10YR4/2) may contain more organic matter

C2 –312-360 cm, stratified sand and peat interbeded, 320-330 cm and 352-360 cm sands are better stratified.

State Line Monolith Description

Ab – 175-223 cm, sandy loam to fine loamy sand, very weak subangular blocky structure, only the top part at 175-187 cm is well expressed (10YR2/1), then 3 obvious sand layers with lighter color (10YR4/3) in 187-188 cm, 197-200 cm, 209-213cm, then 213.5-223 cm gets darker, 10YR3/2, possible Ab.

CA – 223-240 cm, 10YR3/3, fine loamy sand, massive, clear boundary

C – 240-280 cm, 10YR4/4, fine sand, massive, two lighter layers: 240-244 cm (2.5Y6/6), 259-261.5 cm (10YR4/6)

Riverside Monolith Description

Oi – 0-6 cm, grass and roots, abrupt boundary

C1 – 6-11 cm, 2.5Y6/2, sand, single grain, loose, common roots, abrupt boundary

C2 – 11-23.5 cm, 2.5Y5/4, fine sand, single grain, loose, common fine roots, clear boundary

C3 – 13.5-42 cm, 10YR4/4, loamy sand, massive (lower part has weak blocky structure), compared with above horizon, a little bit of firm, few fine roots, gradual boundary

Ab1 – 42-57 cm, 10YR3/3, loam, moderate medium blocky structure, clear boundary

Ab2 – 57-72 cm, 10YR2/1, loam, weak fine blocky structure, few fine roots, clear boundary

Ab3 – 72-78 cm, 10YR3/2, loam, weak blocky structure, clear boundary

C' – 78-96 cm, 10YR3/3, fine sand, massive, loose, clear boundary

Ab' – 96-106 cm, 10YR2/2, sandy loam, no distinct structure (weak blocky structure?), clear boundary

AC – 106-122 cm, 10YR3/2, sandy loam, massive, clear boundary, weak stratifications

Ab'' – 122-154 cm, 10YR2/1, loam, moderate medium granular structure, common pores, clear boundary

ABb – 154-166 cm, 10YR3/2, loam, weak blocky structure, gradual boundary

Bwb – 166-200 cm, 10YR3/4, silty loam, weak blocky structure, gradual boundary

BC – 200-210 cm, 10YR4/3, sandy loam, very weak blocky structure, clear wavy boundary

C'' – 210-250 cm, 2.5Y5/4, loamy sand, massive

224-228 cm, 246-248 cm, sand, 2.5Y6/2; 212-214 cm, part sand

Riverside Core Description

Ap – 0-8 cm, 10YR3/3, fine sand, grass roots, sands are contained in the roots, single grain/massive?, clear boundary

AC – 8-17 cm, 10YR4/4, fine sand to loamy sand, less roots than above horizon, gradual boundary

C – 17-36 cm, 10YR4/4, fine loamy sand, massive, common roots, clear boundary

Ab1 – 36-60 cm, 10YR3/3, loam, moderate medium granular structure, common roots, gradual boundary

Ab2 – 60-75 cm, 10YR3/3, loam (finer than above horizon), weak blocky structure, few roots, clear boundary

Ab3 – 75-80 cm, 10YR3/2, loam, weak blocky structure, clear boundary

C' – 80-89 cm, 10YR4/2, loamy sand, massive, clear boundary

Ab' – 89-94 cm, 10YR3/2, sandy loam, structure is not distinct, clear boundary (darker)

AC – 94-113 cm, 10YR3/2, sandy loam, massive, gradual boundary, charcoal at 109cm

Ab'' – 113-146 cm, 10YR2/1, silty loam, moderate medium blocky structure, common fine pores and roots, clear boundary

ABb – 146-160 cm, 10YR3/2, silty loam, weak blocky structure, clear boundary

Bwb – 160-182 cm, 10YR4/3, loam, weak subangular blocky structure, clear boundary

BCb – 182-200 cm, 10YR4/4, loamy sand to sand, clear boundary

C – 200-293 cm

200-240 cm, 2.5Y5/3, fine sand to sand, massive, 240 cm is the end of the second core section, a lot of charcoal at about 220 cm

240-293 cm, 10YR5/4, sand, several lighter zones (252-255, 276-279, 281-282, 2.5Y6/4), redox features

Bedload – 293-340 cm

293-301 cm, coarse sand and gravels

301-307 cm, fine sand, contain several gravels (1 cm)

307-312 cm, sand, very light color, 2.5Y7/2, depletion features

312-316 cm, several black layers

316-340 cm, bedload, very coarse sand with gravels (1.5-2 cm), 326-332 cm is redder 5YR4/6, oxidized zone)

APPENDIX B

PARTICLE SIZE DATA

Table B1 Particle size data from pipette method and CILAS machine. 10 samples at the Keener site were obtained in a 15 cm intervals and used for pipette analysis. The results were compared with those from the CILAS machine.

Sample	Pipette			CILAS		
	clay %	silt %	sand %	clay %	silt %	sand %
KN 0-3	35.20	45.93	18.88	4.5	79.1	16.4
KN 15-18	35.75	46.75	17.50	4.9	81.7	13.4
KN 29-32	36.29	58.19	5.53	6.6	89.6	3.8
KN 43-46.5	38.76	57.69	3.55	7.6	90.9	1.5
KN 60-63.5	32.42	57.49	10.09	4.5	81.1	14.4
KN 77.5-81	28.88	52.00	19.12	3.8	78.5	17.7
KN 95-98.5	22.42	32.33	45.25	2.3	62.9	34.8
KN 112.5-116	13.33	21.27	65.41	1.3	54.3	44.4
KN 130-133.5	5.02	8.76	86.22	0.8	40	59.2
KN 147.5-150	3.96	6.07	89.97	0.6	38.4	61

Table B2 Sand content from the wet sieve method and the CILAS machine. 10 samples from each of the three sites were selected with similar intervals and used for wet sieve analysis. Sand percentages from the wet sieve and CILAS machine were compared.

Sample	sand %	
	wet sieve %	CILAS%
KN 3-6	17.00	17.40
KN 9-12	17.02	17.50
KN 18-21	13.89	15.50
KN 32-35	2.87	1.10
KN 41-43	3.15	1.70
KN 46.5-50	1.80	2.20
KN 56.5-60	6.24	6.80
KN 74-77.5	8.33	11.70
KN 88-91.5	27.39	26.00
KN 102-105.5	67.38	45.50
SLC 0-7	86.76	56.80
SLC 29-43	82.17	56.80
SLC 66-74	65.00	45.90
SLC 102-116	48.11	33.60
SLC 149-155	44.73	32.50
SLM 175-180	75.95	48.50
SLM 205-209	63.46	37.80
SLM 233-238	72.58	47.00
SLM 259-261.5	87.15	52.20
SLC 280-285	58.22	38.80
RSM 0-6	93.57	66.60
RSM 22-24	86.49	54.00
RSM 46-57	44.42	31.90
RSM 78-89	75.80	50.40
RSM 117-122	64.20	43.30
RSM 130-132	40.74	26.10
RSM 152-154	46.27	34.30
RSM 174-176.5	33.55	30.00
RSM 194-196.5	53.77	39.20
RSM 211.5-214	77.78	50.00

Table B3 The 2-2000 μm particle size data at the Keener site. (from CILAS machine, in Phi scale)

Sample ID	depth(cm)	ϕ -1-0	ϕ 0-1	ϕ 1-2	ϕ 2-3	ϕ 3-4	ϕ 4-5	ϕ 5-6	ϕ 6-7	ϕ 7-8	ϕ 8-9	ϕ>9
KN 0-3	1.50	0.00	0.00	0.00	0.94	15.29	34.28	17.02	19.26	8.15	5.06	0.00
KN 3-6	4.50	0.00	0.00	0.00	1.42	17.26	35.66	16.01	17.74	7.34	4.58	0.00
KN 6-9	7.50	0.00	0.00	0.00	1.55	18.37	35.82	15.09	16.91	7.37	4.90	0.00
KN 9-12	10.50	0.00	0.00	0.00	1.23	17.09	35.30	16.09	17.99	7.57	4.73	0.00
KN 12-15	13.50	0.00	0.00	0.00	1.47	18.16	35.89	15.48	17.36	7.22	4.42	0.00
KN 15-18	16.50	0.00	0.00	0.00	0.23	13.93	35.14	17.46	19.72	8.35	5.16	0.00
KN 18-21	19.50	0.00	0.00	0.00	0.94	15.33	34.35	16.64	19.32	8.26	5.16	0.00
KN 21-24	22.50	0.00	0.00	0.00	0.08	10.02	33.73	18.78	21.99	9.60	5.79	0.00
KN 24-27	25.50	0.00	0.00	0.00	0.08	10.02	33.73	18.78	21.99	9.60	5.79	0.00
KN 27-29	28.50	0.00	0.00	0.00	0.00	6.42	31.84	20.04	24.10	10.82	6.78	0.00
KN 29-32	30.50	0.00	0.00	0.00	0.00	4.09	31.63	20.32	25.33	11.40	7.23	0.00
KN 32-35	33.50	0.00	0.00	0.00	0.00	1.24	27.27	21.32	28.35	13.23	8.59	0.00
KN 35-38	36.50	0.00	0.00	0.00	0.00	0.39	26.12	21.75	29.06	13.75	8.93	0.00
KN 38-41	39.50	0.00	0.00	0.00	0.00	1.61	28.54	21.40	27.61	12.60	8.23	0.00
KN 41-43	42.00	0.00	0.00	0.00	0.00	1.87	29.40	20.81	26.98	12.59	8.35	0.00
KN 43-46.5	44.75	0.00	0.00	0.00	0.00	1.52	26.85	20.57	28.30	13.81	8.96	0.00
KN 46.5-50	48.25	0.00	0.00	0.00	0.00	2.34	27.75	20.19	27.70	13.39	8.63	0.00
KN 50-53	51.50	0.00	0.00	0.00	0.00	2.69	28.36	20.24	27.33	13.09	8.29	0.00
KN 53-56.5	54.75	0.00	0.00	0.00	0.00	5.01	29.97	19.89	25.54	12.00	7.60	0.00
KN 56.5-60	58.25	0.00	0.00	0.00	0.00	7.30	32.74	19.02	23.31	10.79	6.83	0.00
KN 60-63.5	61.75	0.00	0.00	0.00	0.19	14.88	37.92	16.23	18.09	7.78	4.91	0.00
KN 63.5-67	65.25	0.00	0.00	0.00	0.07	11.46	36.86	16.97	19.95	9.00	5.70	0.00
KN 67-70.5	68.75	0.00	0.00	0.00	0.00	7.55	35.57	18.17	22.04	10.13	6.56	0.00
KN 70.5-74	72.25	0.00	0.00	0.00	0.00	8.76	35.79	17.66	21.45	9.94	6.41	0.00
KN 74-77.5	75.75	0.00	0.00	0.00	0.09	12.25	38.32	16.75	18.94	8.30	5.35	0.00
KN 77.5-81	79.25	0.00	0.00	0.00	0.27	18.15	41.45	14.44	15.31	6.30	4.08	0.00
KN 81-84.5	82.75	0.00	0.00	0.00	0.29	18.87	41.32	14.16	15.24	6.21	3.92	0.00
KN 84.5-88	86.25	0.00	0.00	0.00	1.03	20.47	41.11	13.29	14.36	5.94	3.81	0.00

KN 88-91.5	89.75	0.00	0.00	0.00	1.92	24.85	41.47	11.77	12.14	4.85	3.02	0.00
KN 91.5-95	93.25	0.00	0.00	0.00	3.89	27.49	37.37	11.50	11.97	4.75	3.03	0.00
KN 95-98.5	96.75	0.00	0.14	3.74	5.50	26.23	38.90	9.73	9.78	3.66	2.32	0.00
KN 98.5-102	100.25	0.00	0.21	5.61	8.22	27.82	36.77	8.40	8.19	2.95	1.82	0.00
KN 102-105.5	103.75	0.00	0.32	8.32	9.34	27.99	36.66	7.16	6.60	2.24	1.36	0.00
KN 105.5-109	107.25	0.00	0.23	5.86	7.52	28.49	38.17	7.97	7.53	2.67	1.57	0.00
KN 109-112.5	110.75	0.00	0.21	5.26	8.50	31.55	35.38	7.70	7.25	2.60	1.55	0.00
KN 112.5-116	114.25	0.00	0.24	6.04	8.65	30.11	37.10	7.26	6.80	2.37	1.42	0.00
KN 116-119.5	117.75	0.00	0.33	8.69	12.71	31.92	32.26	5.89	5.31	1.80	1.09	0.00
KN 119.5-123	121.25	0.00	0.48	11.85	12.56	29.10	31.50	6.01	5.49	1.87	1.13	0.00
KN 123-126.5	124.75	0.00	0.55	13.56	12.22	27.30	31.73	6.03	5.56	1.89	1.17	0.00
KN 126.5-130	128.25	0.00	0.68	17.14	15.19	26.19	28.17	5.20	4.82	1.61	1.01	0.00
KN 130-133.5	131.75	0.00	0.76	18.70	15.34	24.87	28.11	5.05	4.67	1.53	0.97	0.00
KN 133.5-137	135.25	0.00	0.58	14.71	13.64	26.38	31.01	5.67	5.24	1.71	1.07	0.00
KN 137-140.5	138.75	0.00	0.49	11.80	10.53	26.48	34.05	6.78	6.38	2.16	1.32	0.00
KN 140.5-144	142.25	0.00	0.56	14.26	12.34	26.54	32.67	5.74	5.20	1.67	1.02	0.00
KN 144-147.5	145.75	0.00	0.50	12.05	11.28	28.10	32.62	6.27	5.91	2.02	1.25	0.00
KN 147.5-150	148.75	0.00	0.65	16.77	16.88	27.01	28.92	4.31	3.70	1.07	0.69	0.00

Table B4 The 2-2000 μm particle size data at the State Line site. (from CILAS machine, in Phi scale)

Sample ID	depth(cm)	ϕ -1-0	ϕ 0-1	ϕ 1-2	ϕ 2-3	ϕ 3-4	ϕ 4-5	ϕ 5-6	ϕ 6-7	ϕ 7-8	ϕ 8-9	ϕ>9
SLC 0-7	3.50	0.00	0.44	11.71	14.38	41.99	19.06	5.19	4.67	1.58	0.97	0.00
SLC 7-15	11.00	0.00	0.45	11.80	13.22	43.81	18.94	5.10	4.42	1.41	0.85	0.00
SLC 15-29	22.00	0.00	0.40	11.33	14.42	41.31	20.53	5.10	4.52	1.47	0.92	0.00
SLC 29-43	36.00	0.00	0.36	9.65	11.69	42.56	21.97	5.82	5.17	1.72	1.06	0.00
SLC 43-52	47.50	0.00	0.26	7.71	11.92	41.52	22.80	6.44	5.94	2.10	1.29	0.00
SLC 52-60	56.00	0.00	0.14	4.29	11.06	45.72	22.10	6.80	6.33	2.23	1.32	0.00
SLC 60-66	63.00	0.00	0.00	0.00	3.58	45.57	30.01	8.37	7.94	2.82	1.70	0.00
SLC 66-74	70.00	0.00	0.12	3.56	10.18	44.89	22.71	7.32	7.06	2.58	1.59	0.00
SLC 74-77	75.50	0.00	0.49	14.96	17.53	35.70	19.55	4.82	4.39	1.56	1.00	0.00
SLC 77-88	82.50	0.00	0.00	0.00	2.33	43.31	28.44	9.72	9.85	3.87	2.48	0.00
SLC 88-102	95.00	0.00	0.00	0.00	4.87	43.32	26.21	9.42	9.76	3.88	2.54	0.00
SLC 102-116	109.00	0.00	0.00	0.00	3.93	43.47	26.77	9.42	9.85	3.99	2.57	0.00
SLC 116-130	123.00	0.00	0.00	0.00	3.86	42.22	26.62	9.78	10.39	4.32	2.81	0.00
SLC 130-139	134.50	0.00	0.00	0.00	5.01	44.57	25.99	9.14	9.23	3.67	2.37	0.00
SLC 139-149	144.00	0.00	0.12	3.15	6.54	40.65	24.60	9.25	9.50	3.80	2.40	0.00
SLC 149-155	152.00	0.00	0.00	0.00	3.81	42.11	26.72	9.99	10.40	4.25	2.73	0.00
SLM 175-180	157.00	0.00	0.24	6.32	9.95	45.36	22.64	6.32	5.90	2.01	1.26	0.00
SLM 180-185	161.50	0.00	0.00	0.00	4.54	47.79	27.46	8.06	7.78	2.71	1.65	0.00
SLM 185-190	167.00	0.00	0.00	0.00	4.11	47.56	28.20	8.08	7.70	2.71	1.64	0.00
SLM 190-195	172.50	0.00	0.00	0.00	2.74	47.74	28.64	8.25	8.03	2.86	1.75	0.00
SLM 195-200	177.50	0.00	0.00	0.00	4.76	46.78	25.23	8.75	8.92	3.41	2.16	0.00
SLM 200-205	182.50	0.00	0.00	0.00	4.80	49.71	27.50	7.26	6.90	2.38	1.45	0.00
SLM 205-209	187.50	0.00	0.00	0.00	4.01	49.08	27.97	7.59	7.24	2.56	1.55	0.00
SLM 209-213	192.50	0.00	0.25	6.53	12.71	45.60	20.12	6.14	5.59	1.90	1.15	0.00
SLM 213-218	197.50	0.00	0.16	3.92	7.59	47.80	24.30	6.59	6.20	2.12	1.32	0.00
SLM 218-223	202.50	0.00	0.14	3.47	6.66	47.40	25.66	6.72	6.46	2.14	1.35	0.00
SLM 223-228	207.50	0.00	0.00	0.00	6.68	49.83	23.90	7.72	7.50	2.71	1.65	0.00
SLM 228-233	212.50	0.00	0.15	3.64	8.05	48.46	23.40	6.62	6.27	2.11	1.30	0.00

SLM 233-238	217.50	0.00	0.17	4.35	8.94	47.22	23.04	6.64	6.23	2.13	1.28	0.00
SLM 238-240	222.50	0.00	0.16	3.88	7.41	47.28	24.59	6.86	6.37	2.15	1.29	0.00
SLM 240-244	227.50	0.00	0.31	8.31	11.04	46.81	22.01	5.11	4.33	1.32	0.77	0.00
SLM 244-249	232.50	0.00	0.23	6.20	11.73	47.29	20.14	6.01	5.45	1.84	1.11	0.00
SLM 249-254	237.50	0.00	0.24	6.22	12.37	46.27	20.11	6.07	5.61	1.95	1.15	0.00
SLM 254-259	242.50	0.00	0.21	5.32	10.21	45.91	21.13	6.95	6.61	2.30	1.36	0.00
SLM 259-261.5	247.50	0.00	0.30	7.81	10.32	47.29	22.35	5.36	4.46	1.33	0.78	0.00
SLM261.5-266.5	252.50	0.00	0.29	7.94	14.90	44.37	18.37	5.82	5.36	1.84	1.11	0.00
SLC 260-265	257.50	0.00	0.14	3.22	8.99	48.62	21.83	7.00	6.49	2.33	1.38	0.00
SLC 265-270	262.50	0.00	0.00	0.16	8.77	47.51	22.00	8.34	8.23	3.09	1.90	0.00
SLC 270-275	267.50	0.00	0.13	3.07	8.95	46.02	21.53	7.82	7.77	2.93	1.79	0.00
SLC 275-280	272.50	0.00	0.00	0.00	6.31	47.87	24.25	8.31	8.28	3.10	1.88	0.00
SLC 280-285	277.50	0.00	0.00	0.00	5.03	48.22	25.40	8.30	8.18	3.05	1.83	0.00
SLC 285-290	282.50	0.00	0.00	0.00	6.26	48.06	24.34	8.24	8.20	3.04	1.86	0.00
SLC 290-295	287.50	0.00	0.00	0.00	5.61	49.22	25.86	7.73	7.39	2.61	1.58	0.00
SLC 295-300	292.50	0.00	0.19	4.27	7.52	47.56	23.61	6.76	6.41	2.25	1.42	0.00
SLC 300-306	297.50	0.00	0.18	4.33	6.85	46.08	24.57	7.26	6.87	2.42	1.44	0.00
SLC 306-312	303.00	0.00	0.21	5.12	8.61	47.88	22.88	6.46	5.79	1.93	1.11	0.00

Table B5 The 2-2000 μm particle size data at the Riverside site. (from CILAS machine, in Phi scale)

Sample ID	depth(cm)	ϕ -1-0	ϕ 0-1	ϕ 1-2	ϕ 2-3	ϕ 3-4	ϕ 4-5	ϕ 5-6	ϕ 6-7	ϕ 7-8	ϕ 8-9	ϕ>9
RSM 0-6	3.00	0.00	0.81	21.90	20.96	32.13	14.92	3.84	3.51	1.17	0.76	0.00
RSM 6-11	8.50	0.00	0.68	16.53	13.88	39.80	18.06	4.70	4.16	1.36	0.83	0.00
RSM 11-22	17.50	0.00	0.53	13.83	14.58	40.37	18.67	5.06	4.49	1.53	0.94	0.00
RSM 22-24	23.00	0.00	0.38	10.70	14.26	40.54	20.81	5.45	5.13	1.68	1.05	0.00
RSM 24-35	29.50	0.00	0.34	9.39	12.85	40.84	20.81	6.29	6.07	2.10	1.30	0.00
RSM 35-46	40.50	0.00	0.16	4.24	6.38	42.68	26.98	7.72	7.53	2.68	1.63	0.00
RSM 46-57	51.50	0.00	0.00	0.00	2.61	43.16	28.36	9.77	9.98	3.78	2.33	0.00
RSM 57-68	62.50	0.00	0.00	0.00	3.47	41.11	27.59	10.09	10.77	4.25	2.71	0.00
RSM 68-72	70.00	0.00	0.00	0.00	3.76	42.17	27.09	10.02	10.34	4.05	2.57	0.00
RSM 72-78	75.00	0.00	0.18	4.98	9.12	41.01	24.24	7.93	7.83	2.91	1.80	0.00
RSM 78-89	83.50	0.00	0.24	6.41	11.09	45.58	21.58	6.18	5.81	1.93	1.18	0.00
RSM 89-96	92.50	0.00	0.20	5.42	10.47	45.61	22.16	6.58	6.22	2.09	1.25	0.00
RSM 96-106	101.00	0.00	0.19	5.08	9.02	43.08	24.43	7.44	7.01	2.36	1.39	0.00
RSM 106-117	111.50	0.00	0.24	5.89	8.34	46.17	23.66	6.44	5.98	2.06	1.22	0.00
RSM 117-122	119.50	0.00	0.15	4.26	8.02	44.28	25.51	7.32	6.81	2.31	1.33	0.00
RSM 122-124.5	123.25	0.00	0.12	3.06	6.48	41.14	25.24	9.06	9.16	3.57	2.17	0.00
RSM 124.5-127	125.75	0.00	0.00	0.00	3.65	38.66	26.64	11.56	11.98	4.70	2.82	0.00
RSM 127-130	128.50	0.00	0.00	0.00	2.43	37.33	26.65	12.09	12.86	5.35	3.30	0.00
RSM 130-132	131.00	0.00	0.00	0.00	3.19	34.26	26.18	12.37	14.03	6.18	3.80	0.00
RSM 132-134.5	133.25	0.00	0.00	0.00	2.14	32.20	25.94	13.60	15.29	6.74	4.09	0.00
RSM 134.5-137	135.75	0.00	0.00	0.91	5.50	31.24	24.07	12.90	14.75	6.60	4.03	0.00
RSM 137-139.5	138.25	0.00	0.00	2.54	7.68	33.65	22.89	11.45	12.84	5.53	3.42	0.00
RSM 139.5-142	140.75	0.00	0.00	1.98	5.78	31.27	23.80	12.27	14.38	6.48	4.05	0.00
RSM 142-144.5	143.25	0.00	0.00	0.00	4.21	35.56	25.61	11.87	13.31	5.82	3.63	0.00
RSM 144.5-147	145.75	0.00	0.00	0.00	3.29	36.26	26.71	11.52	13.02	5.71	3.49	0.00
RSM 147-149.5	148.25	0.00	0.00	0.00	3.42	33.79	26.12	12.52	14.14	6.21	3.80	0.00
RSM 149.5-152	150.75	0.00	0.00	1.93	5.67	34.15	24.66	11.66	12.92	5.59	3.43	0.00
RSM 152-154	153.00	0.00	0.00	2.13	6.42	37.61	24.78	10.64	11.12	4.51	2.78	0.00

RSM 154-156.5	155.25	0.00	0.00	0.00	3.25	37.12	26.74	11.74	12.52	5.33	3.30	0.00
RSM 156.5-159	157.75	0.00	0.00	0.00	3.86	38.94	26.55	11.42	11.75	4.66	2.82	0.00
RSM 159-161.5	160.25	0.00	0.00	0.00	3.42	37.02	26.90	11.74	12.49	5.20	3.23	0.00
RSM 161.5-164	162.75	0.00	0.00	0.00	4.08	38.19	26.37	11.39	11.99	4.93	3.03	0.00
RSM 164-166.5	165.25	0.00	0.00	1.96	5.74	37.81	25.36	10.75	11.07	4.54	2.77	0.00
RSM 166.5-169	167.75	0.00	0.00	0.00	2.30	36.72	27.38	12.35	12.93	5.16	3.15	0.00
RSM 169-171.5	170.25	0.00	0.00	0.00	2.43	39.89	27.34	11.51	11.59	4.52	2.72	0.00
RSM 171.5-174	172.75	0.00	0.00	0.00	3.94	39.79	25.96	11.25	11.51	4.63	2.93	0.00
RSM 174-176.5	175.25	0.00	0.00	0.00	2.41	40.57	26.76	11.23	11.50	4.62	2.91	0.00
RSM 176.5-179	177.75	0.00	0.00	0.00	2.38	39.74	26.87	11.46	11.75	4.81	2.99	0.00
RSM 179-181.5	180.25	0.00	0.00	0.00	2.08	41.56	27.72	10.63	10.89	4.37	2.74	0.00
RSM 181.5-184	182.75	0.00	0.00	0.00	2.58	43.43	27.40	9.97	10.13	3.99	2.50	0.00
RSM 184-186.5	185.25	0.00	0.00	0.00	2.77	43.35	26.23	10.41	10.58	4.12	2.55	0.00
RSM 186.5-189	187.75	0.00	0.00	0.00	4.22	43.95	26.27	9.86	9.70	3.76	2.25	0.00
RSM 189-191.5	190.25	0.00	0.00	0.00	5.18	45.80	25.66	9.13	8.85	3.37	2.00	0.00
RSM 191.5-194	192.75	0.00	0.00	0.00	5.38	47.65	25.84	8.16	8.03	3.09	1.85	0.00
RSM 194-196.5	195.25	0.00	0.00	0.00	4.93	48.95	25.85	8.02	7.69	2.84	1.73	0.00
RSM 196.5-199	197.75	0.00	0.00	0.00	4.45	47.07	27.46	8.26	8.07	2.92	1.77	0.00
RSM 199-201.5	200.25	0.00	0.00	0.00	5.01	47.75	27.18	7.97	7.65	2.74	1.68	0.00
RSM 201.5-204	202.75	0.00	0.18	4.14	7.05	47.03	24.40	6.97	6.54	2.32	1.38	0.00
RSM 204-206.5	205.25	0.00	0.19	4.84	8.41	46.77	23.65	6.53	6.14	2.16	1.30	0.00
RSM 206.5-209	207.75	0.00	0.19	4.72	7.28	46.36	25.11	6.69	6.24	2.16	1.25	0.00
RSM 209-211.5	210.25	0.00	0.20	5.32	8.08	45.28	24.57	6.69	6.27	2.23	1.35	0.00
RSM 211.5-214	212.75	0.00	0.29	8.02	10.96	43.78	22.96	5.84	5.32	1.76	1.08	0.00
RSM 214-216.5	215.25	0.00	0.32	8.71	11.37	44.07	22.47	5.59	4.92	1.58	0.97	0.00
RSM 216.5-219	217.75	0.00	0.32	8.70	11.92	44.73	21.91	5.35	4.68	1.49	0.90	0.00
RSM 219-221.5	220.25	0.00	0.43	12.23	18.73	42.26	16.57	4.24	3.68	1.14	0.72	0.00
RSM 221.5-224	222.75	0.00	0.35	10.83	15.52	41.98	21.08	4.54	3.91	1.10	0.69	0.00
RSM 224-226.5	225.25	0.00	0.60	17.46	19.53	36.58	17.60	3.76	3.05	0.86	0.55	0.00
RSM 226.5-228	227.25	0.00	0.55	16.18	19.47	37.78	17.39	3.85	3.22	0.95	0.61	0.00
RSM 228-230.5	229.25	0.00	0.47	13.46	18.47	41.01	17.51	3.95	3.41	1.05	0.66	0.00

RSM 230.5-233	231.75	0.00	0.41	11.09	14.36	43.70	20.04	4.62	3.90	1.17	0.71	0.00
RSM 233-235.5	234.25	0.00	0.38	10.13	13.21	44.55	20.71	4.84	4.15	1.26	0.76	0.00
RSM 235.5-238	236.75	0.00	0.36	9.65	12.21	44.82	22.03	4.91	4.10	1.21	0.71	0.00
RSM 238-240.5	239.25	0.00	0.41	10.94	13.90	44.04	20.21	4.65	3.93	1.19	0.72	0.00
RSM 240.5-243	241.75	0.00	0.30	7.17	6.97	48.38	24.77	5.56	4.68	1.39	0.78	0.00
RSC 227.5-230	244.25	0.00	0.50	13.28	12.72	42.17	21.14	4.61	3.85	1.06	0.67	0.00
RSC 230-232.5	246.75	0.00	0.59	14.80	12.08	42.21	20.47	4.45	3.74	1.03	0.64	0.00
RSC 232.5-235	249.25	0.00	0.66	17.63	16.15	38.29	18.26	3.99	3.41	0.98	0.64	0.00
RSC 235-237.5	251.75	0.00	0.64	16.30	13.22	40.57	19.61	4.36	3.62	1.03	0.65	0.00
RSC 237.5-240	254.25	0.00	0.64	17.84	17.92	37.27	17.58	3.83	3.33	0.94	0.65	0.00
RSC 240-242.5	256.75	0.00	0.54	14.80	12.19	38.54	23.31	4.85	4.01	1.09	0.68	0.00
RSC 242.5-245	259.25	0.00	0.59	15.88	14.71	39.38	19.69	4.38	3.67	1.04	0.66	0.00
RSC 245-247.5	261.75	0.00	0.59	15.88	15.02	39.92	19.36	4.19	3.46	0.98	0.61	0.00
RSC 247.5-250	264.25	0.00	0.61	16.57	15.62	39.45	18.85	4.03	3.33	0.94	0.60	0.00
RSC 250-252.5	266.75	0.00	0.68	19.78	19.88	34.47	17.07	3.65	3.03	0.86	0.58	0.00
RSC 252.5-255	269.25	0.00	0.57	15.97	17.02	39.77	17.93	3.92	3.27	0.93	0.62	0.00
RSC 255-257.5	271.75	0.00	0.64	17.94	17.35	38.11	17.45	3.83	3.16	0.92	0.59	0.00
RSC 257.5-260	274.25	0.00	0.54	13.38	11.62	44.04	20.27	4.63	3.80	1.06	0.66	0.00
RSC 260-262.5	276.75	0.00	0.37	9.77	11.86	45.44	21.26	4.96	4.27	1.28	0.78	0.00
RSC 262.5-265	279.25	0.00	0.49	13.05	14.53	42.53	19.52	4.44	3.70	1.07	0.66	0.00
RSC 265-267.5	281.75	0.00	0.48	12.89	13.37	41.87	21.12	4.66	3.84	1.08	0.68	0.00
RSC 267.5-270	284.25	0.00	0.57	15.75	16.77	39.17	17.71	4.47	3.72	1.13	0.70	0.00
RSC 270-272.5	286.75	0.00	0.58	16.52	18.51	37.80	17.19	4.17	3.49	1.07	0.67	0.00
RSC 272.5-275	289.25	0.00	0.67	18.24	15.83	37.00	19.12	4.12	3.42	0.97	0.63	0.00
RSC 275-277.5	291.75	0.00	0.48	12.58	13.64	43.05	19.87	4.59	3.91	1.17	0.71	0.00
RSC 277.5-280	294.25	0.00	0.39	10.52	12.71	42.91	21.34	5.30	4.57	1.41	0.85	0.00
RSC 280-282.5	296.75	0.00	0.59	15.82	13.66	38.43	21.01	4.69	3.92	1.17	0.71	0.00
RSC 282.5-285	299.25	0.00	0.50	13.34	13.09	42.01	20.69	4.68	3.89	1.12	0.68	0.00
RSC 285-287.5	301.75	0.00	0.76	19.08	14.18	38.19	18.44	4.21	3.49	1.01	0.63	0.00
RSC 287.5-290	304.25	0.00	0.72	17.83	12.96	39.51	19.35	4.33	3.62	1.05	0.64	0.00

APPENDIX C

LOSS-ON-IGNITION (LOI) DATA

Table C1 Loss-On-Ignition (LOI) data at the Keener site

Sample name	Depth (cm)	LOI %
KN 0-3	1.50	23.73
KN 3-6	4.50	21.11
KN 6-9	7.50	19.84
KN 9-12	10.50	18.46
KN 12-15	13.50	17.88
KN 15-18	16.50	18.53
KN 18-21	19.50	19.75
KN 21-24	22.50	19.10
KN 24-27	25.50	20.10
KN 27-29	28.50	20.58
KN 29-32	30.50	20.86
KN 32-35	33.50	22.16
KN 35-38	36.50	22.00
KN 38-41	39.50	21.22
KN 41-43	42.00	21.76
KN 43-46.5	44.75	22.46
KN 46.5-50	48.25	20.47
KN 50-53	51.50	21.63
KN 53-56.5	54.75	19.27
KN 56.5-60	58.25	17.75
KN 60-63.5	61.75	17.02
KN 63.5-67	65.25	16.96
KN 67-70.5	68.75	17.60
KN 70.5-74	72.25	16.32
KN 74-77.5	75.75	15.69
KN 77.5-81	79.25	14.24
KN 81-84.5	82.75	14.25
KN 84.5-88	86.25	13.97
KN 88-91.5	89.75	12.44
KN 91.5-95	93.25	12.80
KN 95-98.5	96.75	10.73
KN 98.5-102	100.25	9.16
KN 102-105.5	103.75	7.99

Table C2 Loss-On-Ignition (LOI) data at the State Line site

Sample name	Depth (cm)	LOI %
SLC 0-7	3.50	4.80
SLC 7-15	11.00	3.75
SLC 15-29	22.00	4.00
SLC 29-43	36.00	4.65
SLC 43-52	47.50	4.78
SLC 52-60	56.00	6.03
SLC 60-66	63.00	6.69
SLC 66-74	70.00	7.07
SLC 74-77	75.50	2.81
SLC 77-88	82.50	9.84
SLC 88-102	95.00	9.95
SLC 102-116	109.00	9.62
SLC 116-130	123.00	10.10
SLC 130-139	134.50	10.00
SLC 139-149	144.00	9.28
SLC 149-155	152.00	10.20
SLM 175-180	157.00	6.12
SLM 180-185	161.50	8.88
SLM 185-190	167.00	8.24
SLM 190-195	172.50	7.37
SLM 195-200	177.50	8.63
SLM 200-205	182.50	6.83
SLM 205-209	187.50	7.44
SLM 209-213	192.50	5.11
SLM 213-218	197.50	7.09
SLM 218-223	202.50	6.51
SLM 223-228	207.50	6.77
SLM 228-233	212.50	6.19
SLM 233-238	217.50	6.13
SLM 238-240	222.50	5.83
SLM 240-244	227.50	3.36
SLM 244-249	232.50	4.66
SLM 249-254	237.50	4.95
SLM 254-259	242.50	5.01
SLM 259-261.5	247.50	3.49
SLM 261.5-266.5	252.50	4.48
SLC 260-265	257.50	6.00
SLC 265-270	262.50	7.22
SLC 270-275	267.50	6.85
SLC 275-280	272.50	7.08
SLC 280-285	277.50	7.82
SLC 285-290	282.50	7.96

SLC 290-295	287.50	7.03
SLC 295-300	292.50	6.25
SLC 300-306	297.50	6.47
SLC 306-312	303.00	6.31

Table C3 Loss-On-Ignition (LOI) data at the Riverside site

Sample name	Depth (cm)	LOI %
RSM 0-6	3.00	2.05
RSM 6-11	8.50	2.40
RSM 11-22	17.50	3.18
RSM 22-24	23.00	3.28
RSM 24-35	29.50	4.38
RSM 35-46	40.50	5.94
RSM 46-57	51.50	8.94
RSM 57-68	62.50	9.13
RSM 68-72	70.00	9.15
RSM 72-78	75.00	7.59
RSM 78-89	83.50	4.98
RSM 89-96	92.50	5.08
RSM 96-106	101.00	6.15
RSM 106-117	111.50	6.10
RSM 117-122	119.50	6.66
RSM 122-124.5	123.25	9.67
RSM 124.5-127	125.75	10.42
RSM 127-130	128.50	11.07
RSM 130-132	131.00	10.01
RSM 132-134.5	133.25	10.55
RSM 134.5-137	135.75	11.07
RSM 137-139.5	138.25	10.37
RSM 139.5-142	140.75	10.39
RSM 142-144.5	143.25	10.46
RSM 144.5-147	145.75	10.36
RSM 147-149.5	148.25	9.93
RSM 149.5-152	150.75	9.55
RSM 152-154	153.00	8.86
RSM 154-156.5	155.25	8.95
RSM 156.5-159	157.75	9.38
RSM 159-161.5	160.25	9.46
RSM 161.5-164	162.75	9.02
RSM 164-166.5	165.25	9.23
RSM 166.5-169	167.75	9.43
RSM 169-171.5	170.25	9.49
RSM 171.5-174	172.75	9.56

RSM 174-176.5	175.25	10.04
RSM 176.5-179	177.75	9.95
RSM 179-181.5	180.25	9.39
RSM 181.5-184	182.75	9.13
RSM 184-186.5	185.25	8.82
RSM 186.5-189	187.75	8.35
RSM 189-191.5	190.25	8.00
RSM 191.5-194	192.75	7.62
RSM 194-196.5	195.25	7.43
RSM 196.5-199	197.75	6.87
RSM 199-201.5	200.25	6.43
RSM 201.5-204	202.75	6.07
RSM 204-206.5	205.25	5.83
RSM 206.5-209	207.75	5.69
RSM 209-211.5	210.25	5.18
RSM 211.5-214	212.75	4.03
RSM 214-216.5	215.25	3.21

APPENDIX D

CHEMICAL DATA

Table D1 35 element concentrations at the Keener Site

SAMPLE	Ag	Al	As	B	Ba	Be	Bi	Ca	Cd	Co	Cr	Cu
	ppm	%	ppm	ppm	ppm	ppm	ppm	%	ppm	ppm	ppm	ppm
KN 0-3	<0.2	5.76	<2	50	210	2.1	<2	0.26	<0.5	19	44	33
KN 3-6	<0.2	6.07	5	30	200	2.2	<2	0.19	<0.5	20	44	34
KN 6-9	<0.2	6.4	4	20	200	2.3	<2	0.14	<0.5	19	47	36
KN 9-12	<0.2	6.37	4	20	190	2.3	<2	0.1	<0.5	19	47	36
KN 12-15	<0.2	6.29	2	10	190	2.3	<2	0.07	<0.5	20	46	34
KN 15-18	<0.2	6.81	3	10	200	2.5	<2	0.06	<0.5	20	49	37
KN 18-21	<0.2	6.78	4	10	200	2.5	<2	0.05	<0.5	20	49	36
KN 21-24	<0.2	6.99	3	10	210	2.6	<2	0.05	<0.5	21	49	38
KN 24-27	<0.2	7.23	4	10	210	2.7	<2	0.05	<0.5	21	51	39
KN 27-29	<0.2	7.8	6	10	230	3	<2	0.04	<0.5	21	56	42
KN 29-32	<0.2	8.44	5	10	240	3.2	<2	0.04	<0.5	21	61	45
KN 32-35	<0.2	8.77	2	10	230	3.3	<2	0.04	<0.5	23	62	48
KN 35-38	<0.2	8.77	5	10	230	3.4	<2	0.04	<0.5	28	62	48
KN 38-41	<0.2	8.26	<2	<10	220	3.3	<2	0.04	<0.5	25	58	46
KN 41-43	<0.2	8.31	<2	<10	220	3.5	<2	0.03	<0.5	25	58	44
KN 43-46.5	0.3	8.01	<2	<10	220	3.6	3	0.03	<0.5	31	56	42
KN 46.5-50	<0.2	8.02	<2	<10	220	3.6	2	0.03	<0.5	28	56	41
KN 50-53	<0.2	8.19	<2	<10	220	3.5	<2	0.03	<0.5	25	58	45
KN 53-56.5	<0.2	8.09	<2	<10	220	3.4	2	0.03	<0.5	24	58	41
KN 56.5-60	<0.2	7.89	2	<10	210	3.2	<2	0.03	<0.5	23	56	37

KN 60-63.5	<0.2	7.52	<2	<10	210	3.1	2	0.03	<0.5	21	55	36
KN 63.5-67	<0.2	7.88	<2	<10	220	3.3	<2	0.03	<0.5	21	57	38
KN 67-70.5	<0.2	7.91	<2	<10	230	3.5	<2	0.03	<0.5	22	58	40
KN 70.5-74	<0.2	7.96	2	<10	230	3.5	<2	0.03	<0.5	21	58	38
KN 74-77.5	<0.2	8.07	2	<10	240	3.5	<2	0.03	<0.5	21	59	38
KN 77.5-81	<0.2	7.44	<2	<10	230	3.4	<2	0.03	<0.5	21	55	36
KN 81-84.5	<0.2	7.4	<2	<10	230	3.3	<2	0.03	<0.5	20	55	37
KN 84.5-88	<0.2	7.04	<2	<10	230	3.2	<2	0.03	<0.5	19	53	35
KN 88-91.5	<0.2	6.42	<2	<10	220	3.1	<2	0.03	<0.5	18	51	32
KN 91.5-95	<0.2	5.77	<2	<10	200	2.7	<2	0.04	<0.5	17	47	29
KN 95-98.5	<0.2	5.31	<2	<10	200	2.6	<2	0.03	<0.5	16	44	27
KN 98.5-102	<0.2	4.26	<2	<10	170	2.2	<2	0.03	<0.5	13	37	22
KN 102-105.5	<0.2	3.38	<2	<10	150	1.7	<2	0.03	<0.5	11	31	17

SAMPLE	Fe	Ga	Hg	K	La	Mg	Mn	Mo	Na	Ni	P	Pb
	%	ppm	ppm	%	ppm	%	ppm	ppm	%	ppm	ppm	ppm
KN 0-3	3.77	20	0.09	0.29	30	0.49	1145	<1	<0.01	25	1030	33
KN 3-6	3.86	20	0.08	0.3	40	0.51	1155	<1	<0.01	24	910	26
KN 6-9	4.14	20	0.09	0.3	40	0.51	1070	<1	<0.01	26	810	29
KN 9-12	4.1	20	0.08	0.3	40	0.51	1065	<1	<0.01	26	770	26
KN 12-15	4.18	20	0.08	0.3	40	0.5	1070	<1	<0.01	26	690	27
KN 15-18	4.28	20	0.08	0.3	40	0.51	1075	1	<0.01	28	720	27
KN 18-21	4.24	20	0.08	0.28	40	0.49	1045	1	<0.01	27	700	27
KN 21-24	4.29	20	0.08	0.28	40	0.49	1150	1	<0.01	28	680	25
KN 24-27	4.37	20	0.08	0.28	40	0.5	1095	1	<0.01	28	720	26
KN 27-29	4.43	20	0.08	0.26	40	0.5	811	<1	<0.01	33	710	28
KN 29-32	4.7	20	0.08	0.27	50	0.53	572	1	<0.01	36	740	27
KN 32-35	5.69	20	0.08	0.24	50	0.5	835	1	<0.01	37	790	27
KN 35-38	6.46	20	0.07	0.23	50	0.5	1240	1	<0.01	35	790	26
KN 38-41	6.22	20	0.06	0.22	50	0.51	1110	<1	0.01	33	770	21
KN 41-43	6.01	20	0.07	0.2	50	0.52	817	<1	0.01	33	800	21
KN 43-46.5	5.8	20	0.07	0.18	50	0.49	974	<1	0.01	30	820	25

KN 46.5-50	4.69	20	0.07	0.17	50	0.5	584	<1	0.01	31	800	27
KN 50-53	4.31	20	0.08	0.19	50	0.53	404	<1	0.01	33	800	20
KN 53-56.5	4.86	20	0.06	0.22	50	0.55	436	<1	0.01	35	720	21
KN 56.5-60	4.58	20	0.06	0.25	40	0.56	400	<1	0.01	34	650	21
KN 60-63.5	4.35	20	0.07	0.27	40	0.58	398	<1	0.01	33	590	20
KN 63.5-67	4.45	20	0.07	0.28	50	0.59	369	<1	0.01	34	620	19
KN 67-70.5	4.93	20	0.08	0.26	50	0.57	390	<1	0.01	35	700	19
KN 70.5-74	5.38	20	0.08	0.27	50	0.58	383	<1	0.01	36	700	21
KN 74-77.5	5.13	20	0.07	0.28	50	0.6	351	<1	0.01	35	650	21
KN 77.5-81	4.92	20	0.06	0.3	50	0.61	338	<1	0.01	36	600	18
KN 81-84.5	4.61	20	0.06	0.31	50	0.62	318	<1	0.01	35	590	17
KN 84.5-88	4.51	20	0.06	0.32	50	0.63	319	<1	0.01	34	550	17
KN 88-91.5	4.25	20	0.05	0.32	50	0.64	300	<1	0.01	33	500	14
KN 91.5-95	3.86	20	0.05	0.3	40	0.59	356	<1	0.01	30	500	14
KN 95-98.5	3.49	20	0.04	0.31	40	0.58	277	<1	0.01	28	430	12
KN 98.5-102	2.91	10	0.04	0.29	30	0.52	250	<1	0.01	23	360	9
KN 102-105.5	2.39	10	0.03	0.27	30	0.47	196	<1	0.01	21	290	7

SAMPLE	S	Sb	Sc	Sr	Th	Ti	Tl	U	V	W	Zn
	%	ppm	ppm	ppm	ppm	%	ppm	ppm	ppm	ppm	ppm
KN 0-3	0.07	<2	6	12	<20	0.16	<10	<10	72	<10	108
KN 3-6	0.06	<2	6	10	<20	0.17	<10	<10	74	<10	107
KN 6-9	0.06	<2	7	9	<20	0.19	<10	<10	79	<10	106
KN 9-12	0.05	<2	7	8	<20	0.19	<10	<10	79	<10	103
KN 12-15	0.05	<2	7	7	<20	0.2	<10	<10	78	<10	102
KN 15-18	0.05	2	8	7	<20	0.2	<10	<10	82	<10	106
KN 18-21	0.05	<2	8	7	<20	0.19	<10	<10	82	<10	102
KN 21-24	0.06	<2	8	7	<20	0.2	<10	<10	84	<10	106
KN 24-27	0.06	<2	8	7	<20	0.2	<10	<10	87	<10	109
KN 27-29	0.06	<2	9	7	<20	0.21	<10	<10	94	<10	113
KN 29-32	0.06	<2	10	8	<20	0.22	<10	<10	103	<10	118
KN 32-35	0.08	3	11	8	<20	0.21	<10	<10	108	<10	113

KN 35-38	0.08	<2	11	7	<20	0.21	<10	<10	108	<10	110
KN 38-41	0.08	<2	10	8	<20	0.2	<10	<10	102	<10	105
KN 41-43	0.08	<2	9	7	<20	0.2	<10	<10	100	<10	105
KN 43-46.5	0.08	<2	8	8	<20	0.19	<10	<10	97	<10	102
KN 46.5-50	0.07	<2	8	7	<20	0.18	<10	<10	94	<10	105
KN 50-53	0.06	<2	8	8	<20	0.19	<10	<10	97	<10	109
KN 53-56.5	0.06	<2	9	7	<20	0.2	<10	<10	97	<10	109
KN 56.5-60	0.05	<2	9	7	<20	0.21	<10	<10	95	<10	107
KN 60-63.5	0.04	<2	9	7	<20	0.22	<10	<10	91	<10	110
KN 63.5-67	0.05	<2	9	7	<20	0.22	<10	<10	95	<10	115
KN 67-70.5	0.05	<2	9	8	<20	0.21	<10	<10	97	<10	120
KN 70.5-74	0.05	<2	9	8	<20	0.22	<10	<10	98	<10	135
KN 74-77.5	0.05	<2	10	8	<20	0.23	<10	<10	97	<10	121
KN 77.5-81	0.04	<2	9	8	<20	0.23	<10	<10	93	<10	120
KN 81-84.5	0.04	<2	9	8	<20	0.23	<10	<10	92	<10	120
KN 84.5-88	0.04	<2	9	7	<20	0.23	<10	<10	89	<10	115
KN 88-91.5	0.03	<2	9	7	<20	0.24	<10	<10	85	<10	109
KN 91.5-95	0.04	<2	8	6	<20	0.22	<10	<10	77	<10	100
KN 95-98.5	0.03	<2	7	6	<20	0.22	<10	<10	73	<10	94
KN 98.5-102	0.02	<2	6	5	<20	0.2	<10	<10	63	<10	82
KN 102-105.5	0.02	<2	5	4	<20	0.18	<10	<10	52	<10	68

Table D2 35 element concentrations at the State Line Site

SAMPLE	Ag	Al	As	B	Ba	Be	Bi	Ca	Cd	Co	Cr	Cu
	ppm	%	ppm	ppm	ppm	ppm	ppm	%	ppm	ppm	ppm	ppm
SLC 0-7	<0.2	1.79	<2	<10	110	0.6	<2	0.04	<0.5	6	19	8
SLC 7-15	<0.2	1.66	<2	<10	90	0.6	<2	0.04	<0.5	6	17	8
SLC 15-29	<0.2	1.74	<2	<10	90	0.6	<2	0.03	<0.5	6	18	8
SLC 29-43	<0.2	2.23	<2	<10	120	0.7	<2	0.03	<0.5	7	21	10
SLC 43-52	<0.2	2.46	<2	<10	130	0.8	<2	0.03	<0.5	9	23	10
SLC 52-60	<0.2	3.13	<2	<10	160	1	<2	0.03	<0.5	10	27	12
SLC 60-66	<0.2	3.37	<2	<10	180	1	<2	0.05	<0.5	10	29	13
SLC 66-74	<0.2	3.4	<2	<10	180	1.1	<2	0.04	<0.5	11	31	14
SLC 74-77	<0.2	1.38	<2	<10	70	<0.5	<2	0.02	<0.5	4	14	5
SLC 77-88	<0.2	5.21	2	<10	180	1.5	<2	0.03	<0.5	13	41	22
SLC 88-102	<0.2	5.05	<2	<10	180	1.4	<2	0.04	<0.5	13	39	21
SLC 102-116	<0.2	4.83	<2	<10	190	1.4	<2	0.04	<0.5	13	38	20
SLC 116-130	<0.2	5.67	<2	<10	230	1.6	<2	0.04	<0.5	17	44	25
SLC 130-139	<0.2	4.97	<2	<10	220	1.5	<2	0.04	<0.5	15	40	22
SLC 139-149	<0.2	4.64	<2	<10	220	1.3	<2	0.04	<0.5	13	36	19
SLC 149-155	<0.2	5.21	<2	<10	280	1.5	<2	0.05	<0.5	14	39	21
SLC 175-180	<0.2	2.84	<2	<10	190	1.1	<2	0.04	<0.5	11	30	13
SLM 180-185	<0.2	4.11	3	<10	220	1.7	<2	0.04	<0.5	14	41	18
SLM 185-190	<0.2	4.09	2	<10	230	1.7	<2	0.04	<0.5	15	41	17
SLM 190-195	<0.2	4.21	<2	<10	240	1.6	<2	0.04	<0.5	15	42	18
SLM 195-200	<0.2	4.91	3	<10	250	1.9	<2	0.04	<0.5	17	45	20
SLM 200-205	<0.2	3.97	3	<10	230	1.6	<2	0.04	<0.5	14	40	17
SLM 205-209	<0.2	4.14	2	<10	240	1.8	<2	0.04	<0.5	15	42	18
SLM 209-213	<0.2	3.18	<2	<10	200	1.3	<2	0.03	<0.5	12	34	13
SLM 213-218	<0.2	3.97	3	<10	240	1.6	<2	0.04	<0.5	15	40	17
SLM 218-223	<0.2	3.97	<2	<10	230	1.6	<2	0.04	<0.5	15	40	17
SLM 223-228	<0.2	4.13	<2	<10	250	1.7	<2	0.04	<0.5	16	41	17

SLM 228-233	<0.2	4.07	2	<10	260	1.7	<2	0.04	<0.5	15	42	17
SLM 233-238	<0.2	3.59	2	<10	230	1.5	<2	0.04	<0.5	14	37	15
SLM 238-240	<0.2	3.83	<2	<10	250	1.6	<2	0.04	<0.5	15	39	15
SLM 240-244	<0.2	2.14	<2	<10	140	0.8	<2	0.03	<0.5	8	24	9
SLM 244-249	<0.2	2.97	3	<10	200	1.2	<2	0.03	<0.5	13	31	12
SLM 249-254	<0.2	3.12	<2	<10	200	1.3	<2	0.03	<0.5	13	33	12
SLM 254-259	<0.2	3.03	2	<10	200	1.3	<2	0.03	<0.5	13	32	12
SLM 259-261.5	<0.2	2.39	<2	<10	160	1	<2	0.03	<0.5	11	26	9
SLM 261.5-266.5	<0.2	2.79	3	<10	180	1.2	<2	0.03	<0.5	11	30	11
SLC 260-265	<0.2	3.81	<2	<10	230	1.5	<2	0.04	<0.5	18	38	16
SLC 265-270	<0.2	4.32	<2	<10	230	1.8	<2	0.04	<0.5	19	42	18
SLC 270-275	<0.2	4.21	<2	<10	230	1.7	<2	0.04	<0.5	18	43	17
SLC 275-280	<0.2	4.41	<2	<10	240	1.8	<2	0.04	<0.5	18	45	18
SLC 280-285	<0.2	4.37	4	<10	230	1.8	<2	0.04	<0.5	16	44	18
SLC 285-290	<0.2	4.9	2	<10	260	2.1	<2	0.04	<0.5	19	50	21
SLC 290-295	<0.2	3.99	<2	<10	220	1.7	<2	0.03	<0.5	15	41	16
SLC 295-300	<0.2	3.63	3	<10	210	1.6	<2	0.03	<0.5	13	38	14
SLC 300-306	<0.2	3.7	<2	<10	210	1.6	<2	0.03	<0.5	12	38	14
SLC 306-312	<0.2	3.33	<2	<10	210	1.5	<2	0.03	<0.5	11	37	15

SAMPLE	Fe	Ga	Hg	K	La	Mg	Mn	Mo	Na	Ni	P	Pb
	%	ppm	ppm	%	ppm	%	ppm	ppm	%	ppm	ppm	ppm
SLC 0-7	1.79	10	0.01	0.31	10	0.38	216	<1	0.01	10	330	4
SLC 7-15	1.63	10	0.01	0.29	10	0.34	189	<1	0.01	9	350	4
SLC 15-29	1.75	10	0.02	0.28	10	0.36	193	<1	0.01	10	280	4
SLC 29-43	2.07	10	0.02	0.36	20	0.45	244	<1	0.01	12	260	7
SLC 43-52	2.2	10	0.02	0.4	20	0.49	260	<1	0.01	14	270	7
SLC 52-60	2.64	10	0.03	0.49	20	0.59	321	<1	0.01	16	320	10
SLC 60-66	2.74	10	0.04	0.47	20	0.58	338	<1	0.01	17	440	12
SLC 66-74	2.78	10	0.04	0.46	20	0.59	347	<1	0.01	18	370	11
SLC 74-77	1.31	10	0.01	0.2	10	0.25	138	<1	0.01	8	160	4
SLC 77-88	3.61	20	0.06	0.47	30	0.64	459	<1	0.01	22	540	17

SLC 88-102	3.53	20	0.05	0.46	30	0.64	493	<1	0.01	22	470	19
SLC 102-116	3.47	10	0.05	0.46	30	0.63	522	<1	0.01	21	410	14
SLC 116-130	4.05	20	0.06	0.49	30	0.7	708	<1	0.01	24	480	15
SLC 130-139	3.65	20	0.05	0.44	30	0.62	663	<1	0.01	22	400	15
SLC 139-149	3.31	10	0.05	0.41	30	0.58	518	<1	0.01	20	380	13
SLC 149-155	3.61	20	0.05	0.44	30	0.63	580	<1	0.01	21	420	15
SLC 175-180	2.63	10	0.01	0.4	20	0.63	373	<1	0.01	19	230	7
SLM 180-185	3.22	10	0.02	0.43	30	0.74	497	<1	0.01	24	320	9
SLM 185-190	3.34	10	0.02	0.49	20	0.81	496	<1	0.01	25	310	10
SLM 190-195	3.45	10	0.02	0.51	30	0.83	517	<1	0.01	25	340	9
SLM 195-200	3.65	10	0.03	0.5	30	0.85	576	<1	0.01	27	410	11
SLM 200-205	3.31	10	0.02	0.49	20	0.81	479	<1	0.01	25	340	8
SLM 205-209	3.45	10	0.02	0.52	30	0.84	525	<1	0.01	27	360	10
SLM 209-213	2.88	10	0.01	0.46	20	0.73	383	<1	0.01	20	270	6
SLM 213-218	3.36	10	0.02	0.51	20	0.83	476	<1	0.01	24	330	7
SLM 218-223	3.28	10	0.02	0.48	30	0.8	490	<1	0.01	25	350	10
SLM 223-228	3.46	10	0.02	0.53	30	0.87	533	<1	0.01	27	350	9
SLM 228-233	3.53	10	0.02	0.56	30	0.89	531	<1	0.01	27	330	10
SLM 233-238	3.19	10	0.02	0.5	20	0.8	489	<1	0.01	24	300	7
SLM 238-240	3.42	10	0.02	0.56	20	0.88	564	<1	0.01	25	310	8
SLM 240-244	2.07	10	0.01	0.3	20	0.46	339	<1	0.01	15	190	4
SLM 244-249	2.8	10	0.01	0.45	20	0.71	501	<1	0.01	20	260	6
SLM 249-254	2.84	10	0.01	0.46	20	0.72	502	<1	0.01	21	280	7
SLM 254-259	2.84	10	0.01	0.47	20	0.73	580	<1	0.01	22	260	6
SLM 259-261.5	2.34	10	0.01	0.38	10	0.58	479	<1	0.01	17	190	4
SLM 261.5-266.5	2.72	10	0.01	0.42	20	0.65	539	<1	0.01	18	240	4
SLC 260-265	3.35	10	0.02	0.52	20	0.84	894	<1	0.01	24	300	9
SLC 265-270	3.52	10	0.02	0.51	30	0.84	830	<1	0.01	26	310	10
SLC 270-275	3.54	10	0.02	0.53	30	0.86	710	<1	0.01	26	310	8
SLC 275-280	3.68	10	0.02	0.54	30	0.89	665	<1	0.01	26	320	11
SLC 280-285	3.6	10	0.02	0.5	30	0.83	539	<1	0.01	26	310	10

SLC 285-290	4.25	20	0.02	0.59	30	0.97	586	<1	0.01	30	360	11
SLC 290-295	3.59	10	0.02	0.51	30	0.84	439	<1	0.01	24	300	8
SLC 295-300	3.84	10	0.02	0.5	20	0.8	354	<1	0.01	23	300	8
SLC 300-306	3.25	10	0.02	0.49	20	0.79	227	<1	0.01	24	320	8
SLC 306-312	3	10	0.02	0.46	20	0.72	204	<1	0.01	22	300	9

SAMPLE	S	Sb	Sc	Sr	Th	Ti	Tl	U	V	W	Zn
	%	ppm	ppm	ppm	ppm	%	ppm	ppm	ppm	ppm	ppm
SLC 0-7	0.02	<2	3	5	<20	0.13	<10	<10	33	<10	47
SLC 7-15	0.02	<2	2	4	<20	0.13	<10	<10	30	<10	44
SLC 15-29	0.02	<2	3	4	<20	0.13	<10	<10	33	<10	43
SLC 29-43	0.02	<2	4	4	<20	0.16	<10	<10	38	<10	53
SLC 43-52	0.02	<2	4	5	<20	0.18	<10	<10	42	<10	58
SLC 52-60	0.02	<2	5	6	<20	0.21	<10	<10	49	<10	72
SLC 60-66	0.03	<2	5	7	<20	0.2	<10	<10	52	<10	74
SLC 66-74	0.03	<2	5	7	<20	0.2	<10	<10	52	<10	74
SLC 74-77	0.01	<2	2	2	<20	0.1	<10	<10	25	<10	31
SLC 77-88	0.04	<2	7	10	<20	0.21	<10	<10	69	<10	88
SLC 88-102	0.04	<2	7	10	<20	0.21	<10	<10	67	<10	88
SLC 102-116	0.04	<2	7	10	<20	0.21	<10	<10	66	<10	85
SLC 116-130	0.04	<2	8	11	<20	0.23	<10	<10	78	<10	95
SLC 130-139	0.02	<2	7	10	<20	0.21	<10	<10	69	<10	84
SLC 139-149	0.02	<2	6	10	<20	0.21	<10	<10	63	<10	78
SLC 149-155	0.02	<2	7	12	<20	0.22	<10	<10	68	<10	83
SLC 175-180	0.01	<2	4	7	<20	0.2	<10	<10	48	<10	68
SLM 180-185	0.01	<2	6	9	<20	0.24	<10	<10	61	<10	84
SLM 185-190	0.01	<2	6	9	<20	0.25	<10	<10	63	<10	88
SLM 190-195	0.01	2	6	9	<20	0.26	<10	<10	65	<10	89
SLM 195-200	0.02	<2	7	9	<20	0.27	<10	<10	68	<10	93
SLM 200-205	0.01	<2	6	8	<20	0.26	<10	<10	62	<10	85
SLM 205-209	0.01	<2	6	8	<20	0.26	<10	<10	65	<10	91
SLM 209-213	0.01	3	5	7	<20	0.23	<10	<10	53	<10	75

SLM 213-218	0.01	<2	6	8	<20	0.26	<10	<10	62	<10	88
SLM 218-223	0.01	<2	6	8	<20	0.25	<10	<10	62	<10	86
SLM 223-228	0.01	<2	6	9	<20	0.27	<10	<10	64	<10	91
SLM 228-233	0.01	2	6	9	<20	0.27	<10	<10	65	<10	94
SLM 233-238	0.01	<2	5	8	<20	0.25	<10	<10	59	<10	84
SLM 238-240	0.01	<2	6	8	<20	0.27	<10	<10	62	<10	91
SLM 240-244	<0.01	<2	3	5	<20	0.17	<10	<10	39	<10	50
SLM 244-249	0.01	2	5	6	<20	0.22	<10	<10	51	<10	73
SLM 249-254	0.01	<2	5	7	<20	0.23	<10	<10	52	<10	75
SLM 254-259	0.01	2	5	7	<20	0.23	<10	<10	52	<10	75
SLM 259-261.5	<0.01	<2	4	5	<20	0.19	<10	<10	42	<10	60
SLM 261.5-266.5	0.01	<2	4	6	<20	0.21	<10	<10	48	<10	66
SLC 260-265	0.01	2	6	8	<20	0.26	<10	<10	62	<10	88
SLC 265-270	0.02	<2	6	8	<20	0.26	<10	<10	65	<10	93
SLC 270-275	0.01	<2	6	8	<20	0.27	<10	<10	66	<10	92
SLC 275-280	0.01	<2	6	9	<20	0.28	<10	<10	68	<10	96
SLC 280-285	0.01	<2	6	8	<20	0.26	<10	<10	66	<10	92
SLC 285-290	0.01	2	7	9	<20	0.3	<10	<10	76	<10	106
SLC 290-295	0.01	<2	6	7	<20	0.26	<10	<10	63	<10	89
SLC 295-300	0.01	2	6	7	<20	0.25	<10	<10	59	<10	84
SLC 300-306	<0.01	<2	6	6	<20	0.25	<10	<10	60	<10	85
SLC 306-312	<0.01	<2	5	6	<20	0.24	<10	<10	57	<10	78

Table D3 35 element concentrations at the Riverside Site

SAMPLE	Ag	Al	As	B	Ba	Be	Bi	Ca	Cd	Co	Cr	Cu
	ppm	%	ppm	ppm	ppm	ppm	ppm	%	ppm	ppm	ppm	ppm
RSM 0-6	<0.2	0.91	<2	<10	50	<0.5	<2	0.14	<0.5	4	16	4
RSM 6-11	<0.2	1.27	2	<10	80	0.5	<2	0.03	<0.5	5	16	6
RSM 11-22	<0.2	1.4	2	<10	90	0.5	<2	0.06	<0.5	5	20	7
RSM 22-24	0.2	1.66	2	<10	100	0.6	<2	0.06	<0.5	6	19	8
RSM 24-35	<0.2	1.96	2	<10	110	0.6	<2	0.06	<0.5	7	21	10
RSM 35-46	<0.2	2.95	<2	<10	170	1	<2	0.04	<0.5	11	29	15
RSM 46-57	<0.2	4.48	2	<10	220	1.4	2	0.07	<0.5	15	39	23
RSM 57-68	<0.2	4.54	<2	<10	230	1.4	<2	0.1	<0.5	16	40	24
RSM 68-72	<0.2	4.54	<2	<10	240	1.6	<2	0.1	<0.5	16	41	24
RSM 72-78	<0.2	3.14	<2	<10	200	1.2	<2	0.08	<0.5	12	32	17
RSM 78-89	<0.2	2.54	<2	<10	170	1	<2	0.05	<0.5	11	28	12
RSM 89-96	<0.2	2.74	<2	<10	180	1.1	<2	0.05	<0.5	11	31	12
RSM 96-106	<0.2	3.27	<2	<10	200	1.3	<2	0.06	<0.5	13	35	16
RSM 106-117	<0.2	3.03	<2	<10	180	1.3	<2	0.05	<0.5	12	32	14
RSM 117-122	<0.2	3.27	<2	<10	190	1.4	<2	0.05	<0.5	14	35	16
RSM 122-124.5	0.2	4.09	<2	<10	210	1.9	<2	0.05	<0.5	16	40	21
RSM 124.5-127	<0.2	4.59	2	<10	220	2.1	<2	0.05	<0.5	17	44	24
RSM 127-130	<0.2	4.83	2	<10	220	2.1	<2	0.05	<0.5	17	44	25
RSM 130-132	<0.2	5.03	<2	<10	240	2.2	<2	0.06	<0.5	18	46	26
RSM 132-134.5	<0.2	5.01	<2	<10	240	2.2	<2	0.06	<0.5	18	46	26
RSM 134.5-137	<0.2	5.01	<2	<10	240	2.2	<2	0.06	<0.5	18	45	28
RSM 137-139.5	<0.2	4.81	<2	<10	230	2.2	<2	0.05	<0.5	17	44	26
RSM 139.5-142	<0.2	4.89	<2	<10	240	2.2	<2	0.05	<0.5	18	45	27
RSM 142-144.5	<0.2	4.75	<2	<10	230	2.1	<2	0.05	<0.5	18	44	26
RSM 144.5-147	<0.2	4.91	<2	<10	240	2.2	<2	0.05	<0.5	18	45	27
RSM 147-149.5	<0.2	4.7	2	<10	240	2.1	<2	0.05	<0.5	17	43	26
RSM 149.5-152	<0.2	4.65	<2	<10	230	2.1	<2	0.05	<0.5	17	44	25

RSM 152-154	<0.2	4.54	<2	<10	230	2	<2	0.05	<0.5	17	43	24
RSM 154-156.5	<0.2	4.8	<2	<10	240	2.1	<2	0.05	<0.5	18	45	25
RSM 156.5-159	<0.2	4.78	<2	<10	230	2.1	<2	0.05	<0.5	18	45	25
RSM 159-161.5	<0.2	4.72	<2	<10	230	2.1	<2	0.05	<0.5	18	45	25
RSM 161.5-164	<0.2	4.47	<2	<10	220	1.9	<2	0.04	<0.5	17	43	24
RSM 164-166.5	<0.2	4.89	<2	<10	230	2.1	<2	0.05	<0.5	18	47	26
RSM 166.5-169	<0.2	5.07	<2	<10	230	2.1	<2	0.05	<0.5	18	49	26
RSM 169-117.5	<0.2	5.08	<2	<10	230	2.1	<2	0.05	<0.5	19	49	26
RSM 117.5-174	<0.2	5.11	<2	<10	230	2.1	<2	0.05	<0.5	19	50	26
RSM 174-176.5	<0.2	5.43	<2	<10	250	2.2	<2	0.05	<0.5	19	52	27
RSM 176.5-179	<0.2	5.64	<2	<10	260	2.3	<2	0.05	<0.5	19	54	29
RSM 179-181.5	<0.2	5.45	2	<10	250	2.3	<2	0.05	<0.5	19	52	27
RSM 181.5-184	<0.2	5.21	2	<10	250	2.2	<2	0.05	<0.5	19	52	26
RSM 184-186.5	<0.2	4.76	<2	<10	230	2.1	<2	0.03	<0.5	18	48	23
RSM 186.5-189	0.2	4.58	<2	<10	230	2	<2	0.03	<0.5	18	48	22
RSM 189-191.5	<0.2	4.6	3	<10	230	2	2	0.03	<0.5	19	48	22
RSM 191.5-194	<0.2	4.41	<2	<10	230	2	<2	0.02	<0.5	19	47	21
RSM 194-196.5	<0.2	4.2	<2	<10	220	1.9	<2	0.02	<0.5	18	44	20
RSM 196.5-199	<0.2	3.76	<2	<10	200	1.7	2	0.02	<0.5	16	41	18
RSM 199-201.5	<0.2	4.23	<2	<10	230	1.8	<2	0.02	<0.5	17	48	21
RSM 201.5-204	<0.2	3.72	<2	<10	210	1.6	<2	0.02	<0.5	15	42	18
RSM 204-206.5	<0.2	3.66	<2	<10	210	1.6	2	0.02	<0.5	15	40	17
RSM 206.5-209	<0.2	3.32	<2	<10	190	1.5	<2	0.02	<0.5	15	37	15
RSM 209-211.5	<0.2	2.73	<2	<10	160	1.2	<2	0.01	<0.5	12	32	12
RSM 211.5-214	<0.2	2.44	<2	<10	150	1.1	<2	0.01	<0.5	11	30	11
RSM 214-216.5	<0.2	1.64	<2	<10	110	0.7	<2	<0.01	<0.5	8	21	7

SAMPLE	Fe	Ga	Hg	K	La	Mg	Mn	Mo	Na	Ni	P	Pb
	%	ppm	ppm	%	ppm	%	ppm	ppm	%	ppm	ppm	ppm
RSM 0-6	1.4	<10	0.01	0.16	10	0.23	119	<1	<0.01	6	200	3
RSM 6-11	1.43	<10	0.01	0.21	10	0.28	160	<1	<0.01	10	160	4
RSM 11-22	1.77	10	0.01	0.21	10	0.29	177	<1	<0.01	9	220	5

RSM 22-24	1.72	10	0.01	0.25	10	0.35	192	<1	0.01	11	210	4
RSM 24-35	1.95	10	0.02	0.27	10	0.38	232	<1	<0.01	11	270	6
RSM 35-46	2.76	10	0.03	0.42	20	0.57	338	<1	<0.01	16	350	11
RSM 46-57	3.58	10	0.06	0.44	30	0.68	516	<1	0.01	24	510	14
RSM 57-68	3.66	10	0.05	0.4	30	0.66	602	<1	0.01	23	440	15
RSM 68-72	3.74	10	0.04	0.43	30	0.7	670	<1	0.01	24	420	13
RSM 72-78	2.83	10	0.02	0.36	20	0.6	461	<1	0.01	21	310	7
RSM 78-89	2.54	10	0.01	0.38	20	0.61	314	<1	<0.01	17	200	4
RSM 89-96	2.76	10	0.01	0.41	20	0.67	338	<1	0.01	19	210	4
RSM 96-106	3.01	10	0.02	0.39	20	0.7	434	<1	0.01	20	280	6
RSM 106-117	2.84	10	0.02	0.38	20	0.63	415	<1	0.01	20	280	5
RSM 117-122	3.03	10	0.02	0.4	30	0.68	412	<1	0.01	20	300	6
RSM 122-124.5	3.39	10	0.03	0.41	30	0.73	540	<1	0.01	24	390	9
RSM 124.5-127	3.65	10	0.02	0.41	40	0.76	706	<1	0.01	26	480	10
RSM 127-130	3.73	10	0.03	0.39	40	0.75	795	<1	0.01	27	510	10
RSM 130-132	3.88	10	0.03	0.39	40	0.77	821	<1	0.01	29	550	10
RSM 132-134.5	3.8	10	0.03	0.37	40	0.74	804	<1	0.01	28	560	10
RSM 134.5-137	3.83	10	0.04	0.38	40	0.76	760	<1	0.01	26	550	10
RSM 137-139.5	3.73	10	0.04	0.37	40	0.73	706	<1	0.01	26	530	10
RSM 139.5-142	3.74	10	0.04	0.39	40	0.75	749	<1	0.01	27	540	11
RSM 142-144.5	3.64	10	0.03	0.4	40	0.74	764	<1	0.01	25	560	10
RSM 144.5-147	3.74	10	0.03	0.41	40	0.77	794	<1	0.01	28	560	11
RSM 147-149.5	3.64	10	0.03	0.41	40	0.75	746	<1	0.01	27	520	11
RSM 149.5-152	3.62	10	0.03	0.41	40	0.74	748	<1	0.01	27	500	11
RSM 152-154	3.6	10	0.03	0.42	40	0.75	728	<1	0.01	26	490	9
RSM 154-156.5	3.79	10	0.03	0.44	40	0.8	745	<1	0.01	28	510	11
RSM 156.5-159	3.79	10	0.03	0.43	40	0.78	728	<1	0.01	27	500	11
RSM 159-161.5	3.74	10	0.03	0.43	40	0.77	732	<1	0.01	27	520	11
RSM 161.5-164	3.63	10	0.03	0.43	30	0.76	663	<1	0.01	26	470	11
RSM 164-166.5	3.9	10	0.03	0.44	40	0.8	698	<1	0.01	28	520	10
RSM 166.5-169	4.02	20	0.03	0.45	40	0.83	662	<1	0.01	28	490	12

RSM 169-117.5	4.01	20	0.03	0.45	40	0.83	673	<1	0.01	29	480	12
RSM 117.5-174	4.03	20	0.03	0.46	40	0.84	700	<1	0.01	28	460	12
RSM 174-176.5	4.21	20	0.03	0.47	40	0.88	746	<1	0.01	30	510	13
RSM 176.5-179	4.38	20	0.03	0.5	40	0.91	747	<1	0.01	32	490	12
RSM 179-181.5	4.25	20	0.03	0.48	40	0.89	736	<1	0.01	30	470	11
RSM 181.5-184	4.23	20	0.03	0.5	40	0.91	710	<1	0.01	32	450	12
RSM 184-186.5	3.97	10	0.03	0.47	30	0.85	678	<1	<0.01	28	420	12
RSM 186.5-189	3.93	10	0.03	0.48	30	0.87	669	<1	<0.01	28	410	12
RSM 189-191.5	4.01	10	0.03	0.52	30	0.91	672	<1	0.01	26	430	12
RSM 191.5-194	3.92	10	0.03	0.51	30	0.88	648	<1	0.01	26	430	9
RSM 194-196.5	3.73	10	0.03	0.48	30	0.83	627	<1	<0.01	27	420	11
RSM 196.5-199	3.45	10	0.02	0.45	30	0.77	523	<1	<0.01	24	390	10
RSM 199-201.5	3.86	10	0.02	0.52	30	0.89	535	<1	<0.01	27	430	11
RSM 201.5-204	3.48	10	0.02	0.48	30	0.81	474	<1	<0.01	24	380	9
RSM 204-206.5	3.46	10	0.02	0.49	30	0.81	503	<1	<0.01	24	390	10
RSM 206.5-209	3.19	10	0.02	0.45	20	0.74	482	<1	<0.01	22	360	7
RSM 209-211.5	2.71	10	0.02	0.38	20	0.62	368	<1	<0.01	18	310	11
RSM 211.5-214	2.54	10	0.01	0.4	20	0.63	297	<1	<0.01	17	260	7
RSM 214-216.5	1.83	10	0.01	0.29	10	0.44	206	<1	<0.01	11	170	5

SAMPLE	S	Sb	Sc	Sr	Th	Ti	Tl	U	V	W	Zn
	%	ppm	ppm	ppm	ppm	%	ppm	ppm	ppm	ppm	ppm
RSM 0-6	<0.01	<2	2	4	<20	0.11	<10	<10	33	<10	28
RSM 6-11	<0.01	<2	2	3	<20	0.11	<10	<10	28	<10	33
RSM 11-22	<0.01	<2	2	4	<20	0.14	<10	<10	38	<10	37
RSM 22-24	<0.01	<2	3	5	<20	0.13	<10	<10	34	<10	41
RSM 24-35	0.01	<2	3	5	<20	0.14	<10	<10	36	<10	48
RSM 35-46	0.01	2	5	7	<20	0.19	<10	<10	49	<10	71
RSM 46-57	0.02	2	7	12	<20	0.21	<10	<10	64	<10	94
RSM 57-68	0.02	2	7	16	<20	0.21	<10	<10	65	<10	87
RSM 68-72	0.02	<2	6	17	<20	0.22	<10	<10	66	<10	88
RSM 72-78	0.02	<2	4	12	<20	0.19	<10	<10	51	<10	69

RSM 78-89	0.01	2	4	7	<20	0.19	<10	<10	44	<10	60
RSM 89-96	0.01	2	4	8	<20	0.21	<10	<10	48	<10	66
RSM 96-106	0.01	<2	5	10	<20	0.22	<10	<10	54	<10	74
RSM 106-117	0.01	<2	4	8	<20	0.21	<10	<10	50	<10	68
RSM 117-122	0.01	<2	5	8	<20	0.22	<10	<10	53	<10	74
RSM 122-124.5	0.02	2	6	9	<20	0.23	<10	<10	60	<10	86
RSM 124.5-127	0.03	<2	6	10	<20	0.24	<10	<10	65	<10	94
RSM 127-130	0.03	<2	6	10	<20	0.24	<10	<10	66	<10	97
RSM 130-132	0.03	<2	7	10	<20	0.25	<10	<10	69	<10	101
RSM 132-134.5	0.03	<2	7	10	<20	0.23	<10	<10	68	<10	99
RSM 134.5-137	0.03	2	6	10	<20	0.23	<10	<10	67	<10	100
RSM 137-139.5	0.03	2	6	10	<20	0.23	<10	<10	67	<10	98
RSM 139.5-142	0.03	2	6	10	<20	0.23	<10	<10	67	<10	99
RSM 142-144.5	0.03	3	6	9	<20	0.23	<10	<10	65	<10	97
RSM 144.5-147	0.03	2	6	10	<20	0.23	<10	<10	67	<10	101
RSM 147-149.5	0.03	<2	6	10	<20	0.23	<10	<10	65	<10	97
RSM 149.5-152	0.03	2	6	10	<20	0.23	<10	<10	65	<10	97
RSM 152-154	0.03	2	6	9	<20	0.23	<10	<10	65	<10	95
RSM 154-156.5	0.03	3	7	10	<20	0.24	<10	<10	68	<10	99
RSM 156.5-159	0.02	<2	7	10	<20	0.24	<10	<10	68	<10	98
RSM 159-161.5	0.03	<2	7	10	<20	0.24	<10	<10	68	<10	97
RSM 161.5-164	0.02	<2	6	9	<20	0.23	<10	<10	65	<10	93
RSM 164-166.5	0.03	<2	7	10	<20	0.25	<10	<10	70	<10	100
RSM 166.5-169	0.03	2	7	10	<20	0.26	<10	<10	72	<10	100
RSM 169-117.5	0.02	3	7	10	<20	0.26	<10	<10	72	<10	99
RSM 117.5-174	0.03	2	7	10	<20	0.26	<10	<10	72	<10	100
RSM 174-176.5	0.03	<2	8	11	<20	0.27	<10	<10	75	<10	104
RSM 176.5-179	0.03	2	8	11	<20	0.28	<10	<10	78	<10	108
RSM 179-181.5	0.03	2	8	11	<20	0.28	<10	<10	76	<10	105
RSM 181.5-184	0.02	2	8	11	<20	0.28	<10	<10	75	<10	103
RSM 184-186.5	0.02	<2	7	9	<20	0.26	<10	<10	72	<10	98

RSM 186.5-189	0.02	<2	7	9	<20	0.26	<10	<10	71	<10	94
RSM 189-191.5	0.02	<2	7	9	<20	0.27	<10	<10	72	<10	96
RSM 191.5-194	0.02	2	7	9	<20	0.26	<10	<10	70	<10	95
RSM 194-196.5	0.02	2	7	9	<20	0.25	<10	<10	66	<10	89
RSM 196.5-199	0.01	2	6	8	<20	0.24	<10	<10	62	<10	82
RSM 199-201.5	0.01	<2	7	8	<20	0.27	<10	<10	69	<10	92
RSM 201.5-204	0.01	<2	6	8	<20	0.25	<10	<10	62	<10	83
RSM 204-206.5	0.01	2	6	8	<20	0.24	<10	<10	61	<10	82
RSM 206.5-209	0.01	2	5	7	<20	0.23	<10	<10	57	<10	75
RSM 209-211.5	0.01	<2	4	6	<20	0.2	<10	<10	48	<10	63
RSM 211.5-214	0.01	<2	4	5	<20	0.19	<10	<10	44	<10	60
RSM 214-216.5	<0.01	<2	3	3	<20	0.15	<10	<10	33	<10	41

APPENDIX E

CESIUM-137 DATA FOR THE KEENER SITE

Table E Cesium-137 data for the Keener site

sample ID	depth(cm)	^{137}Cs (Bq/Kg)
kn_0-2	1	15.75
kn_2-4	3	12.91
kn_4-6	5	13.96
kn_6-8	7	14.65
kn_8-10	9	12.15
kn_10-12	11	12.12
kn_12-14	13	12.58
kn_14-16	15	11.97
kn_16-18	17	10.70
kn_18-20	19	6.03
kn_20-22	21	1.44
kn_22-24	23	3.62
kn_24-26	25	9.19
kn_26-28	27	2.16
kn_28-30	29	2.11
kn_30-32	31	1.87
kn_32-34	33	1.71
kn_34-36	35	1.43
kn_36-38	37	1.22
kn_38-40	39	1.16